AD-A093 214 RAYTHEON CO GOLETA CALIF ELECTROMAGNETIC SYSTEMS DIV F/G 9/5

AGILE POLARIZATION FEED ARRAY FOR 3-D DOME ANTENNA.(U)

NOV 80 D T THOMAS, S D BIXLER, C J LAUER N00014-78-C-0690

UNCLASSIFIED NL

1 of 2

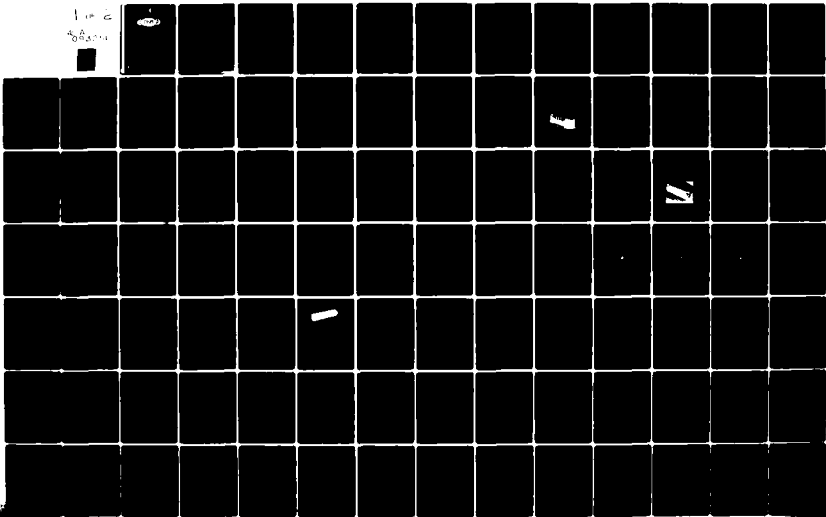

LEVEL (12)

Report ONR 252-008-2

AD A093214

OFFICE OF NAVAL RESEARCH

AGILE POLARIZATION FEED ARRAY FOR 3-D DOME ANTENNA

DR. DAVID T. THOMAS
S. DOUGLAS BIXLER
CARL J. LAUER
MICHAEL J. MAYBELL

RAYTHEON COMPANY
ELECTROMAGNETIC SYSTEMS DIVISION
6380 HOLLISTER AVENUE
GOLETA, CALIFORNIA 93117

CONTRACT N00014-78-C-0690
ONR TASK 252-008-2

NOVEMBER 1980

FINAL TECHNICAL REPORT FOR PERIOD 1 OCT 78 - 30 SEP 79

PREPARED FOR THE

OFFICE OF NAVAL RESEARCH • 800 N. QUINCY ST. • ARLINGTON • VA • 22217

NOTICES

Change of Address

Organizations receiving reports on the initial distribution list should confirm correct address. This list is located at the end of the report. Any change of address or distribution should be conveyed to the Office of Naval Research, Arlington, VA 22217, Attn: Code 221.

Disposition

When this report is no longer needed, it may be transmitted to other authorized organizations. Do not return it to the originator or the monitoring office.

Disclaimer

The findings in this report are not to be construed as an official Department of Defense or Military Department position unless so designated by other official documents.

Reproduction

UNCLASSIFIED

SECURITY CLASSIFICATION OF THIS PAGE (When Data Entered)

REPORT DOCUMENTATION PAGE

READ INSTRUCTIONS BEFORE COMPLETING FORM

1. REPORT NUMBER
ONR 252-008-2

2. GOVT ACCESSION NO.
AD-A093 214

3. RECIPIENT'S CATALOG NUMBER

(9) Final Technical Report,
1 Oct[redacted] 1978 [redacted] 30 Sep[redacted] 1979

4. TITLE (and Subtitle)

(6) Agile Polarization Feed Array for 3-D Dome Antenna.

5. TYPE OF REPORT & PERIOD COVERED

6. PERFORMING ORG. REPORT NUMBER
-

7. AUTHOR(s)
(10) Dr. David T. Thomas, S. Douglas Bixler et al
Carl J. Hauck Michael J. Mainbell

8. CONTRACT OR GRANT NUMBER(s)
(15) N00014-78-C-0690

9. PERFORMING ORGANIZATION NAME AND ADDRESS
Raytheon Company
Electromagnetic Systems Division
6380 Hollister Avenue
Goleta, California 93117

10. PROGRAM ELEMENT, PROJECT, TASK AREA & WORK UNIT NUMBERS
ONR TASK 252-008-2

11. CONTROLLING OFFICE NAME AND ADDRESS
Department of the Navy
Office of Naval Research
Arlington, Virginia 22217

12. REPORT DATE
(11) Nov[redacted] 1980

13. NUMBER OF PAGES
106

14. MONITORING AGENCY NAME & ADDRESS (if different from Controlling Office)
(12) 107

15. SECURITY CLASS. (of this report)
UNCLASSIFIED

15a. DECLASSIFICATION/DOWNGRADING SCHEDULE

16. DISTRIBUTION STATEMENT (of this Report)

Approved for public release; distribution unlimited.

17. DISTRIBUTION STATEMENT (of the abstract entered in Block 20, if different from Report)

18. SUPPLEMENTARY NOTES

19. KEY WORDS (Continue on reverse side if necessary and identify by block number)

Agile polarization, Concave array, Cross notch elements, Dual polarization, E-notch elements, Multistage phase shifters, 3-D dome antenna.

20. ABSTRACT (Continue on reverse side if necessary and identify by block number)

This final report describes an investigation of polarization agility for octave-bandwidth feed arrays in a 3-D dome antenna system. Both studies and experimental investigations were performed on this program.

The studies include analyses of the polarization needs of 3-D dome antenna systems (~~section~~ I,2), especially the feed array portion, and investigation of techniques for implementation, including octave-bandwidth, dual-polarization array elements (~~Section~~ II) and circuits for agile polarization (~~Section~~ III).

(continued)

DD FORM 1 JAN 73 1473 EDITION OF 1 NOV 65 IS OBSOLETE

UNCLASSIFIED

SECURITY CLASSIFICATION OF THIS PAGE (When Data Entered)

20. (concl)

The experimental investigations have consisted of design, fabrication, and test of two small arrays of orthogonal notch elements and of a similar, linear-notch array. Both dual-polarization elements exhibit wide azimuth scan capability over at least an octave bandwidth (data summary in section 2.1). Beamwidths of the coincident-center notch element remain uniformly broad over the octave band.

A bibliography is included which lists 7 references on polarization analysis, 23 references on elements, and 13 references on array performance.

TABLE OF CONTENTS

LIST OF ILLUSTRATIONS

SECTION I
INTRODUCTION

1.1 PROGRAM DESCRIPTION

Dome polarization characteristics have previously been studied by others[1], but only in the context of narrow-band radar. Investigation was made of the effects of array scan for various scan expansion factors K, with primary attention directed to the polarization transfer characteristics of the dome for linearly polarized plane waves. The study concluded with an outline of feed networks suitable for generating diverse polarizations, presenting loss budgets and relative costs for particular networks.

When dome configurations are considered for other applications, it is necessary to understand their polarization characteristics more fully. In particular, functions such as ESM, ECM, and communications required wider bands than the usual radar requirements studies by Sperry. The implementation of polarization agility using multibeam feed arrays requires consideration of the following factors:

1. Both the dome and feed array must contain element types capable of covering octave or greater bandwidths. This forces electrically dense arrays in the lower half of the band. Special attention must be given to the tight element coupling in both the feed array and dome.
2. The feed and polarization networks must be wide band.
3. Polarization interactions between the feed array and dome must be reexamined in the context of large bandwidth and high element density.
4. Rapid polarization agility is imperative in the EW context, and represents an important topic for study.

1 "Dome Antenna, Phase II Final Report," Sperry Gyroscope Division, Great Neck, NY, Nov. 1972, Report No. SGD-4261-0570 (SECRET)

1.2 3-D DOME POLARIZATION STUDIES

1.2.1 INTRODUCTION

The 3-D dome allows wide-angle scanning over regions exceeding a hemisphere. Feed arrays for dome applications are simplest if they provide a fixed linear polarization. However, for such feed arrays, whether flat or curved, the polarization incident on the dome will vary with azimuth direction, resulting in scan-dependent polarization characteristics. For example, a linearly polarized feed array consisting of dipole elements will provide vertical polarization for the plane containing the dipole axis, and horizontal polarization for the orthogonal plane. For intermediate azimuth positions, the polarization will still be linear, but rotating from vertical to horizontal and back again as azimuth angle is varied. This situation may be circumvented by employing circular polarization in the feed array, but this solution is restrictive and successful only if polarization purity is maintained.

In general, system designs employing dome antennas require some specific polarization over the operating hemisphere. Furthermore, modern systems are increasingly turning to polarization agility to accomplish their goals. Both situations require that the feed array be capable of providing multiple polarizations, perhaps with high switching rates between the various polarization states. Previous analyses have shown that the dome will transmit any incident polarization with essentially no change. The burden of providing polarization agility is therefore placed on the feed array.

One technique for generating multiple polarizations employs a crossed, linear-array element[2] fed with some appropriate polarization selection circuit. Many crossed (dual) linear elements may be employed, including crossed dipoles,

2 This approach was used in one Sperry dome. See Final Technical Report, "Hemisphere Coverage Antenna", Contract DAAK 40-74-C-0334, Nov. 1978 (Confidential report).

crossed slots, square or circular waveguide, etc. For this study, the crossed slot was selected as representative of the polarization characteristics of dual linear elements in general. An analysis has been conducted, with the results programmed for computer. Computations of polarization state over the forward hemisphere have been conducted for the element excited to produce right-hand circular polarization; the analyses and computed results are presented below. A discussion of the feed circuits capable of generating multiple polarizations is reserved for a later section.

1.2.2 ANALYSIS

Figure 1 shows a single slot element in the xy-plane with all parameters indicated. The electric field amplitude pattern for a single slot in an infinite ground plane is given by Kraus[3] as:

$$E = \frac{\cos\left[(\pi/2)(\cos\alpha)\right]}{\sin\alpha} \tag{1}$$

where α is the angle between the slot axis and the ray $\overline{OP}$ to the far-field point. Expressing the slot pattern in terms of spherical coordinates (θ, ϕ), ϕ' denotes the inclination of the slot relative to $\phi = 0°$, and the unit vector in the direction of the slot axis with ϕ' orientation is given by:

$$a_1 = \overline{a_x}\cos\phi' + \overline{a_y}\sin\phi' \tag{2}$$

To represent a crossed-slot element, we required a second slot oriented 90 degrees relative to the first. For the second slot, the unit position vector is given by:

$$a_2 = \overline{a_x}\sin\phi' + \overline{a_y}\cos\phi' \tag{3}$$

3 Kraus, J.D. Antennas. McGraw-Hill Book Co., 1950, p. 358.

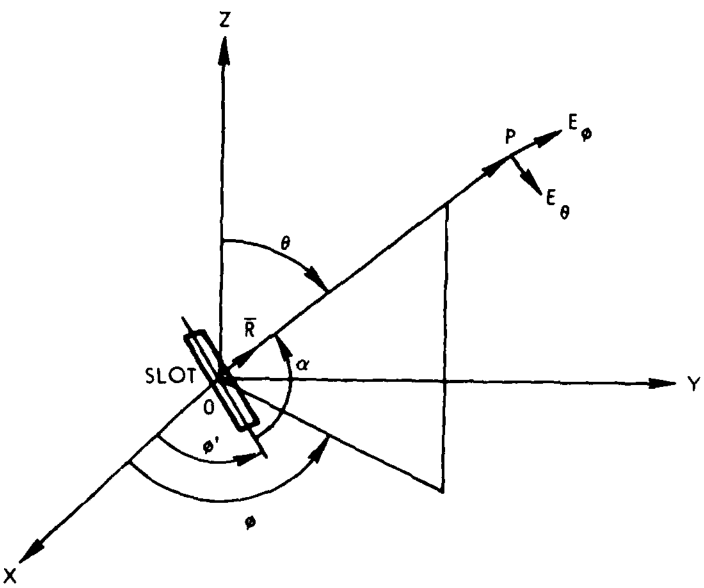

Figure 1. Half-Wavelength Slot in XY-Plane

The unit vector in the direction OP is given by:

$$R = \overline{a_x}\sin\theta\cos\phi + \overline{a_y}\sin\theta + \overline{a_z}\cos\theta. \tag{4}$$

The values of α are now given by:

$$\cos\alpha_1 = \overline{a_1} \cdot \overline{R} = \sin\theta\cos(\phi - \phi'), \text{ and}$$

$$\cos\alpha_2 = \overline{a_2} \cdot \overline{R} = \sin\theta\sin(\phi - \phi'). \tag{5}$$

Substitution into (1) gives:

$$E_1 = \frac{\cos[\pi/2 \cdot \sin\theta\cos(\phi - \phi')]}{\sqrt{1-\sin^2\theta\cos^2(\phi - \phi')}}, \text{ and} \tag{6}$$

$$E_2 = \frac{\cos[\pi/2 \cdot \sin\theta\sin(\phi - \phi')]}{\sqrt{1-\sin^2\theta\sin^2(\phi - \phi)}}.$$

Equation (6) may also be obtained from (5) by letting $\phi' \to \phi' + 90°$.

We must now determine the components of E in the θ and ϕ directions. The procedure consists of finding the angle (or cosine of the angle) between the electric field vector at the far-field point P and the θ and ϕ directions at that point. The direction of the electric field at a point in space is given in principle by projecting the vectors $\overline{a_1}$ and $\overline{a_2}$ (coincident with the slot) onto the tangent plane at the point, rotating the vector 90 degrees (polarization property of a slot), and finding the angle between this vector and the θ and ϕ directions. This is most readily accomplished by finding the components of $\overline{a_1}$, $\overline{a_2}$ along the θ and ϕ directions (inasmuch as $\overline{a_\theta}$ and $\overline{a_\phi}$ are orthogonal vectors in the tangent plane), and working with these components.

The unit vectors in the θ and ϕ directions are:

$$\overline{a_\theta} = \overline{a_x}\cos\theta\cos\phi + \overline{a_y}\cos\theta\sin\phi - \sin\theta\,\overline{a_z}, \text{ and} \tag{7}$$

$$\overline{a_\phi} = -\overline{a_x}\sin\phi + \overline{a_y}\cos\phi. \tag{8}$$

Then, the components of a_1 and a_2 in the θ and ϕ directions are:

$$\overline{a_1} \cdot \overline{a_\phi} = -\sin(\phi - \phi'),$$

$$\overline{a_1} \cdot \overline{a_\theta} = \cos\theta\cos(\phi - \phi'),$$

$$\overline{a_2} \cdot \overline{a_\phi} = \cos(\phi - \phi'), \text{ and}$$

$$\overline{a_2} \cdot \overline{a_\theta} = \cos\theta\sin(\phi - \phi').$$

The resultant vectors in the tangent plane are written as:

$$\overline{S}_1 = -\overline{a_\phi}\sin(\phi - \phi') + \overline{a_\theta}\cos\theta\cos(\phi - \phi'), \text{ and}$$

$$\overline{S}_2 = \overline{a_\phi}\cos(\phi - \phi') + \overline{a_\theta}\cos\theta\sin(\phi - \phi').$$

A positive 90-degree rotation of each vector is required to account for slot polarization. This gives:

$$\overline{S}_1' = -\overline{a_\phi}\cos\theta\cos(\phi - \phi') - \overline{a_\theta}\sin(\phi - \phi'), \text{ and} \tag{9}$$

$$\overline{S}_2' = -\overline{a_\phi}\cos\theta\sin(\phi - \phi') + \overline{a_\theta}\cos(\phi - \phi'). \tag{10}$$

The cosine of the angle between $\overline{S_1}'$ and $\overline{a_\theta}$ is:

$$\cos\beta_1 = \frac{-\sin(\phi - \phi')}{\sqrt{\sin^2(\phi - \phi') + \cos^2\theta\cos^2(\phi - \phi')}}, \tag{11}$$

While the cosine of the angle between S_1, and a_ϕ becomes:

$$\cos\gamma_1 = \frac{-\cos\theta\cos(\phi - \phi')}{\sqrt{\sin^2(\phi - \phi') + \cos^2\theta\cos^2(\phi - \phi')}}. \tag{12}$$

Similarly for S_2' we have:

$$\cos\beta_2 = \frac{\cos(\phi - \phi')}{\sqrt{\cos^2(\phi - \phi') + \cos^2\theta\sin^2(\phi - \phi')}}, \text{ and} \tag{13}$$

$$\cos\gamma_2 = \frac{-\cos\phi\sin(\phi - \phi')}{\sqrt{\cos^2(\phi - \phi') + \cos^2\theta\sin^2(\phi - \phi')}}. \tag{14}$$

Using these results, the E_θ and $E\phi$ components of the far field are:

$$E_{\theta_1} = E_1\cos\beta_1,$$

$$E_{\theta_2} = E_2\cos\beta_2,$$

$$E_{\theta_1} = E_1\cos\gamma_1, \text{ and}$$

$$E_{\theta_2} = E_2\cos\gamma_2.$$

The total field is given by ($\pm i$ for phase quadrature between slots):

$$E_{\theta_1} = E_1\cos\beta_1 \pm iE_2\cos\beta_2, \text{ and} \tag{15}$$

$$E_{\theta_2} = E_1\cos\gamma_1 \pm iE_2\cos\gamma_2. \tag{16}$$

The magnitudes of E_θ and E_ϕ are the linearly polarized field patterns of the crossed-slot antenna in an infinite ground plane.

1.2.3 REPRESENTATION OF POLARIZATION STATE

The circularly polarized field from the crossed-slot element may be represented as the sum of two oppositely rotating, circularly polarized waves. From Jordan and Balmain[4] we have:

$$E_R = 1/2(E_\phi + iE_\theta), \text{ and} \tag{17}$$

$$E_L = 1/2(E_\phi - iE_\theta), \tag{18}$$

where E_R and E_L are right-hand and left-hand circularly polarized waves, respectively. The polarization factor is defined as:

$$Q = \frac{E_R}{E_L} = |Q|e^{i\xi}, \tag{19}$$

where $E_R = A_R e^{i\xi_R}$, $E_L = A_L e^{i\xi_L}$, so that $|Q| = A_R/A_L$ and $\xi = \xi_L - \xi_R$.

In terms of the quantities derived previously, the field components are written in general terms as:

$$E_\theta = E_{\theta r} \pm E_{\theta i}, \text{ and} \tag{20}$$

$$E_\phi = E_{\phi r} \pm E_{\phi i}, \tag{21}$$

where r and i represent real and imaginary, respectively. The choice of plus or minus sign depends on the choice of right or left-hand circular polarization for the element.

---

4 Jordan, E.C., and K.G. Balmain. Electromagnetic Waves and Radiating Systems, 2nd ed., Prentice-Hall, 1968, pp. 459-462.

For this investigation, the CP sense is arbitrary, so we choose +i for right-hand circular. Substituting (20) and (21) into (17) and (18) and recombining terms gives:

$$E_R = 1/2[(E_{\phi r} - E_{\theta i}) + i(E_{\phi i} + E_{\theta r})], \text{ and}$$

$$E_L = 1/2[(E_{\phi r} + E_{\theta i}) + i(E_{\phi i} - E_{\theta r})].$$

Then, in the notation of Jordan and Balmain:

$$A_R = 1/2 \sqrt{(E_{\phi r} - E_{\theta i})^2 + (E_{\phi i} + E_{\theta r})^2} \ , \tag{22}$$

$$A_L = 1/2 \sqrt{(E_{\phi r} + E_{\theta i})^2 + (E_{\phi i} - E_{\theta r})^2} \ , \tag{23}$$

$$\xi_R = \tan^{-1} \left[\frac{E_{\phi i} + E_{\theta r}}{E_{\phi r} - E_{\theta i}} \right] , \text{ and} \tag{24}$$

$$\xi_L = \tan^{-1} \left[\frac{E_{\phi i} + E_{\theta r}}{E_{\phi r} - E_{\theta i}} \right] . \tag{25}$$

Q is then given as:

$$Q = \frac{A_L e^{i\xi_L}}{A_R e^{i\xi_R}} = \left| \frac{A_L}{A_R} \right| e^{i(\xi_L - \xi_R)}$$

with values of A and ξ given by equations (22) through (25). The axial ratio is:

$$AR = \left| \frac{1 + |Q|}{1 - |Q|} \right| , \tag{26}$$

with the tilt angle:

$$\psi = 1/2(\xi_R - \xi_L) + m\pi. \tag{27}$$

The axial ratio is defined to give a value AR > 1, while ψ is measured from the local vertical.

1.2.4 RESULTS

Cross-slot polarization computations were made, with polarization state presented as a function of elevation angle for several azimuth (ϕ) plane cuts.

The vertical polarization component is nearly constant as a function of θ, while the horizontal component varies approximately as the cosine. For θ = 90 degrees, the horizontal (E_ϕ) polarization component vanishes along the infinite ground plane, leaving only vertical linear polarization. This behavior is shown in Figure 2, which is fairly typical of all ϕ-plane cuts. E_θ and E_ϕ field amplitudes obviously diverge greatly for large values of θ, giving rise to large axial ratios.

Axial ratio data are summarized in Figure 3 as a function of elevation angle. The curve for ϕ = 45 degrees corresponds to the crossed-dipole data found in the Microwave Engineer's Handbook[5]. Note, however, that the axial ratio in ϕ planes containing the slot axes are worse than the handbook values by as much as 2 dB. For any fixed value of θ, the axial ratio varies between the limits indicated in the figure.

---

5 Saad, T.S., ed., Microwave Engineers Handbook, Vol. 2. Artech House, Inc., 1971, p. 50.

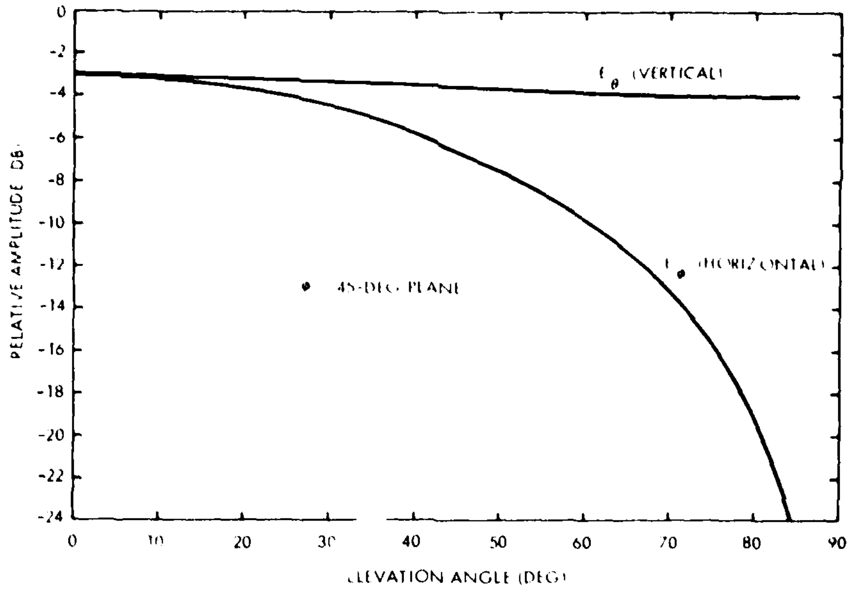

Figure 2. Relative Amplitude of E_θ and E_ϕ as a Function of Elevation Angle

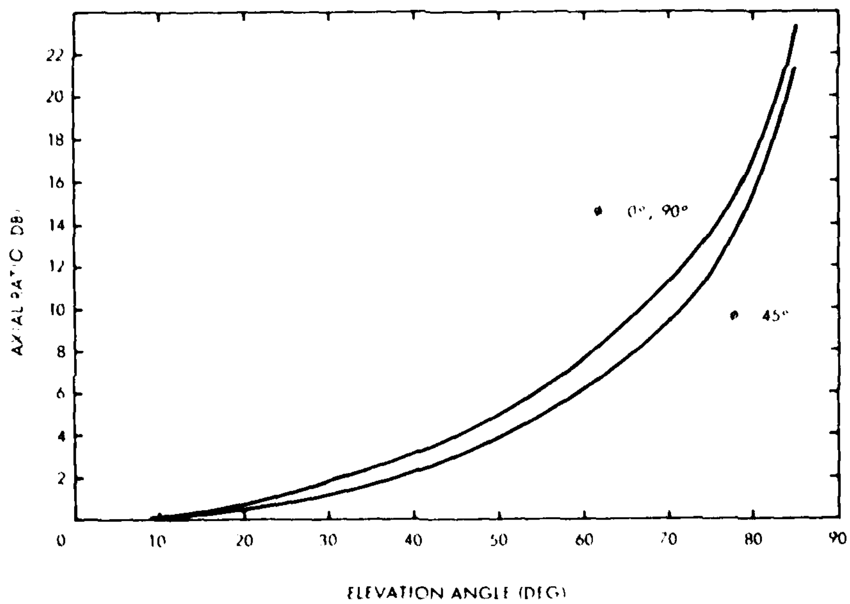

Figure 3. Axial Ratio as a Function of Elevation Angle

The V/H ratio is always positive, indicating that vertical polarization is dominant throughout the hemisphere. In fact, the tilt angle (and thus the major axis of the polarization ellipse) ranges between ± 5 degrees about local vertical as θ and ϕ are varied. Because of this, the axial ratio and the V/H ratio are very nearly equal everywhere, and are exactly equal for $\phi = 45$ degrees, where $\psi = 0$ degree. This result also indicates that the dome polarization is now independent of azimuth angle. The feed array polarization ellipse is always oriented with the major axis essentially vertical for all values of ϕ, even though the axial ratio may become very large for values of θ approaching 90 degrees. A review of the data shows that, for all values of ϕ, the feed array polarization is essentially circular from zenith to $\theta < 60$ degrees, becoming vertical for $\theta > 70$ to 90 degrees (the feed array groundplane).

For $\theta = 0$ degree and any value of ϕ, the tilt angle ψ is not defined. At $\theta = 0$ degree, the computer program provided values equal to $\phi/2$ which are not significant.

SECTION II
FEED ARRAY HARDWARE INVESTIGATION

2.1 ELEMENT TRADEOFF AND SELECTION

Feed array elements capable of providing polarization diversity over octave-plus bandwidths offer a significant design challenge. Several existing elements are potential candidates, and performance characteristics must be examined closely for feed array geometries. The maintenance of prescribed arbitrary polarization states will require a precise control of the element polarization in the array environment. Element polarization will be determined by impressed excitations and element interactions in the feed array. The high element densities in the lower portion of the band produce very tight element coupling, which must be controlled to provide optimum performance. Analyses[6] and tests of tightly coupled elements have previously been conducted at Raytheon ESD for linear arrays.

At this time, it appears that an element capable of generating dual, orthogonal, linear polarizations will provide best performance. Existing elements with a high degree of physical and electrical symmetry appear to offer the best chance of compensating for mutual coupling effects with scan. One such dual-polarized element which has been studied at Raytheon consists of two orthogonal, stripline-fed, tapered-notch elements.[7] Another potential candidate recently studied is a broadband, crossed-slot element; i.e., printed-stripline slot with balanced, symmetrical feed lines.

---

6 Ludwig, A.C. "Mutual Coupling, Gain and Directivity of an Array of Two Identical Antenns." IEEE Trans AP-24, Nov. 1976, p. 837.

7 Lewis, L.R., M. Fassett, and J. Hunt. "A Broadband Stripline Array Element." 1974 IEEE/AP-S International Symposium Digest, June 10-12, 1974, Atlanta, GA, pp 335-337.

A third candidate is the "quad-ridge" waveguide element[8] using either circular or square waveguide. Higher-order modes may limit the bandwidth with this element to less than an octave; in addition, it will be more expensive to fabricate. On the plus side, the quad-ridge element should limit mutual coupling and prevent some types of surface wave modes which occur in other elements, such as the printed notch.

An investigation of square quad-ridge waveguide elements is currently being conducted in a Raytheon internal development program. Orthogonal, printed-notch elements were selected for experimental investigation on this program. The bases for selection are: (1) prior work which indicates that wide-scan, octave-bandwidth performance for dual polarizations should be possible; and (2) the relatively inexpensive fabrication of large arrays which would result.

Two versions of orthogonal printed-notch elements were fabricated and tested. The results are described below.

2.2 CROSSED-NOTCH ARRAY

The stripline crossed-notch element was selected for hardware evaluation as the most likely to meet the requirements for the 3-D Dome Feed Array. This choice was based on a knowledge of the scan and wide-band capabilities of linearly polarized notch arrays, and an indication from previous work[9] of success in integrating two notch elements orthogonal to one another to achieve the required polarization agility.

---

8 Chen, C.C. "Quadruple Ridge-Loaded Circular Waveguide Phased Arrays," IEEE Trans, Vol AP-22, May 1974, pp 481-483.

9 Lawrence, R.L., and J. Pozgay. "Broadband Antenna Study," Report AF CRL-TR-75-01 78. Raytheon Co., Bedford, MA, March 1975.
Monser, G.J., al. "Closely Spaced Orthogonal Dipole Array," U.S. Patent 3,836,976, 17 Sep. 1974.

Two orientation configurations of the orthogonal notches were pursued in parallel within the developmental effort on this project. These were the noncoincident-crossed-notch (NCN) geometry, and the coincident-crossed-notch (CCN) geometry. The two configurations are shown in Figure 4.

Fifteen-element linear arrays in both the NCN and CCN geometries were fabricated and tested. Both arrays were designed to have intra-element spacing of 0.5 λ at 8.5 GHz. Both element configurations developed here can operate in a two-dimensional array geometry.

The CCN array has the advantage of coincident phase centers, resulting from physical centering of the orthogonal elements in the same place. For a linear array, this geometry is symmetrical, and lends itself to symmetrical patterns. The NCN array has a possibility of greater electrical independence between the vertically polarized (VP) and horizontally polarized (HP) elements, resulting from the greater physical separation between the two. This could result in improved performance for the NCN array.

Each array has about an octave bandwidth over which its performance is satisfactory -- 4.5 to 9.25 GHz for the 15-element NCN array, and 3.75 to 7.5 GHz for the 15-element CCN array. The estimated directivity for the CCN array element is shown in Figure 5.

2.3 LINEAR NOTCH ARRAY

The first step taken in the hardware generation was the fabrication of a 15-element, horizontally polarized, linear-notch array. Figure 6 is a photograph of the array. The element design followed the guidelines of reference 1. Figure 7 details the geometry of the array. A 50-ohm stripline feed is tapered to 67 ohms at the notch feed point. The printed-circuit substrate is Duroid 5880, which has a dielectric constant of 2.22. The stripline dielectric thickness is 0.120 inch.

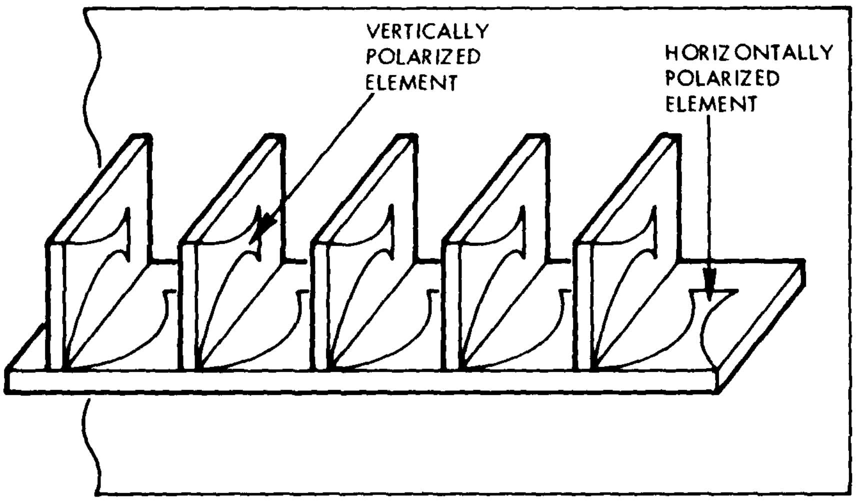

(A) NON-COINCIDENT, CROSSED-NOTCH GEOMETRY

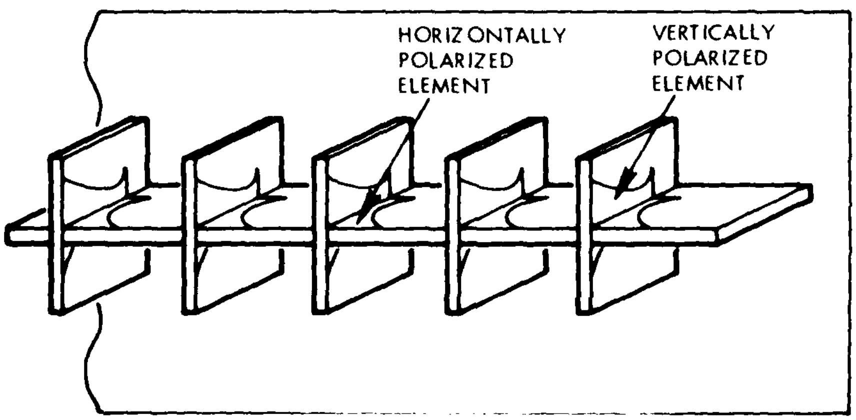

(B) COINCIDENT, CROSSED-NOTCH GEOMETRY

Figure 4. Crossed-Notch Geometry

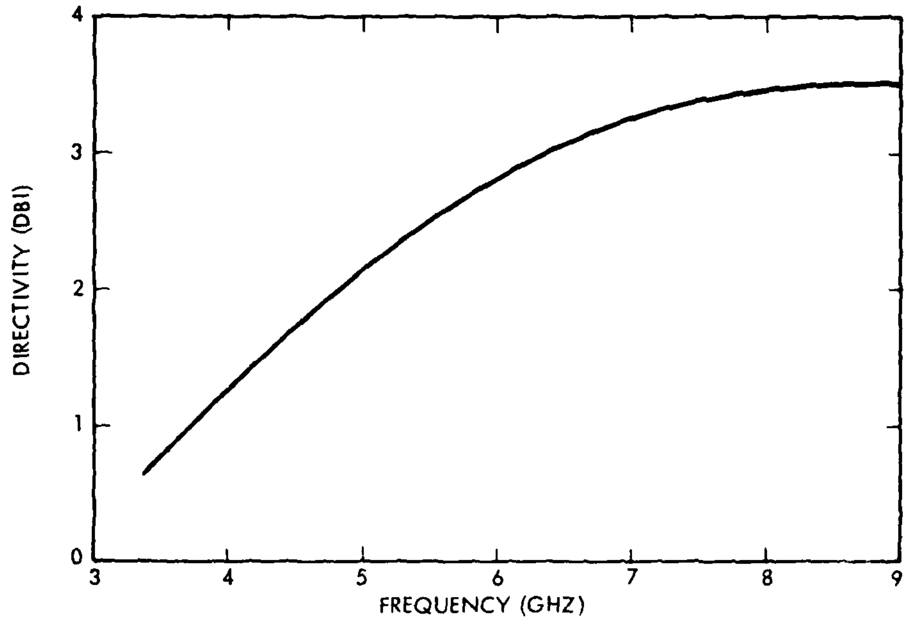

Figure 5. Estimated Directivity of CCN Array Element

14651

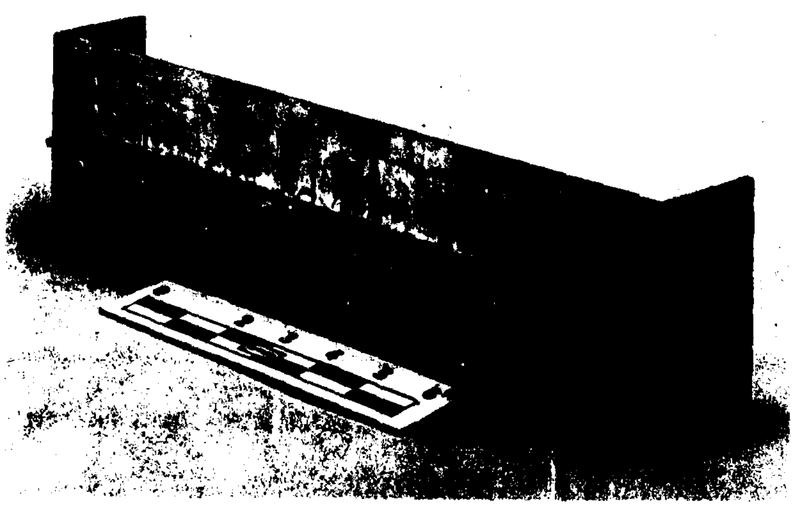

Figure 6. Photograph of Horizontally Polarized, Linear Notch Array

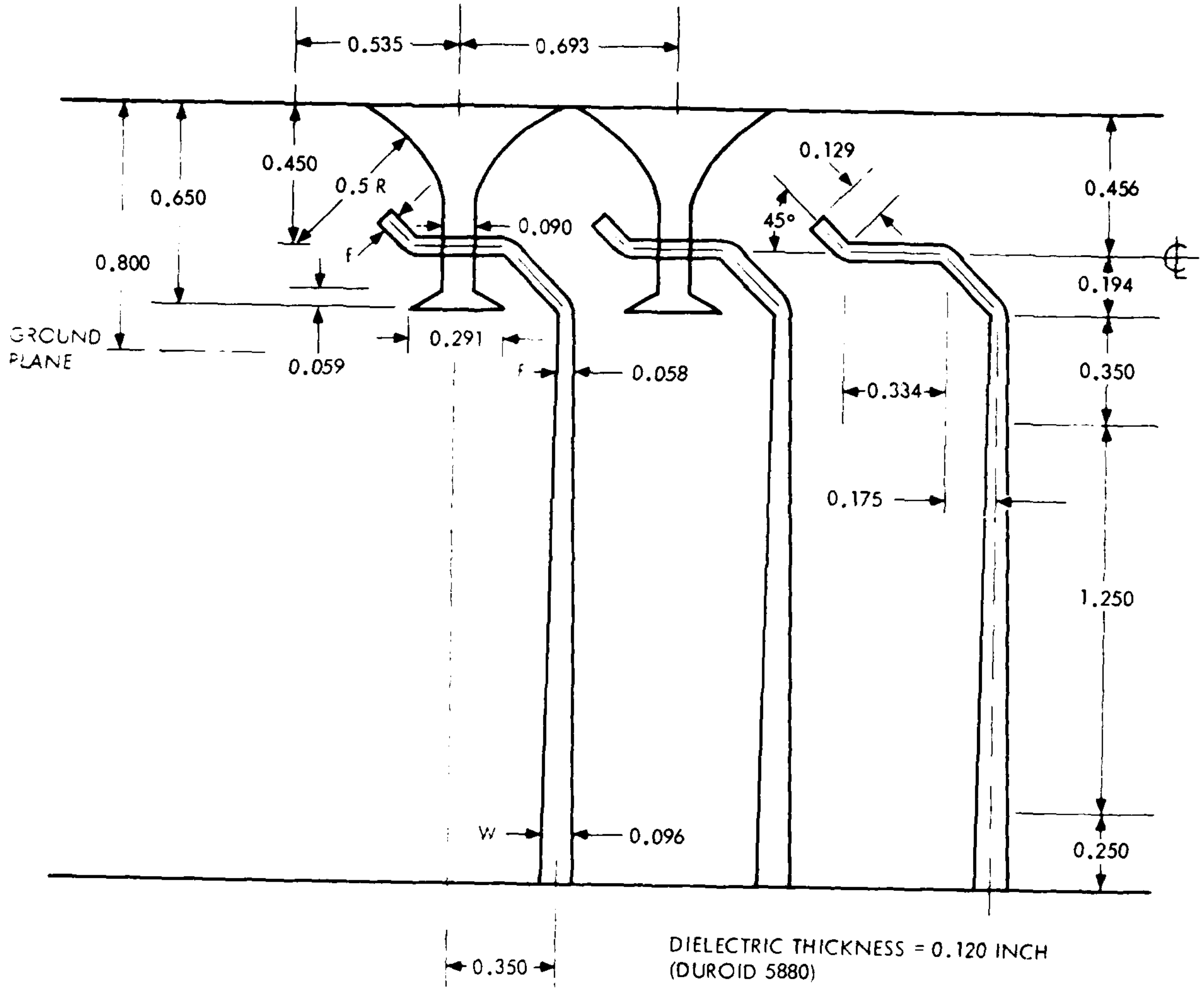

Figure 7. Notch Array Element Geometry

The array performance was optimized over the 3.0 to 9.25-GHz frequency band. All data included here were taken on the center array element. Representative azimuth imbedded element patterns are shown in Figure 8. The azimuth 3-dB beamwidth is equal to or greater than 110 degrees. The azimuth patterns do have some "lumps," and it should be noted that the 3-dB beamwidth point was selected at the angle at which the power is down 3 dB from broadside, and continues to be down 3 dB for all larger angles.

Figures 9 and 10 shown the passive VSWR and active VSWR for 0, 40, and 60-degree scan angles as plotted on an automatic network analyzer. Passive VSWR is less than 2.6, and active VSWR is less than 5 out to a 60-degree scan.

The test array was fabricated with an adjustable ground-plane spacing which was optimized at a distance of 0.8 inch from the antenna face.

The elevation patterns and measured gain of this array are of interest in establishing the estimated gain of the dual-polarized array. In its present configuration, it does not truly reflect the two-dimensional array geometry. The elevation patterns shown in Figure 11 are quite regular, as would be expected from vertical trough stripline elements. Measured gain of the horizontally polarized linear array is shown in Figure 12.

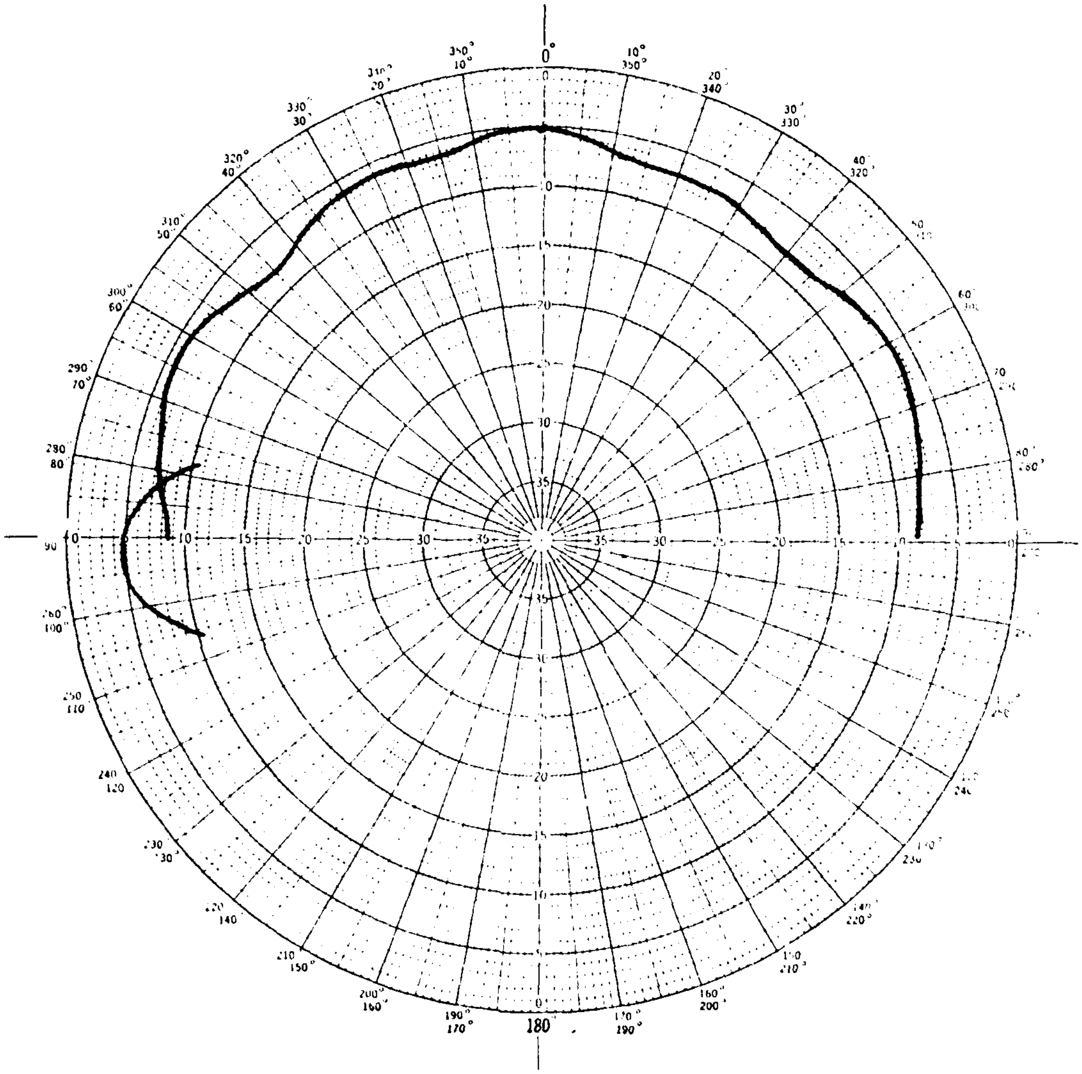

3 GHZ

Figure 8. Representative Embedded-Element Azimuth Pattern (Sheet 1 of 4)

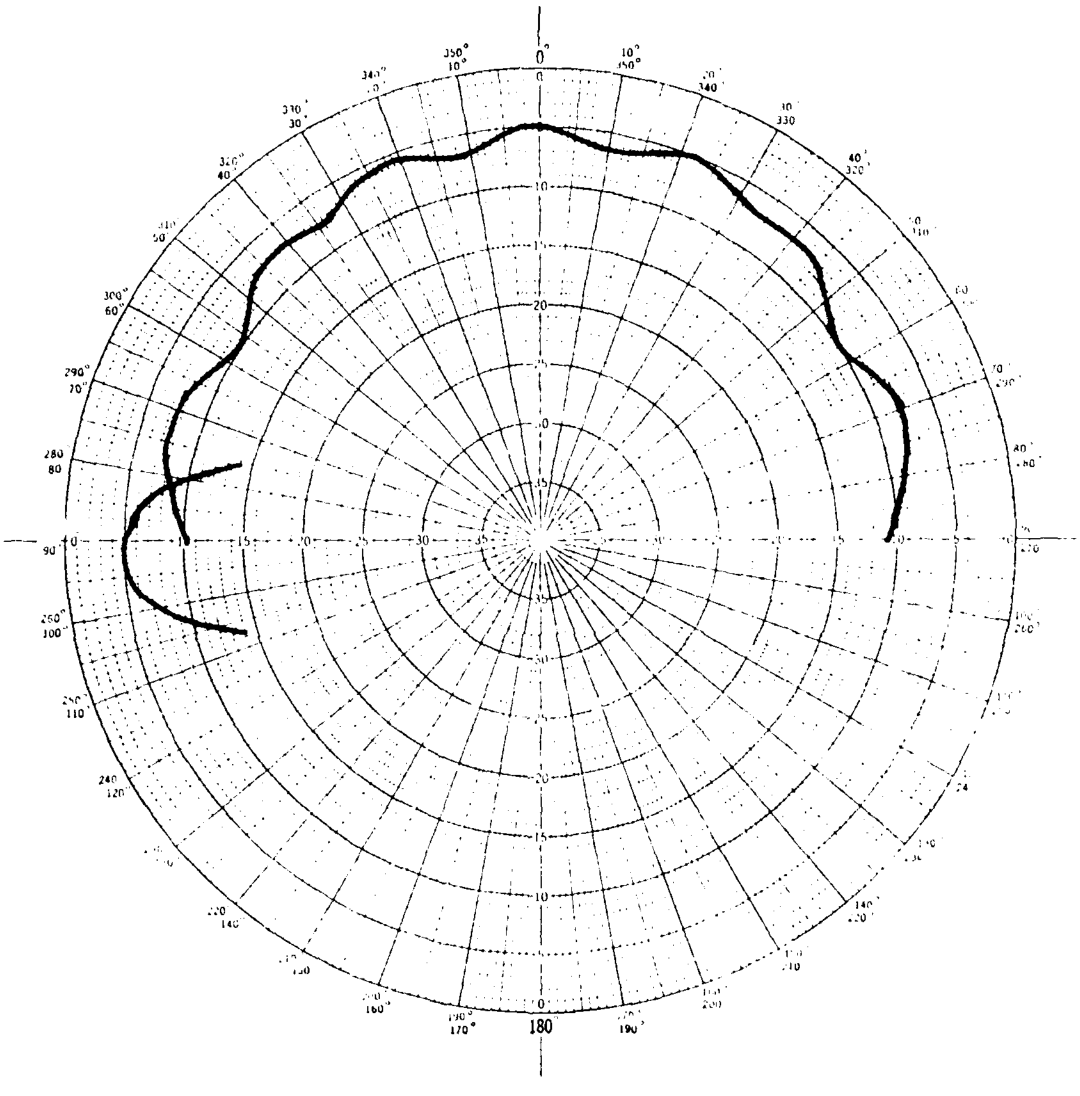

5 GHZ

Figure 8. Representative Embedded-Element Azimuth Pattern (Sheet 2 of 4)

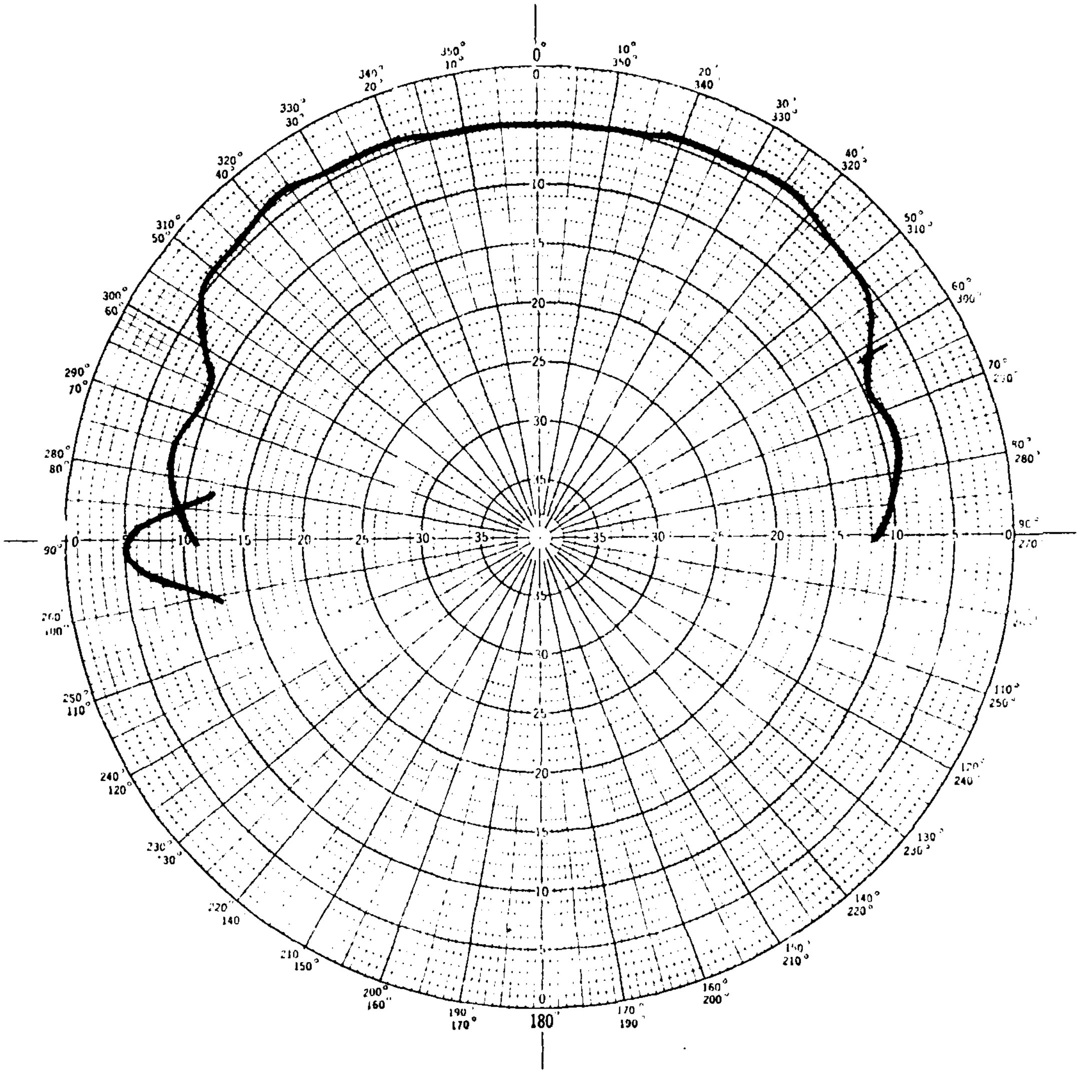

7 GHZ

Figure 8. Representative Embedded-Element Azimuth Pattern (Sheet 3 of 4)

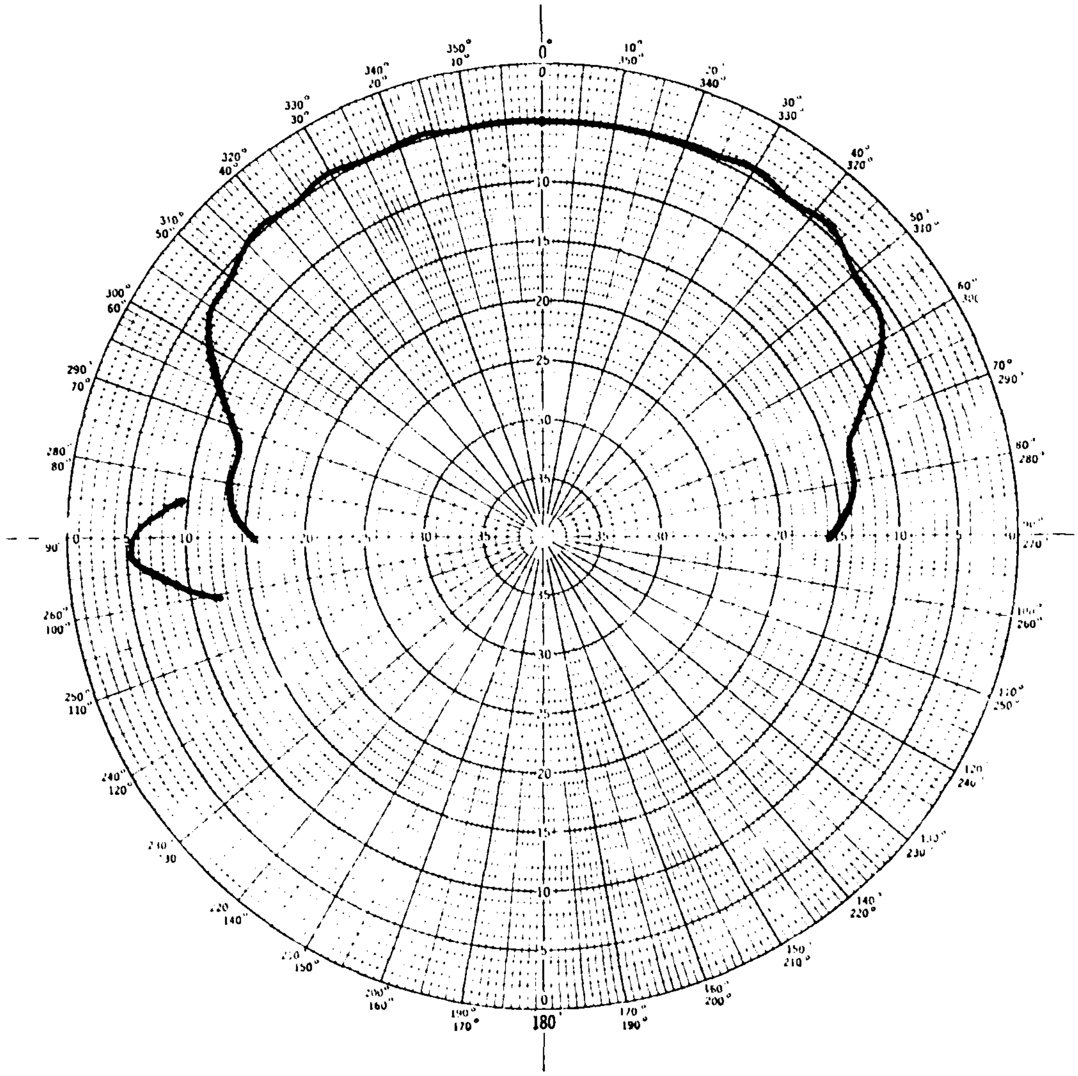

9 GHZ

Figure 8. Representative Embedded-Element
Azimuth Pattern (Sheet 4 of 4)

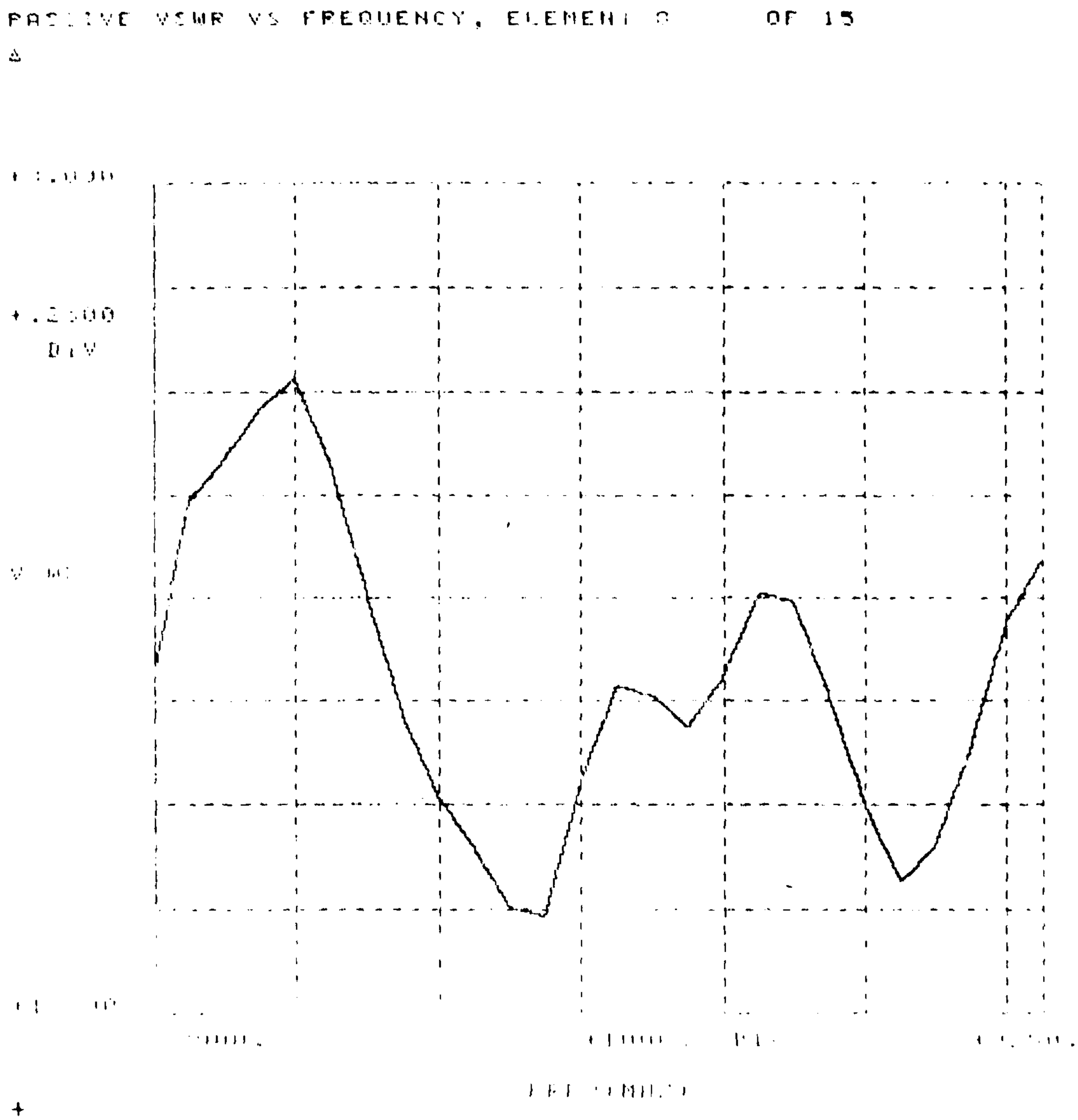

Figure 9. Passive VSWR as a Function of Frequency

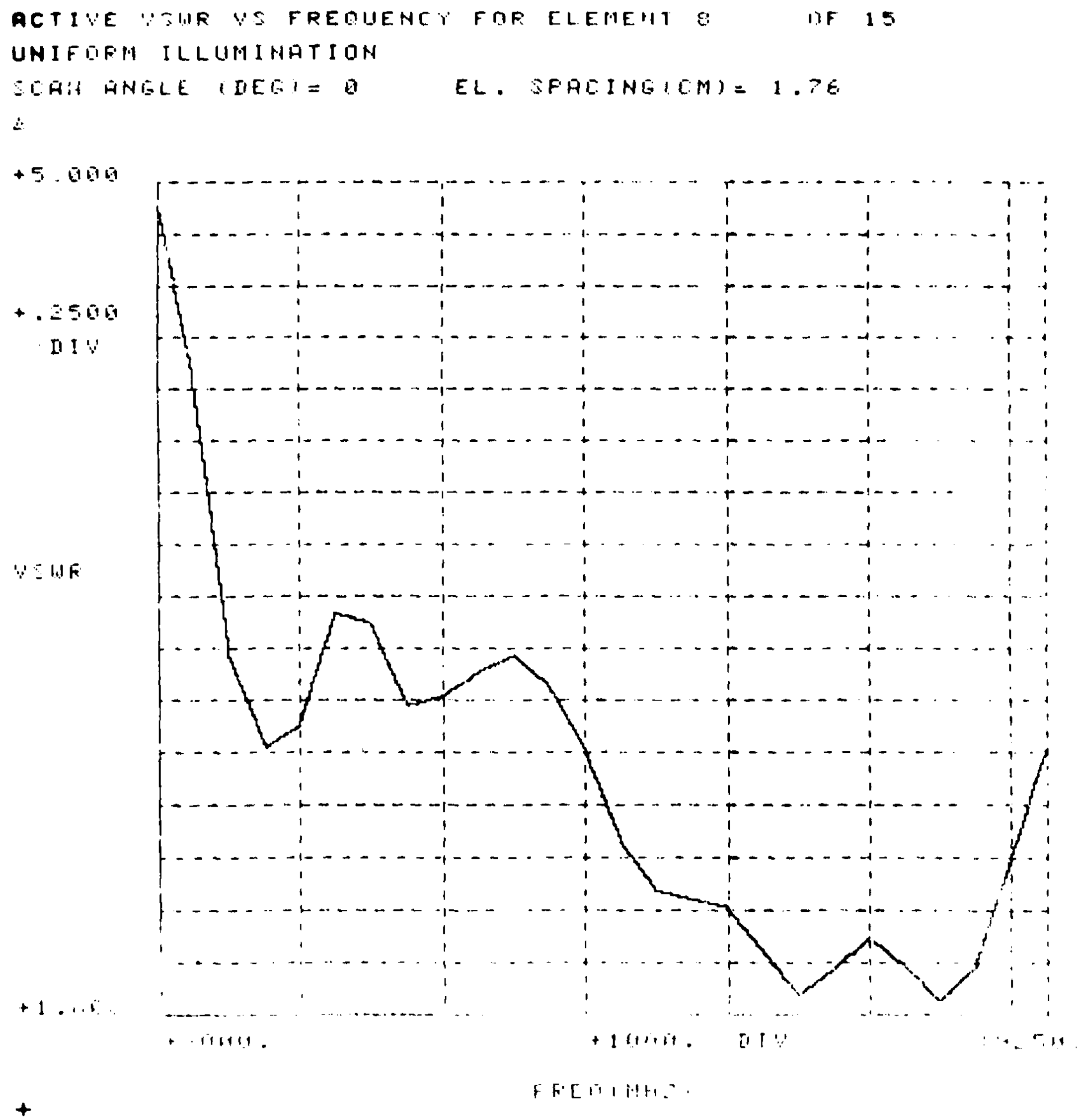

Figure 10. Active VSWR as a Function of Frequency
(Sheet 1 of 3)

ACTIVE VSWR VS FREQUENCY FOR ELEMENT 8 OF 15
UNIFORM ILLUMINATION
SCAN ANGLE (DEG)= 40 EL. SPACING(CM)= 1.76

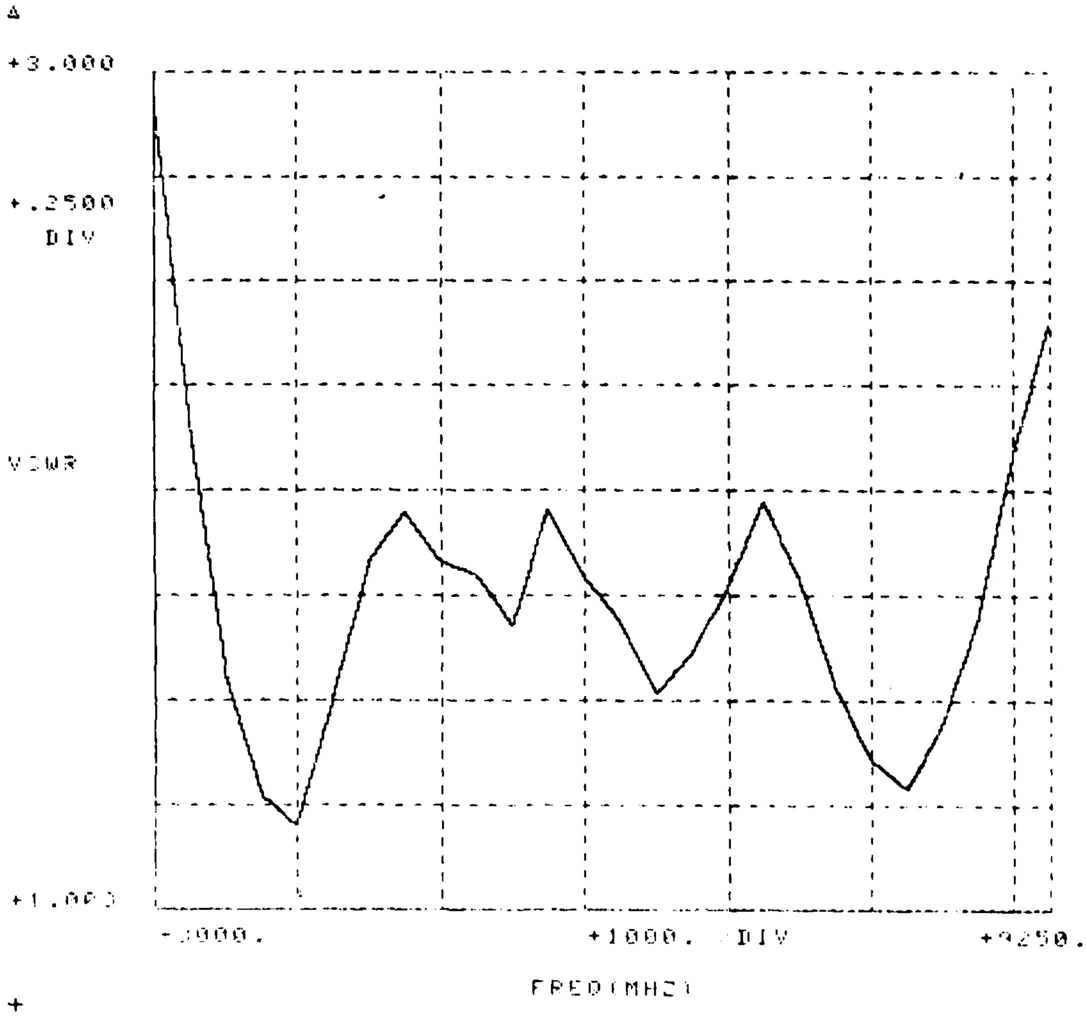

Figure 10. Active VSWR as a Function of Frequency
(Sheet 2 of 3)

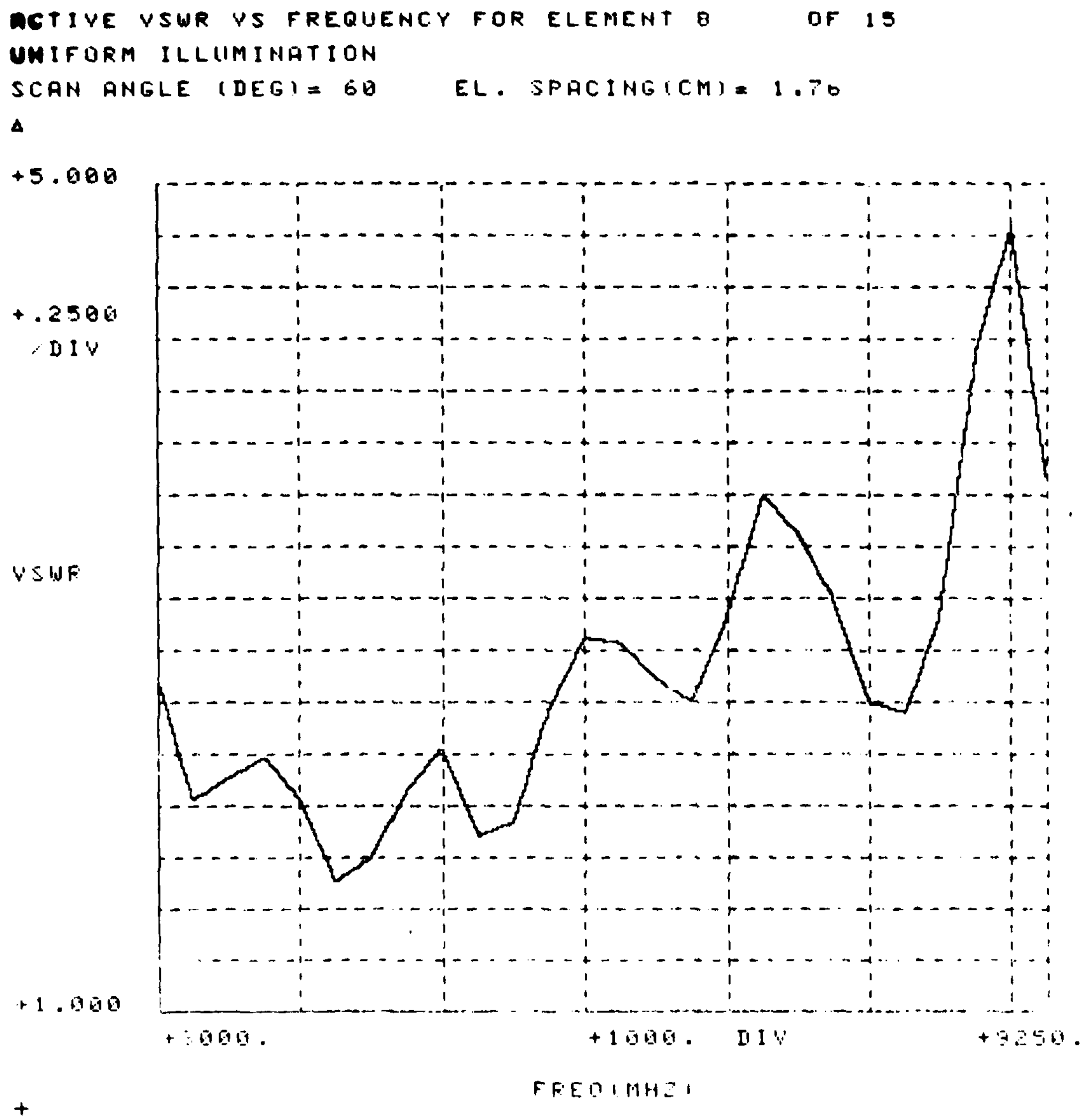

Figure 10. Active VSWR as a Function of Frequency
(Sheet 3 of 3)

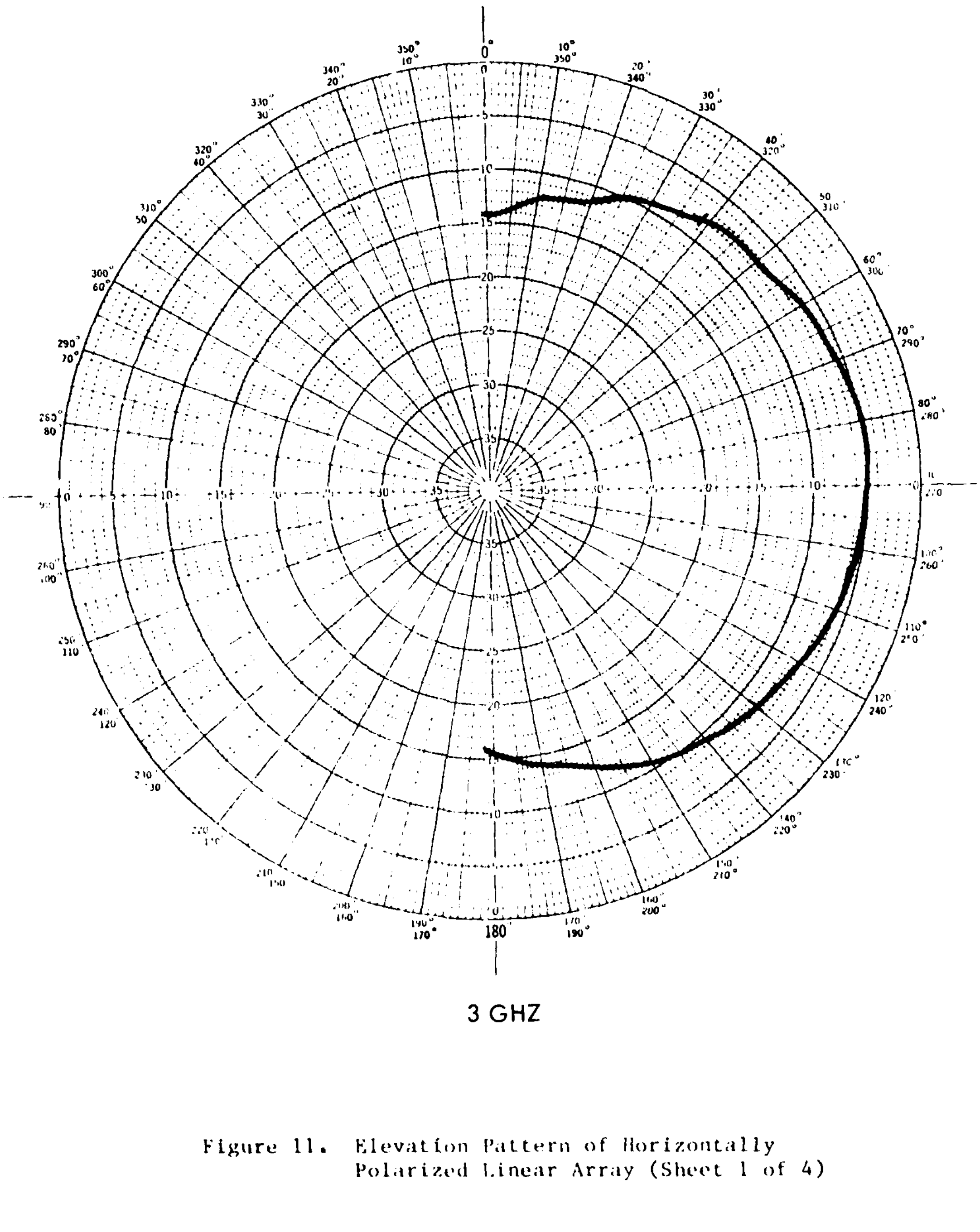

3 GHZ

Figure 11. Elevation Pattern of Horizontally Polarized Linear Array (Sheet 1 of 4)

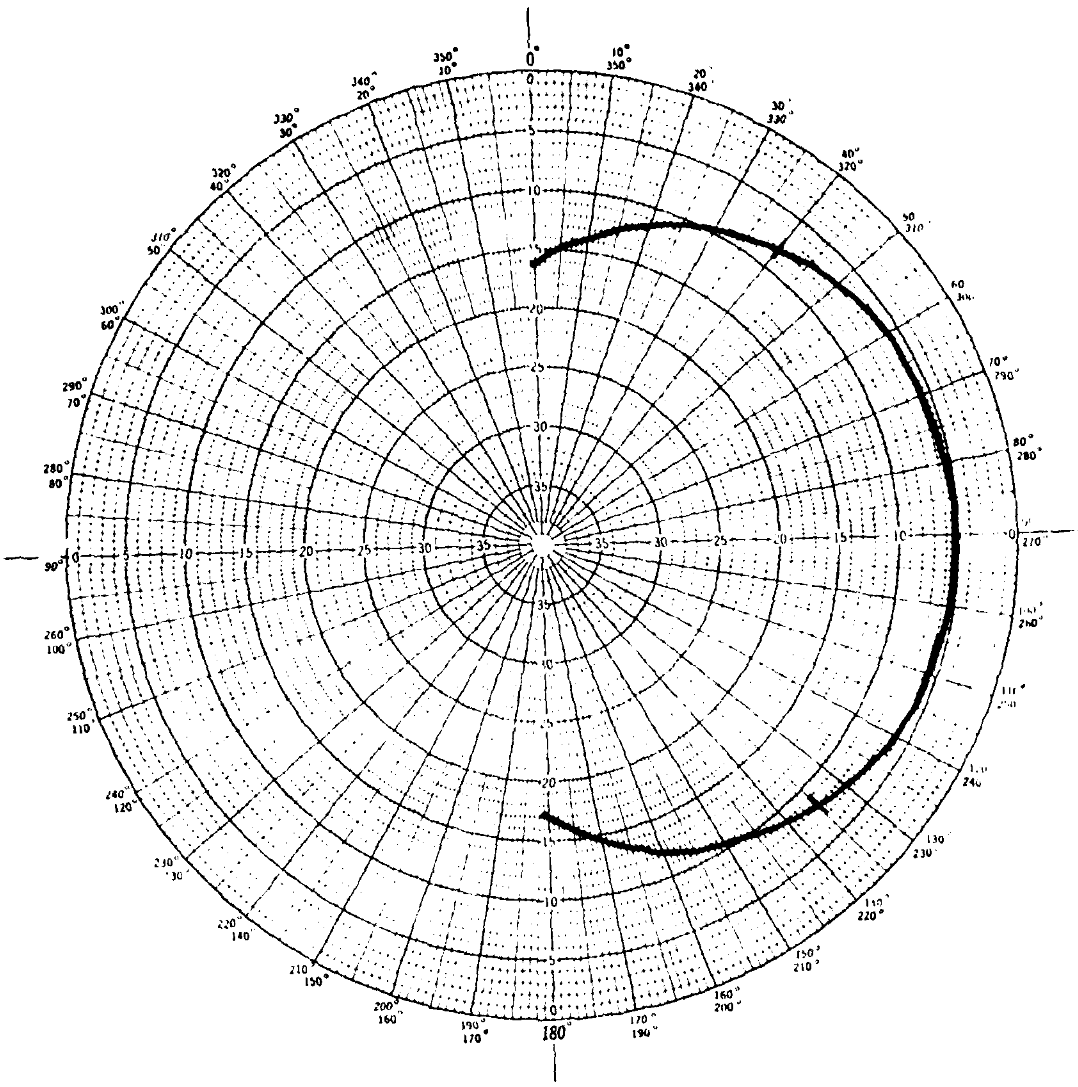

Figure 11. Elevation Pattern of Horizontally
Polarized Linear Array (Sheet 2 of 4)

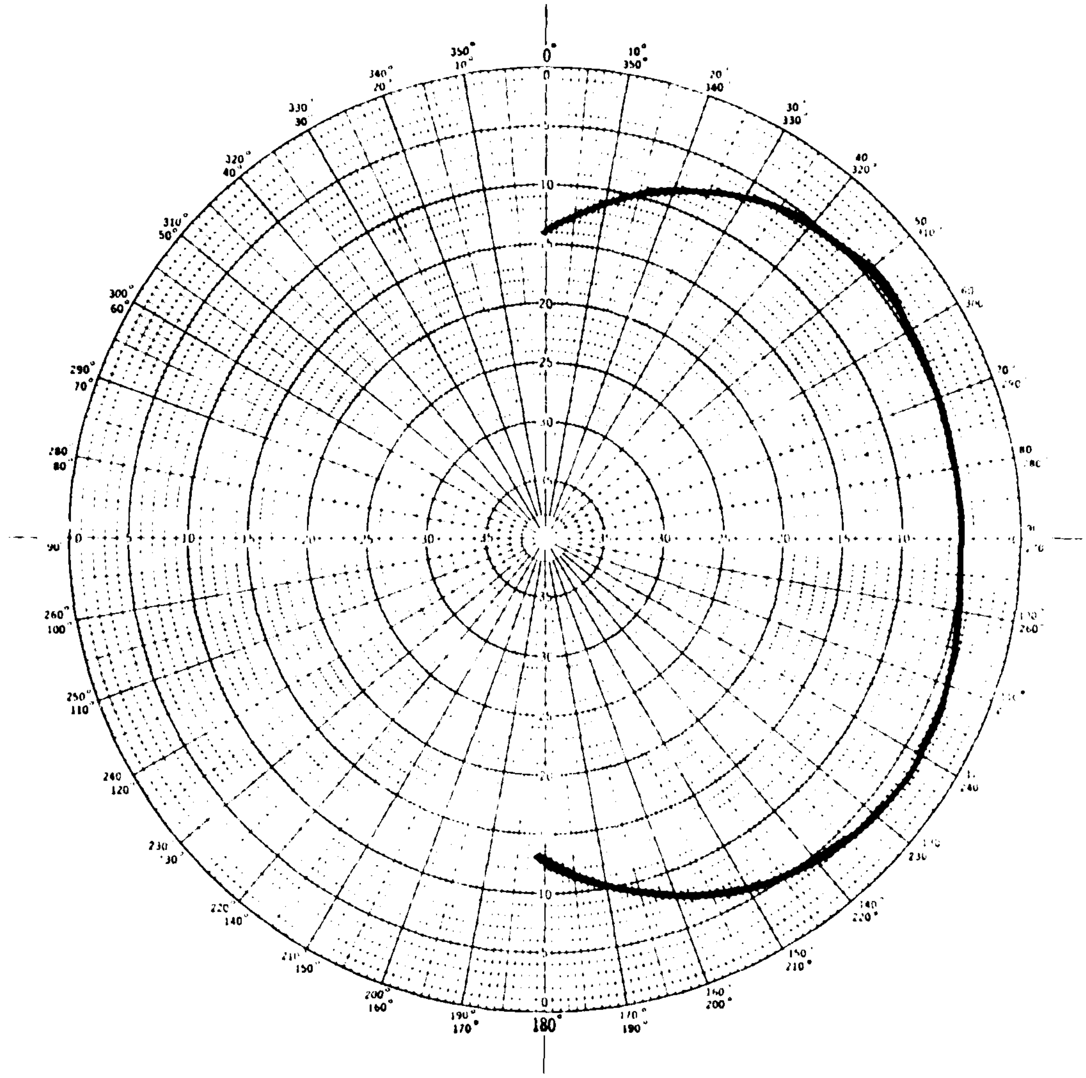

Figure 11. Elevation Pattern of Horizontally Polarized Linear Array (Sheet 3 of 4)

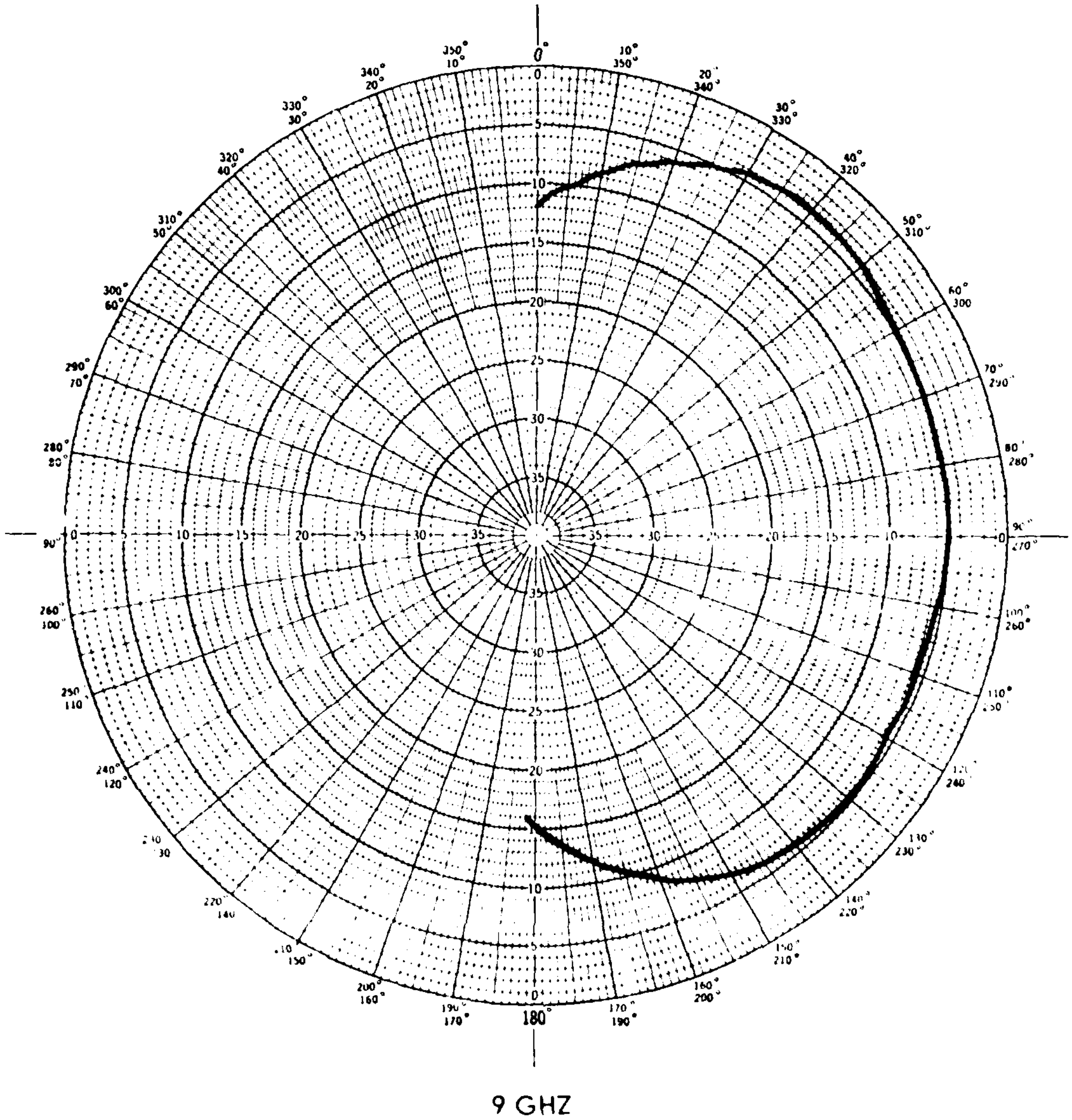

Figure 11. Elevation Pattern of Horizontally Polarized Linear Array (Sheet 4 of 4)

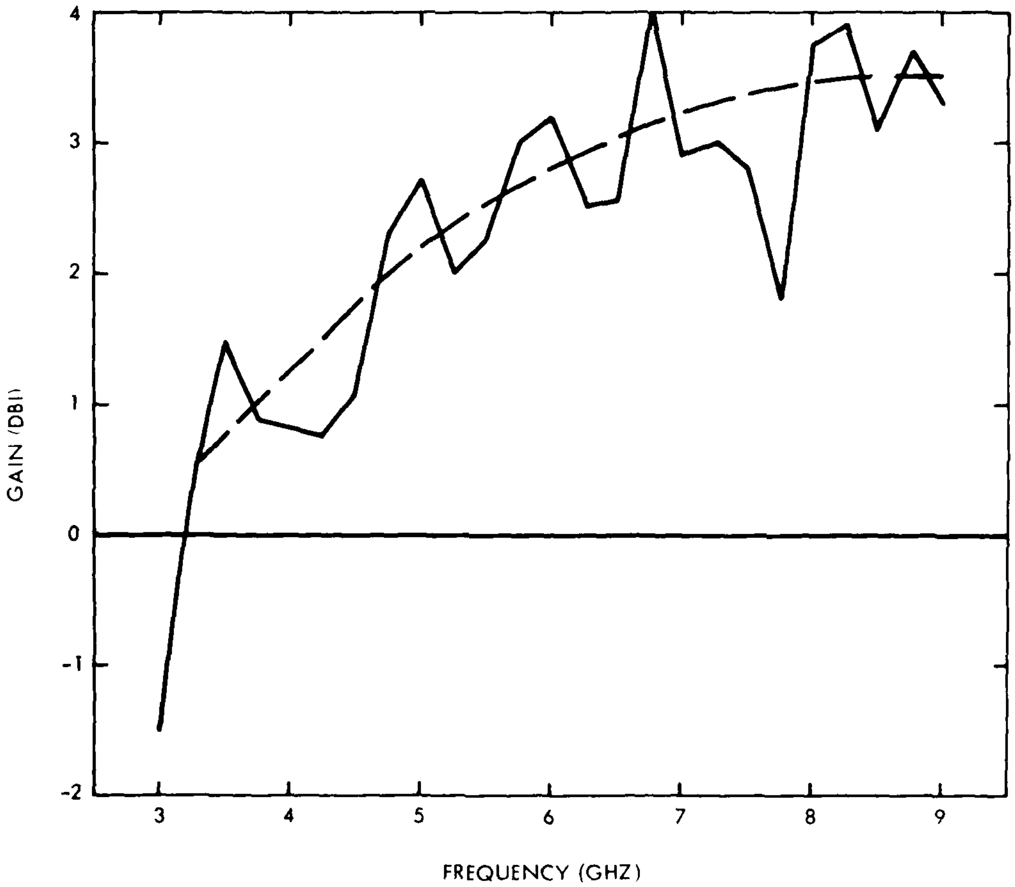

Figure 12. Measured Gain of Horizontally Polarized Linear Array

2.4 NONCOINCIDENT-CROSSED-NOTCH (NCN) ARRAY

Vertical elements were next placed between the horizontal elements to achieve the NCN configuration. Figure 13 is a picture of the completed array. The vertically polarized (VP) element design was identical to that of the horizontally polarized (HP) element design (Figure 7), which is a desirable feature for extension to a two-dimensional array.

Embedded element patterns and gain and impedance measurements were taken every 0.25 GHz from 3.0 to 9.25 GHz. These data suggest that the array performance is good in the 4.5 to 9.25-GHz frequency band over the scan volumes cited below.

14571

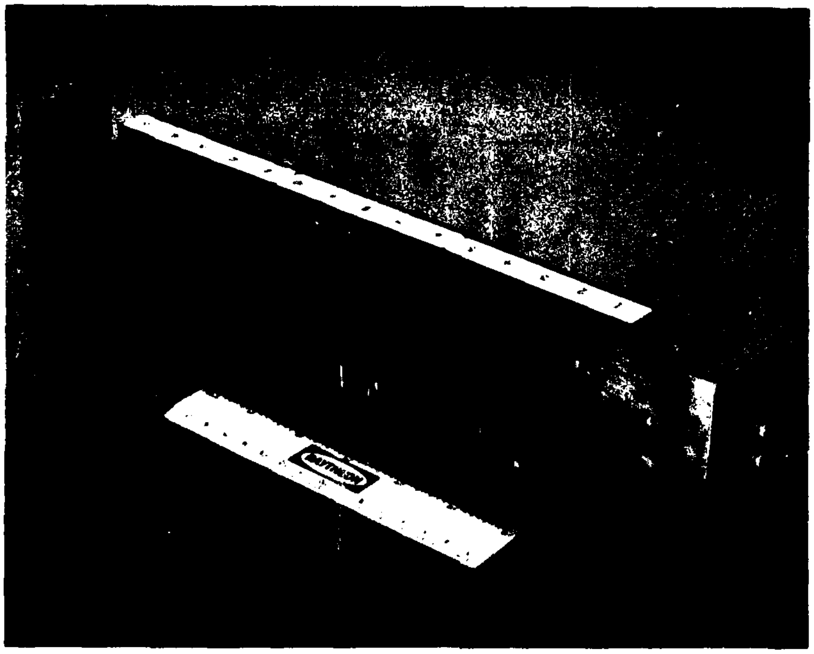

Figure 13. Photograph of Noncoincident-Crossed-Notch (NCN) Array

Figures 14 and 15 show plots of active VSWR at 0, 40, and 60-degree scan on the center VP and HP elements as measured on the automatic network analyzer. Over the 4.5 to 9.25-GHz band, passive VSWR is under 2.75:1 for both polarizations and all frequencies, and active VSWR on the VP element is under 3.7:1 out to 40 degrees and under 5.25:1 out to 60 degrees. The active match on the HP element is under 3.35:1 out to 60 degrees.

Selected embedded element patterns over the 4.5 to 9.0-GHz band are shown in Figures 16 and 17, respectively, for the center HP and VP elements.

Pattern measurements were made to test the polarization isolation of the VP element to HP incident radiation, and vice versa. Figures 18 and 19 give some representative measurements. The VP isolation of the HP element (Figure 18) is 20 dB minimum broadside, and degrades at the low frequencies. Isolation is better at the higher frequencies. HP isolation of the VP element (Figure 19) is 23 dB minimum broadside, and again degrades at the lower frequencies. Isolation improves at the higher frequencies for the VP element, also. This poor isolation at the low frequencies stems in part from the asymmetry of the NCN array.

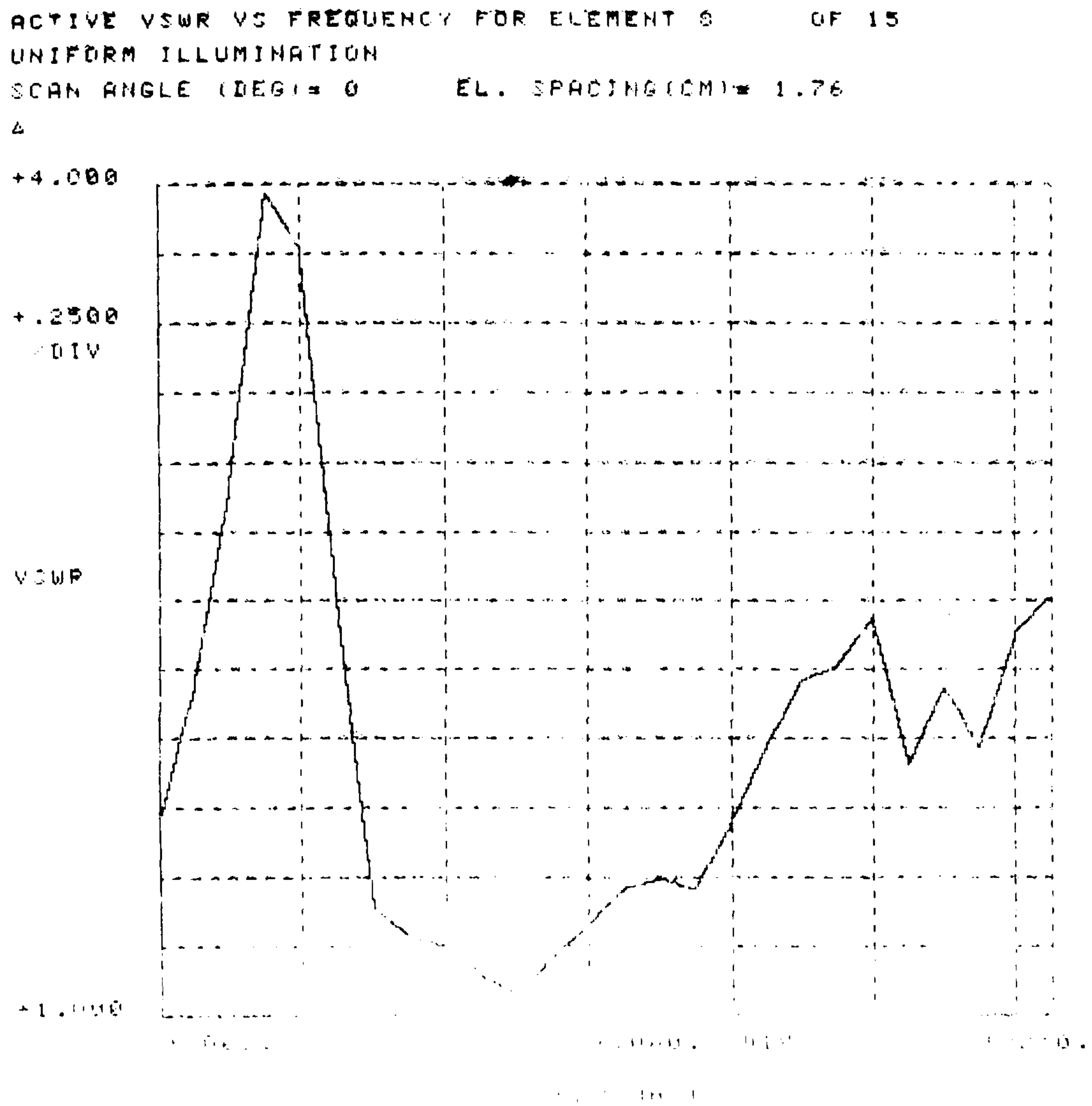

Figure 14. Active VSWR of Vertically Polarized NCN Array Element (Sheet 1 of 3)

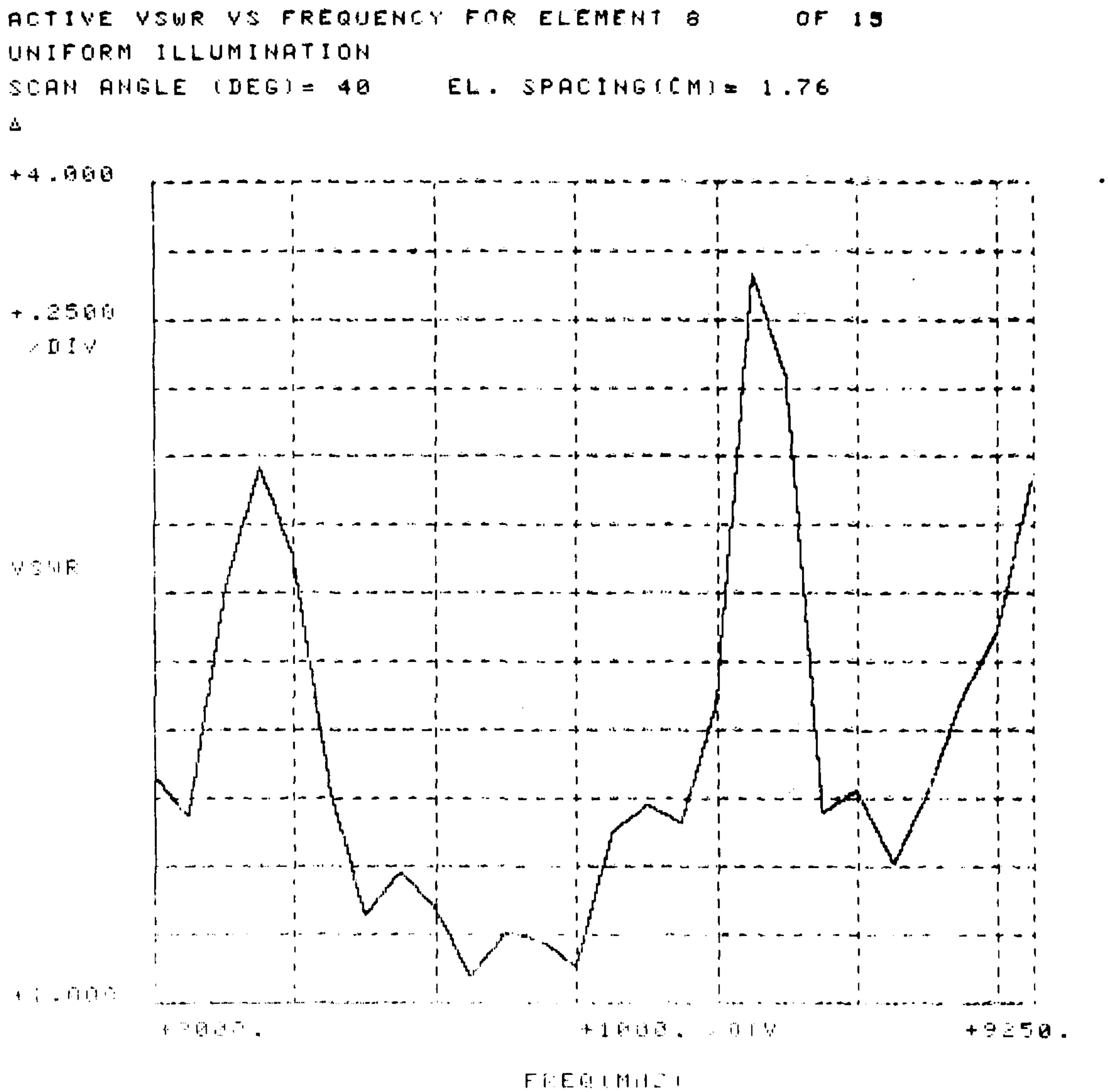

Figure 14. Active VSWR of Vertically Polarized NCN Array Element (Sheet 2 of 3)

ACTIVE VSWR VS FREQUENCY FOR ELEMENT 6 OF 15
UNIFORM ILLUMINATION
SCAN ANGLE (DEG)= 60 EL. SPACING(CM)= 1.76

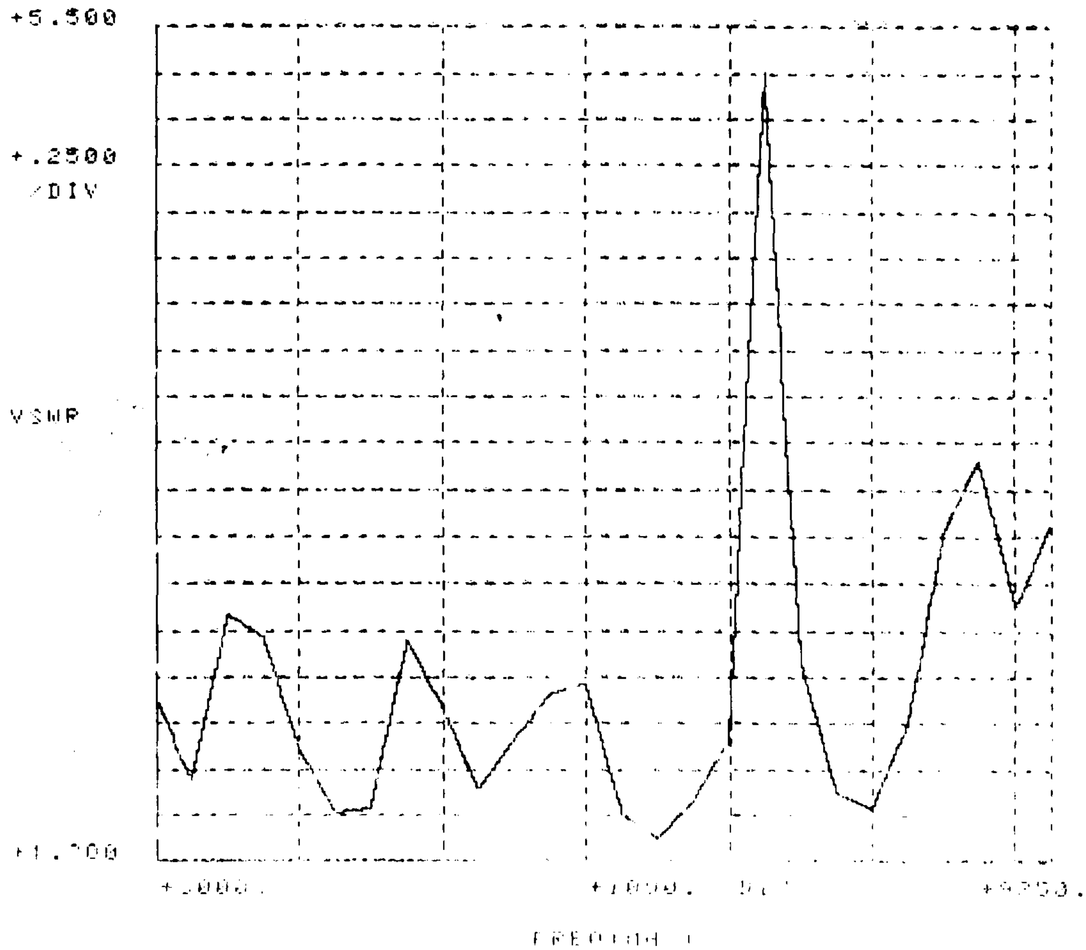

Figure 14. Active VSWR of Vertically Polarized NCN Array Element (Sheet 3 of 3)

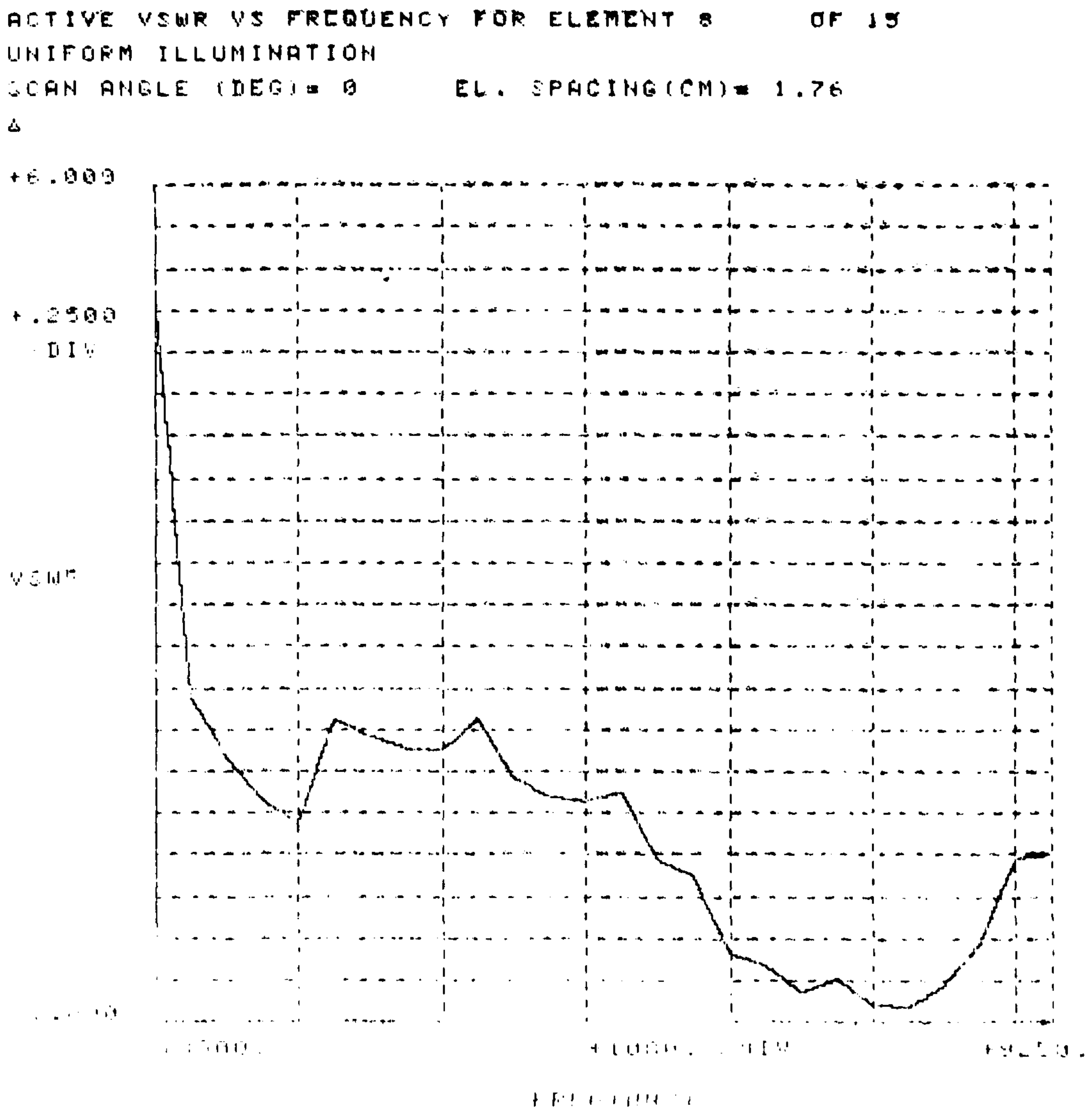

Figure 15. Active VSWR of Horizontally Polarized NCN Array Element (Sheet 1 of 3)

ACTIVE VSWR vs FREQUENCY FOR ELEMENT 8 OF 15
UNIFORM ILLUMINATION
SCAN ANGLE (DEG)= 40 EL. SPACING(CM)= 1.76

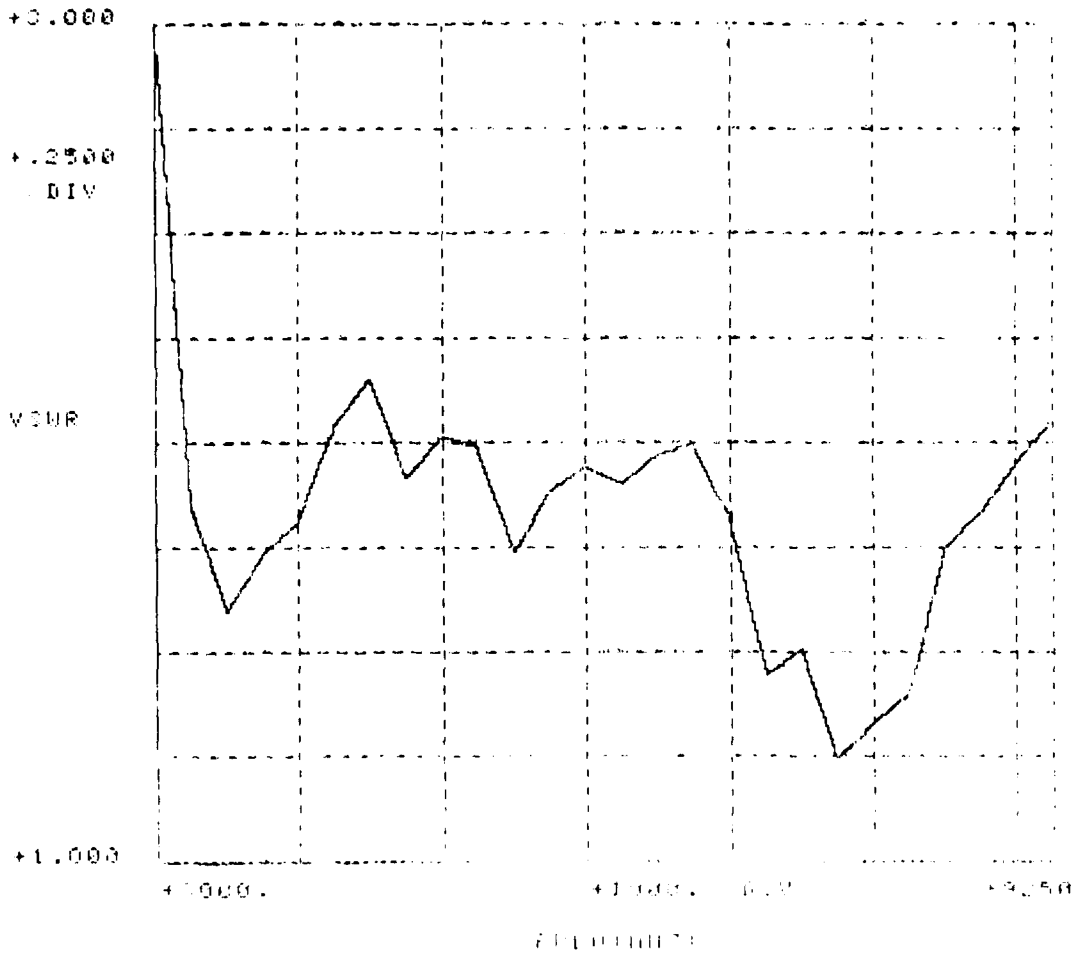

Figure 15. Active VSWR of Horizontally Polarized
NCN Array Element (Sheet 2 of 3)

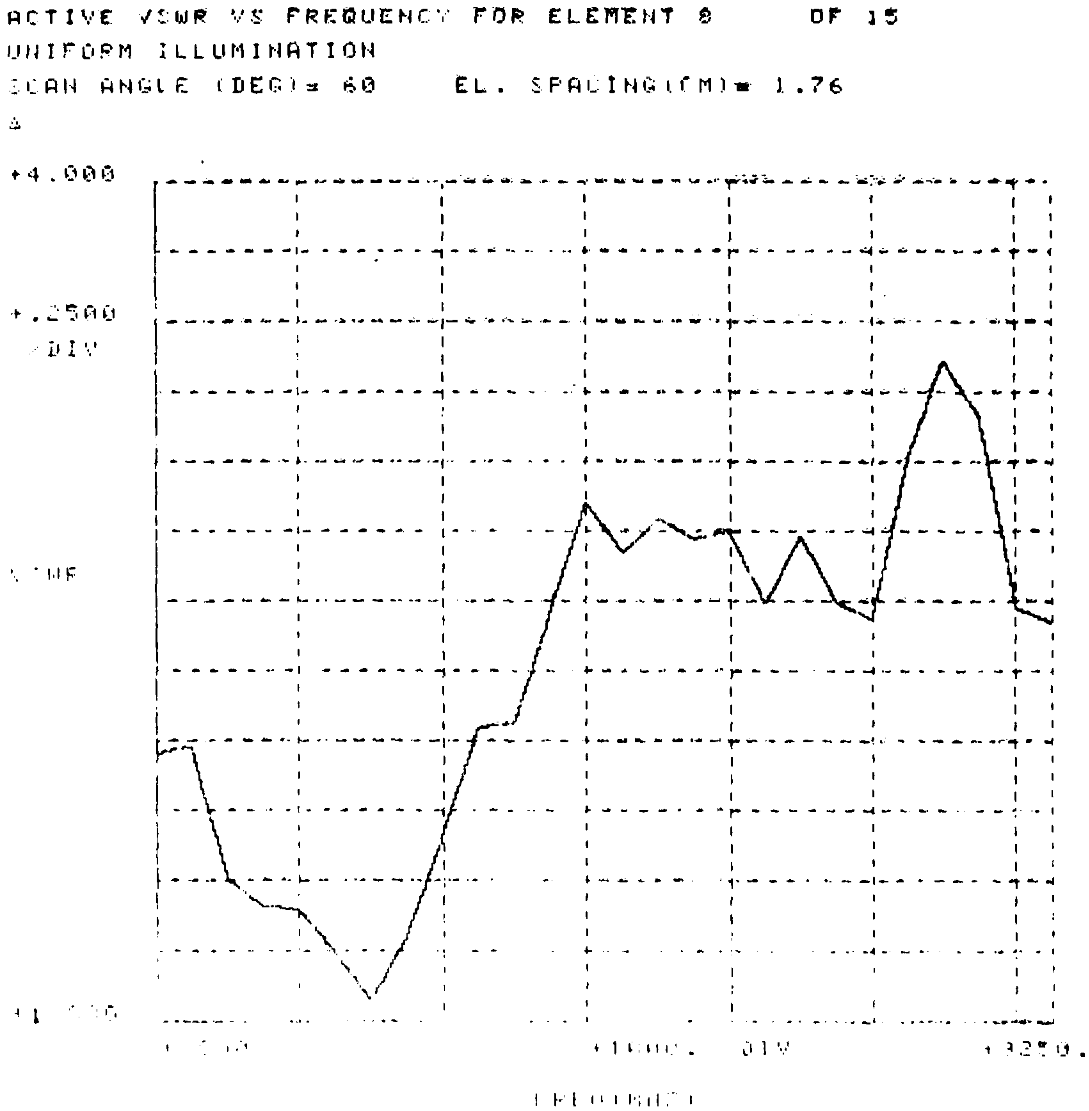

Figure 15. Active VSWR of Horizontally Polarized NCN Array Element (Sheet 3 of 3)

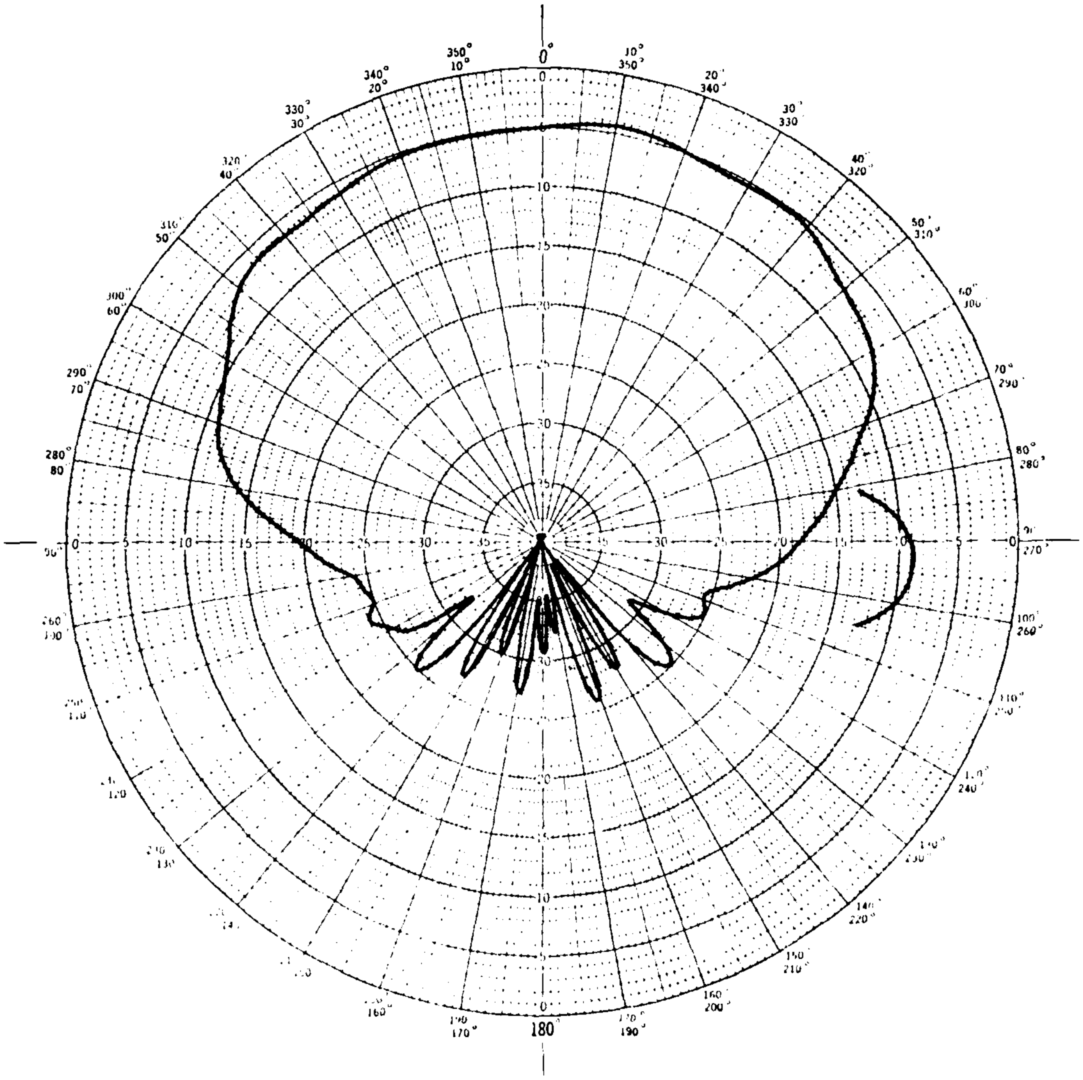

Figure 16. Azimuth Pattern of Horizontally Polarized NCN Array Element (Sheet 1 of 4)

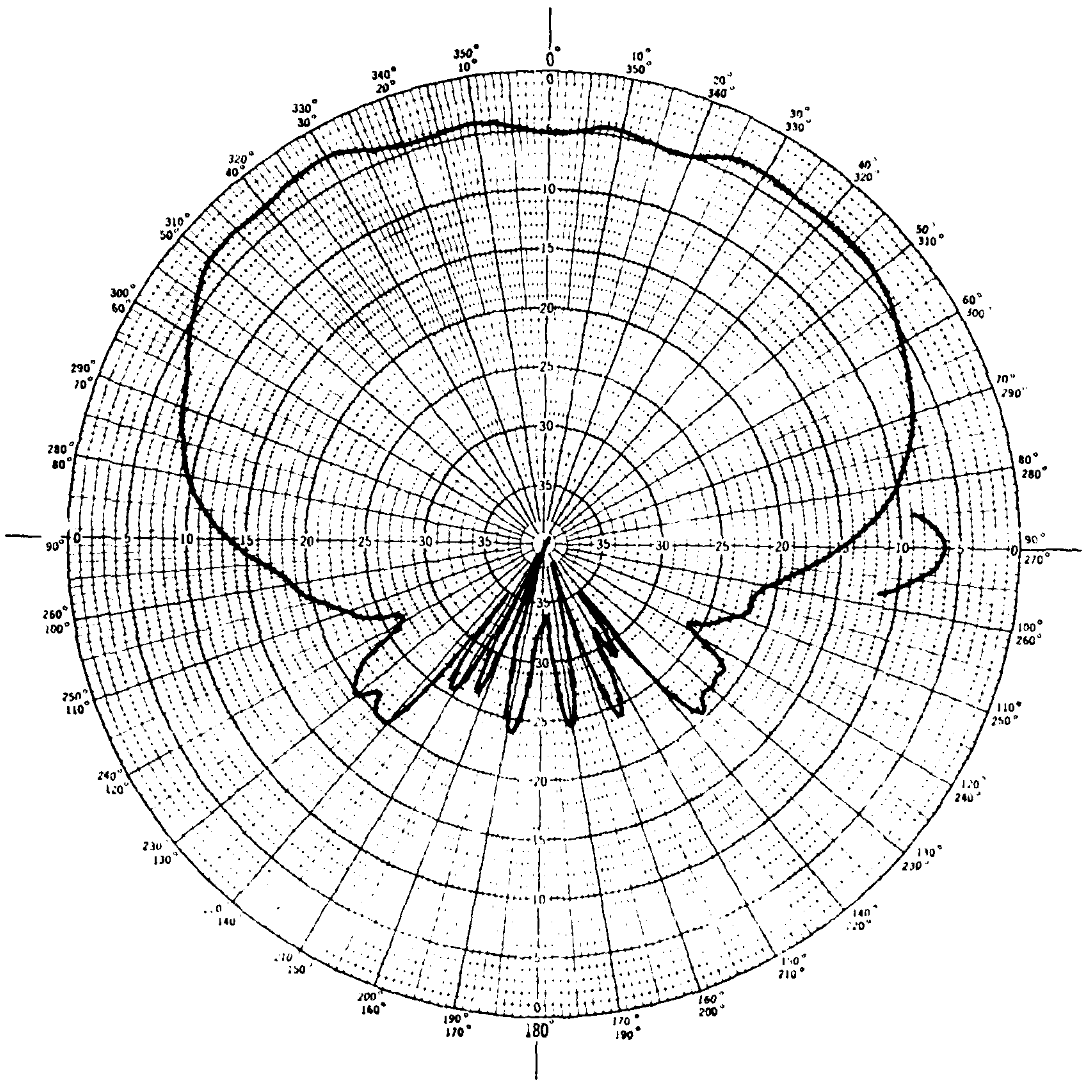

5 GHZ

Figure 16. Azimuth Pattern of Horizontally Polarized NCN Array Element (Sheet 2 of 4)

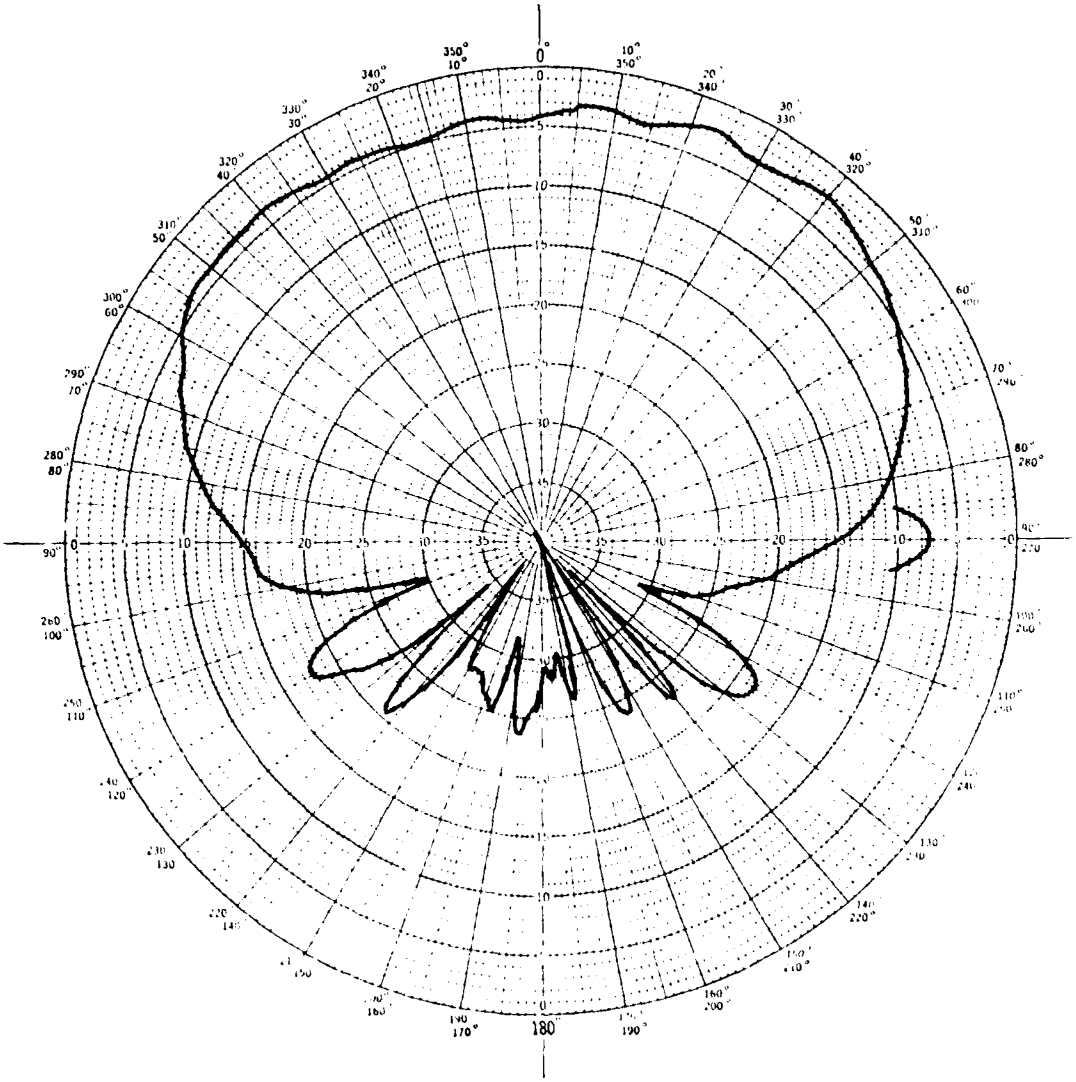

7.5 GHZ

Figure 16. Azimuth Pattern of Horizontally Polarized
NCN Array Element (Sheet 3 of 4)

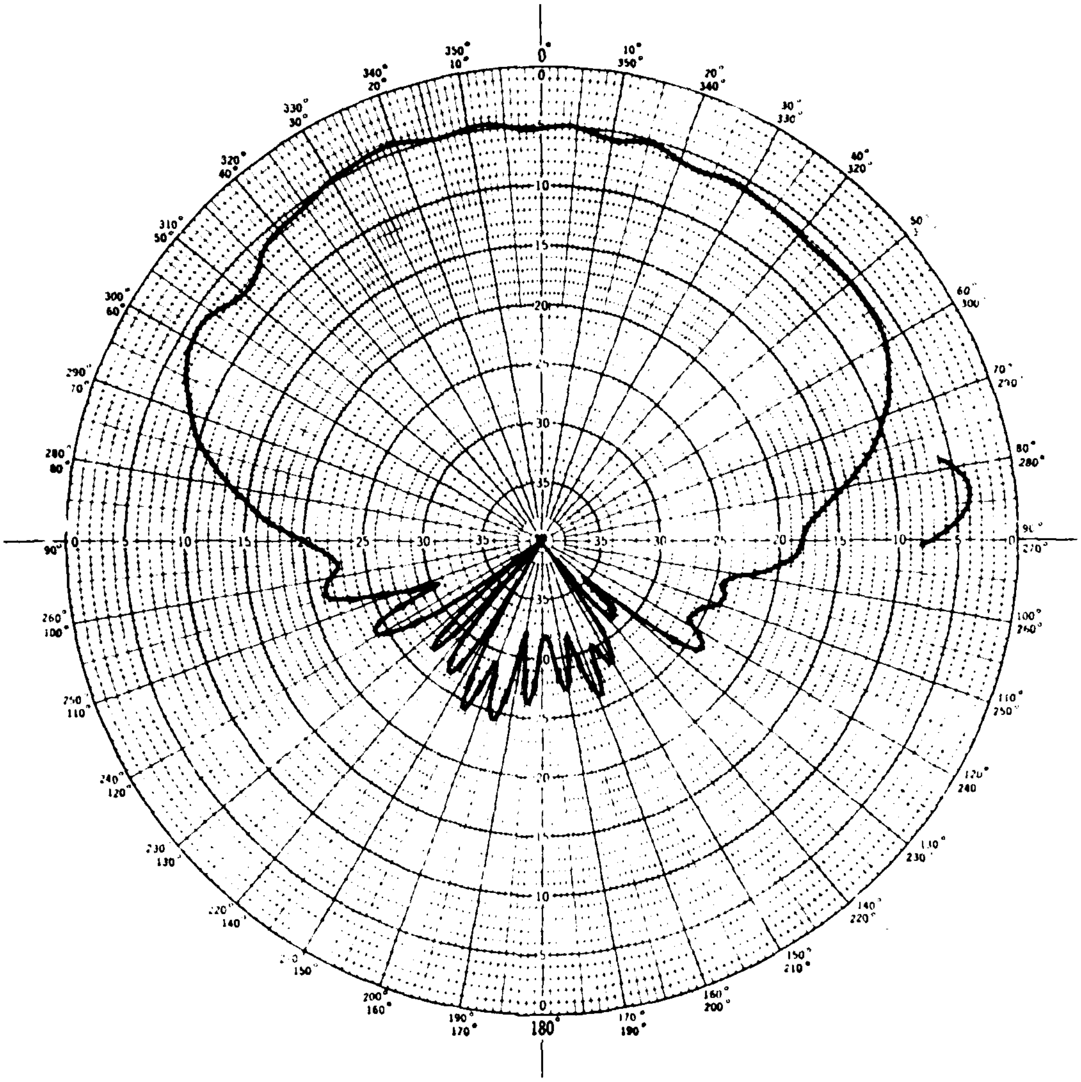

9 GHZ

Figure 16. Azimuth Pattern of Horizontally Polarized NCN Array Element (Sheet 4 of 4)

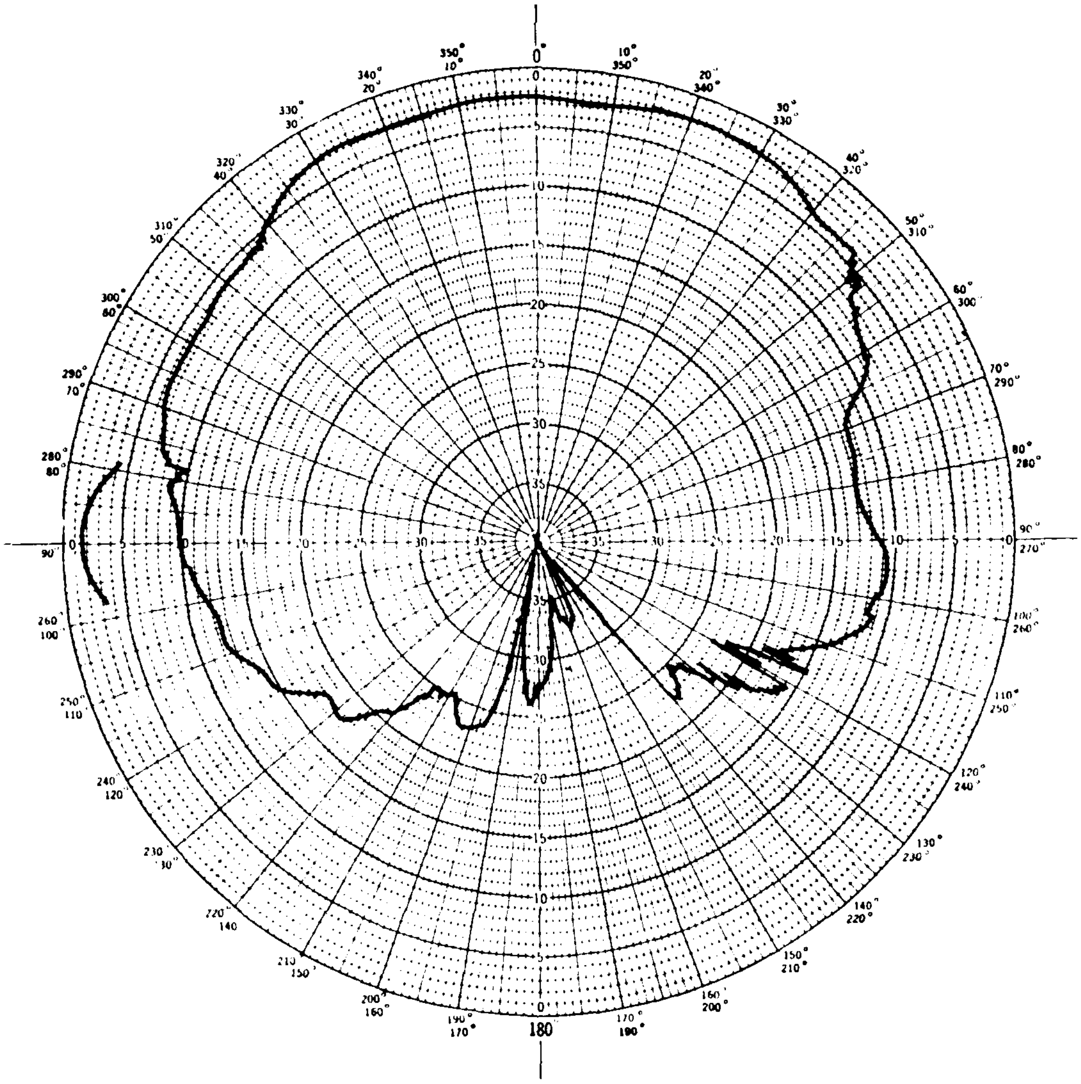

4.5 GHZ

Figure 17. Azimuth Pattern of Vertically Polarized NCN Array Element (Sheet 1 of 4)

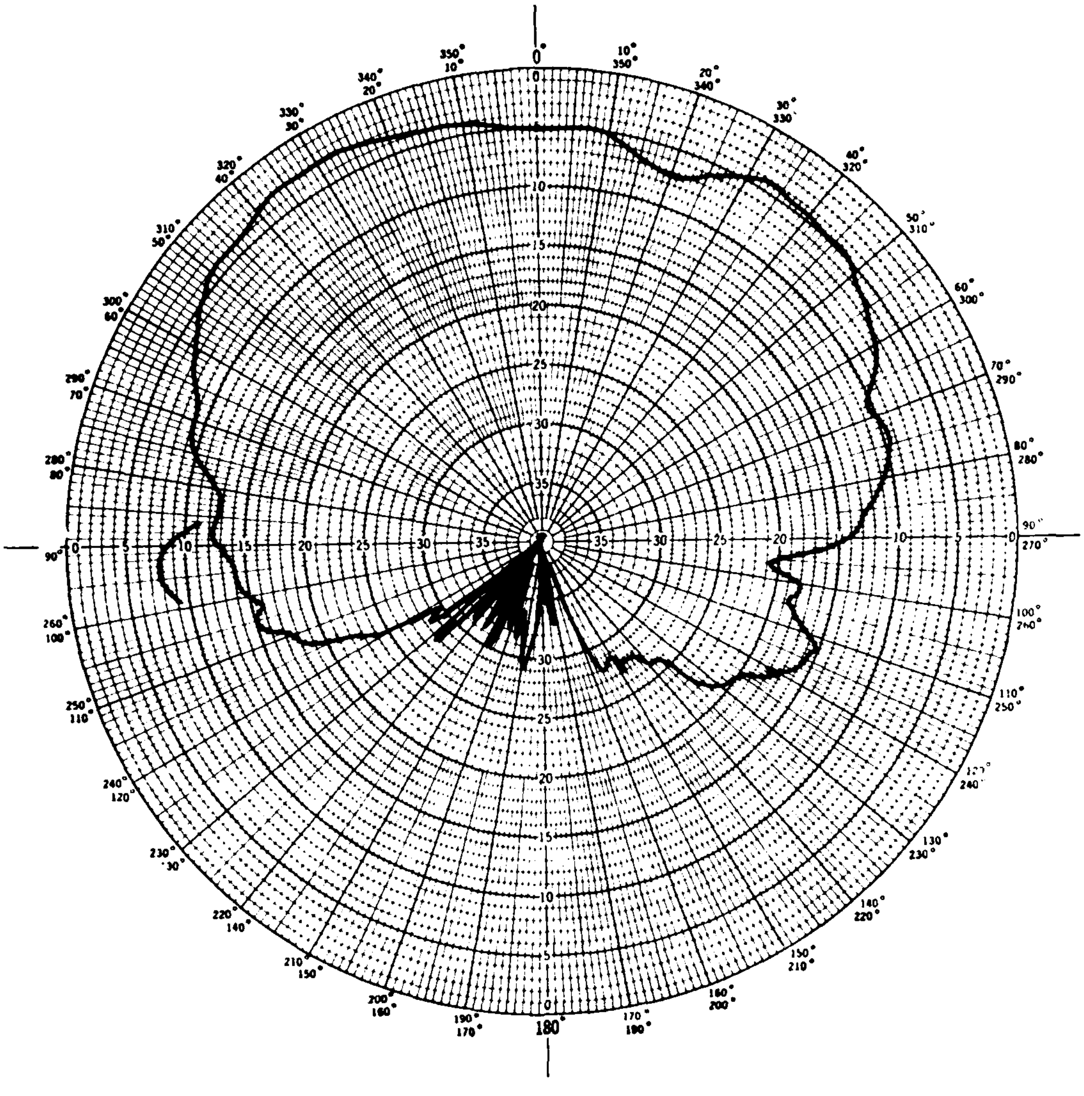

6 GHZ

Figure 17. Azimuth Pattern of Vertically Polarized
NCN Array Element (Sheet 2 of 4)

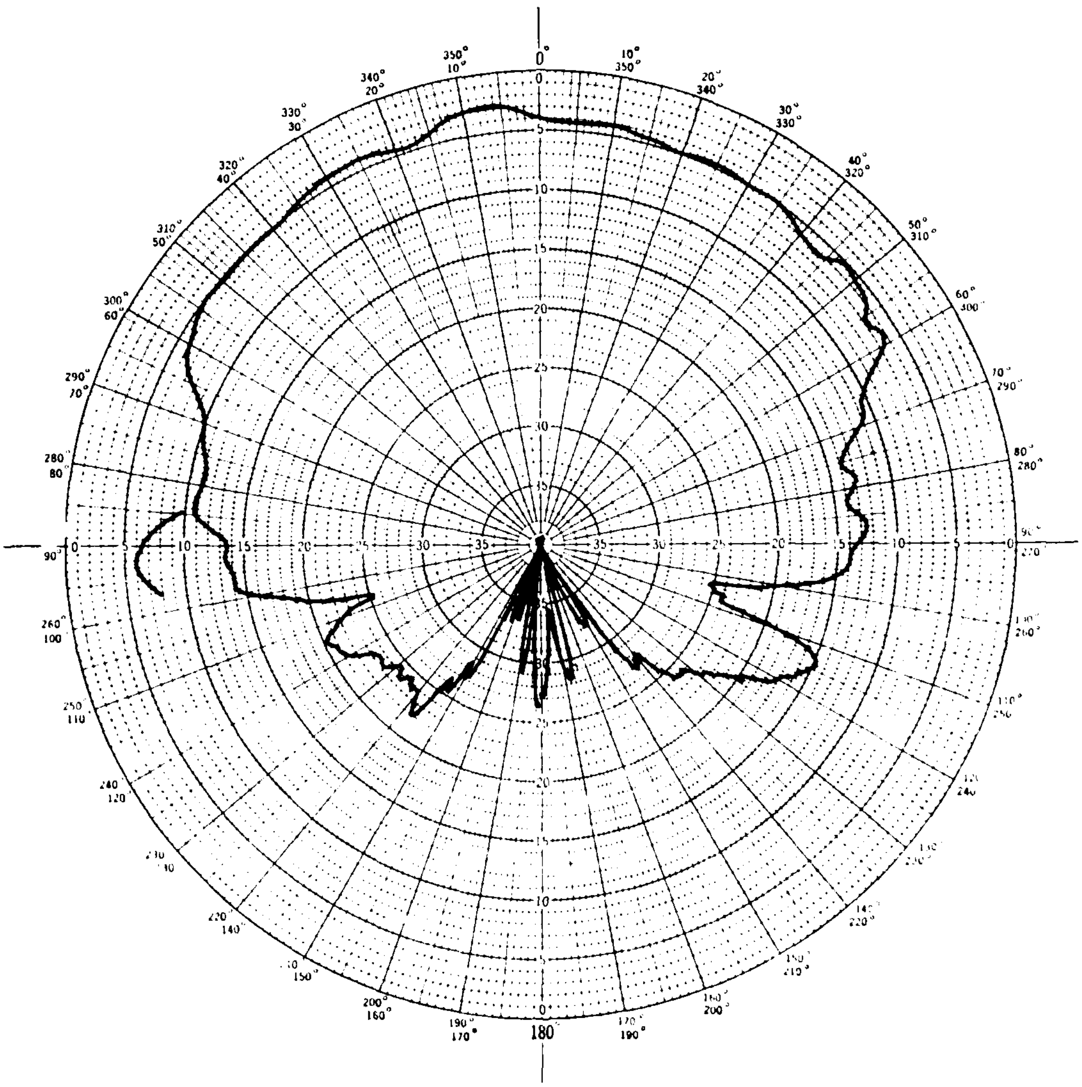

Figure 17. Azimuth Pattern of Vertically Polarized NCN Array Element (Sheet 3 of 4)

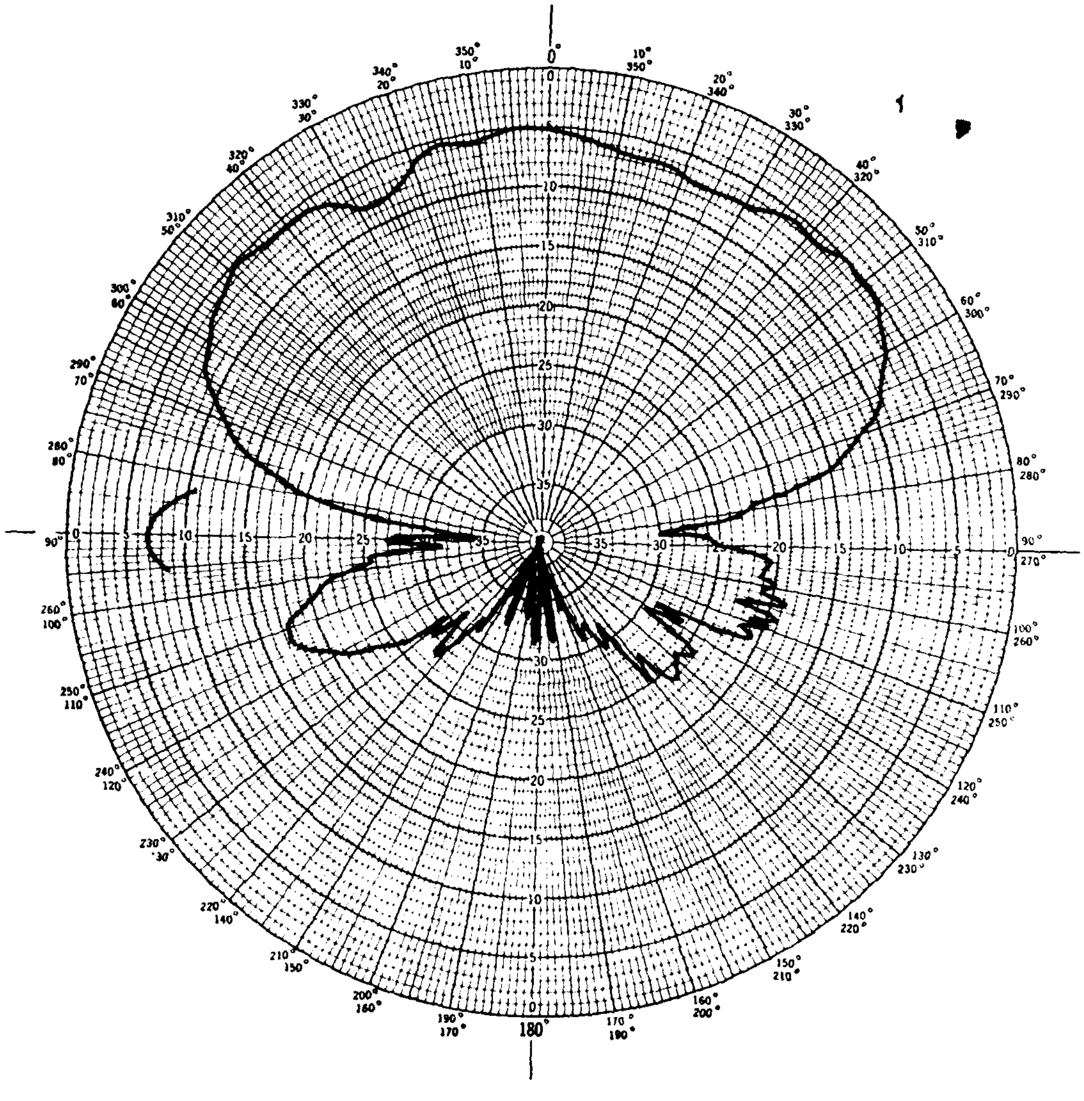

Figure 17. Azimuth Pattern of Vertically Polarized NCN Array Element (Sheet 4 of 4)

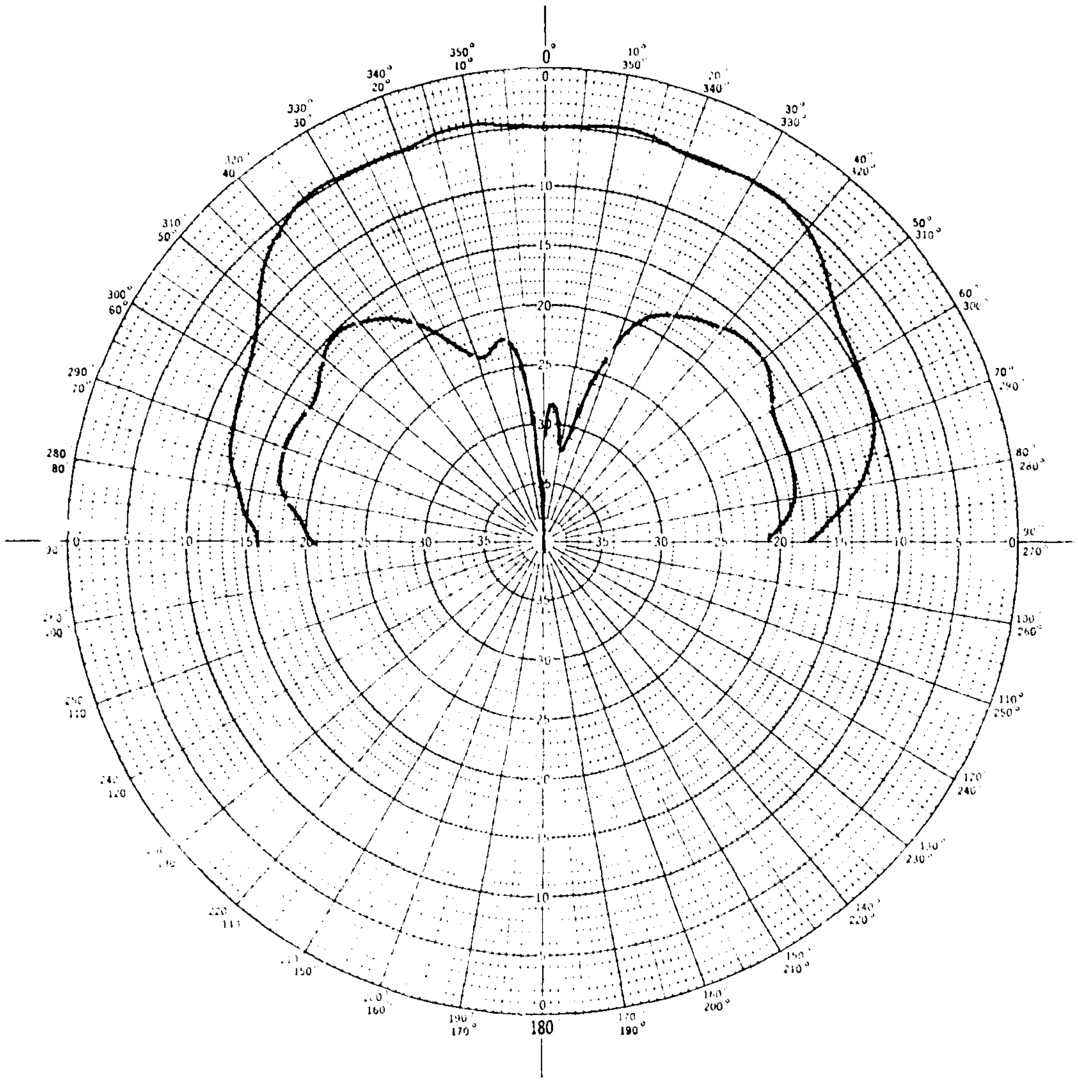

5 GHZ

Figure 18. Cross-Polarization (HV) Patterns of NCN Array Element (Sheet 1 of 2)

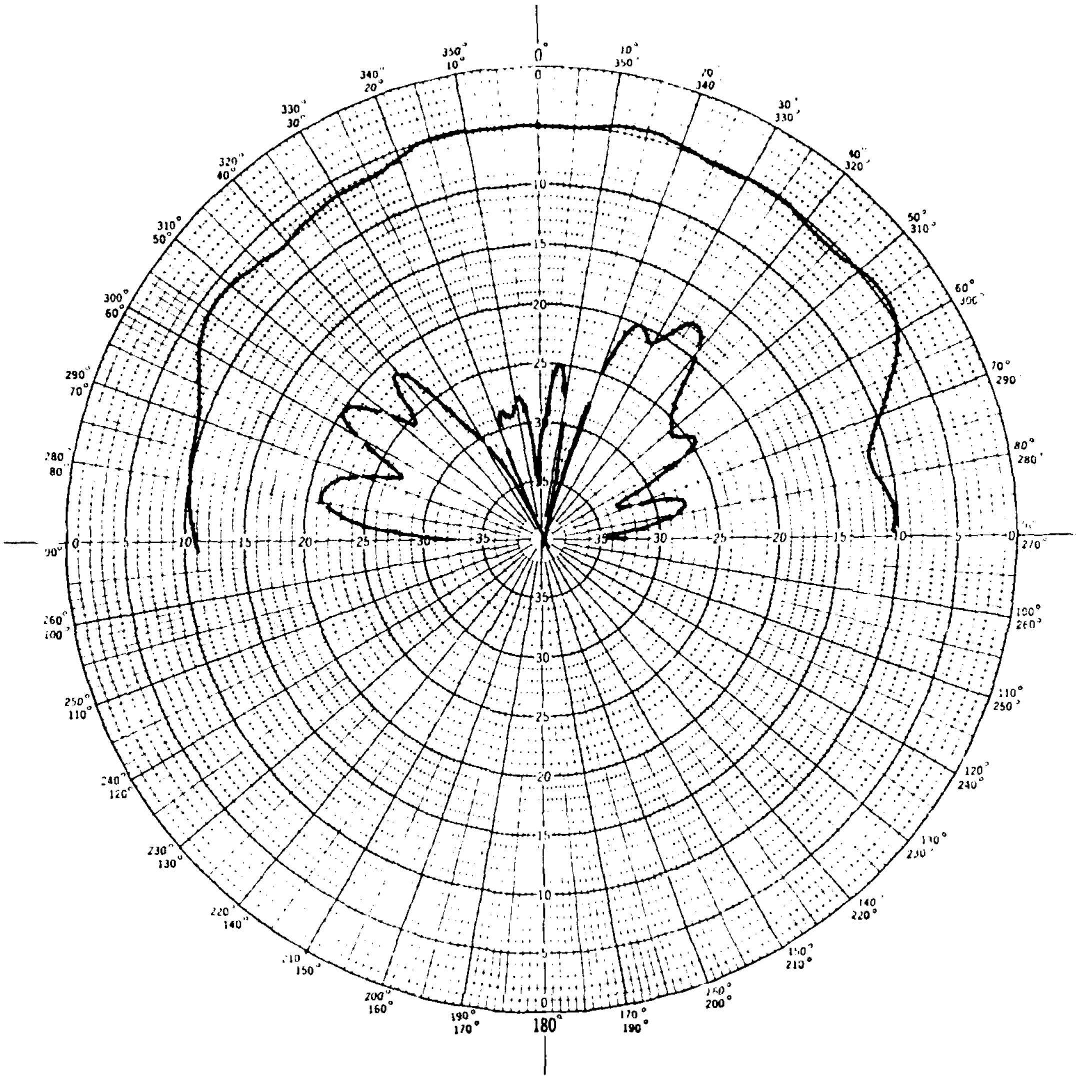

8 GHZ

Figure 18. Cross-Polarization (HV) Patterns of NCN Array Element (Sheet 2 of 2)

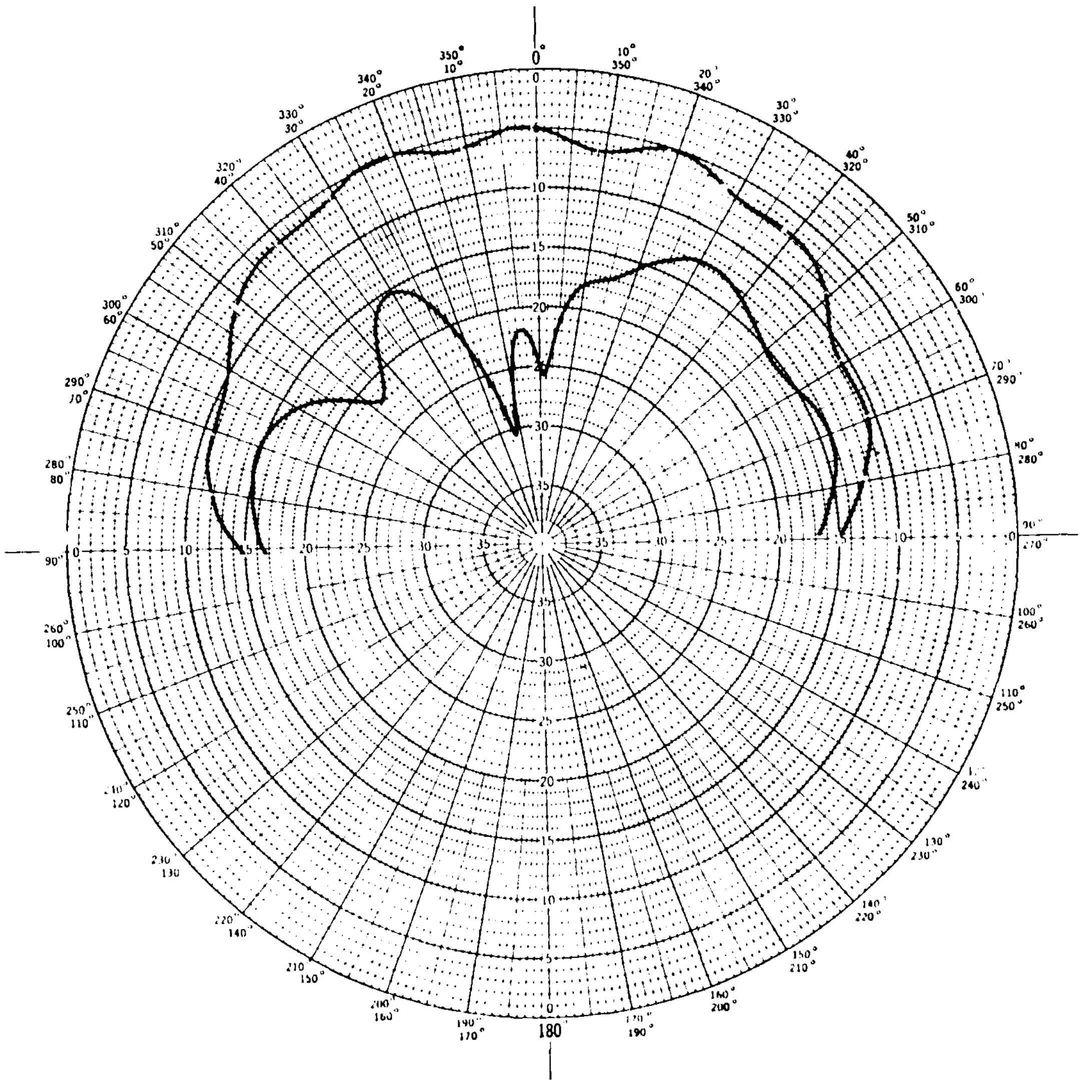

Figure 19. Cross-Polarization (VH) Patterns of
NCS Array Element (Sheet 1 of 2)

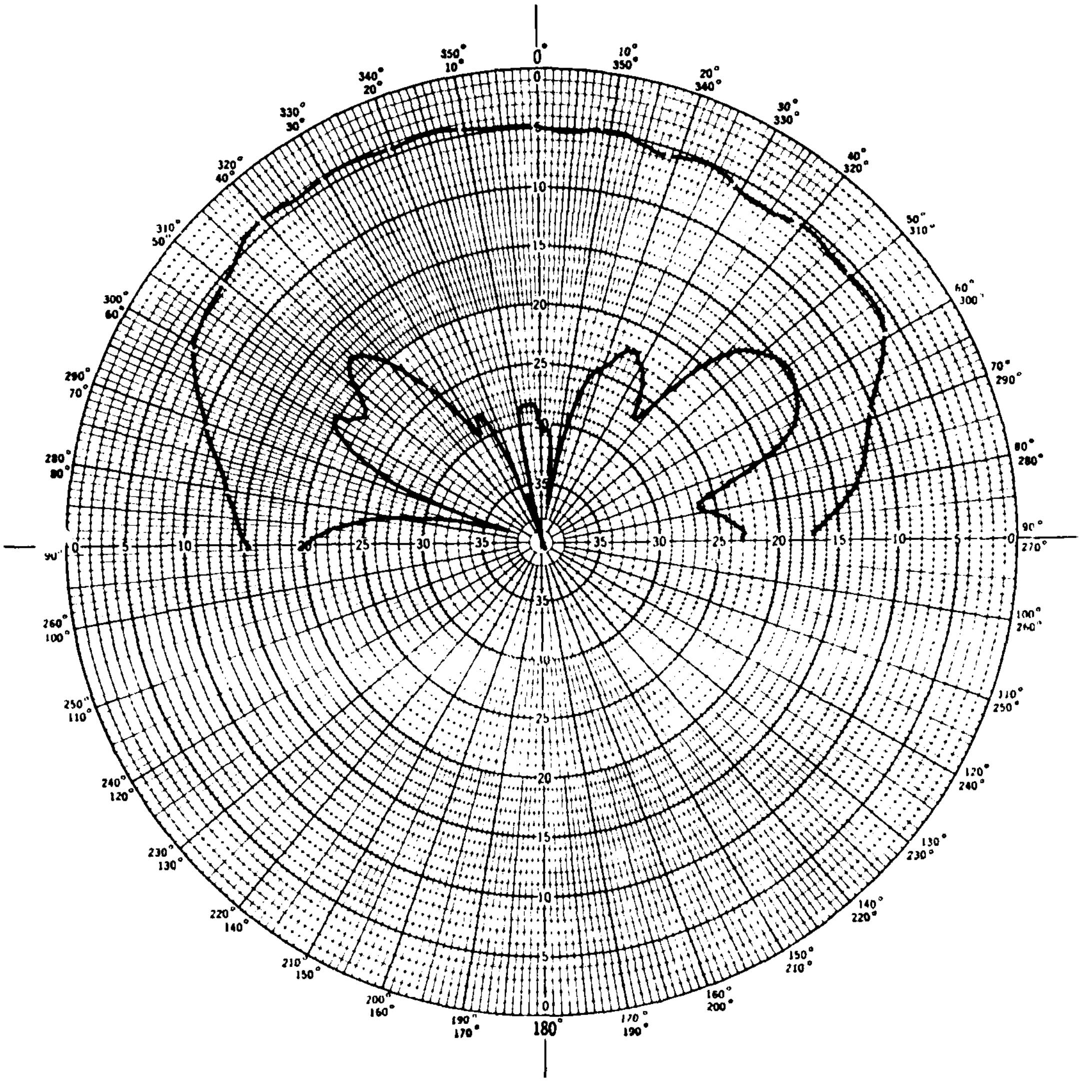

8 GHZ

Figure 19. Cross-Polarization (VH) Patterns of NCN Array Element (Sheet 2 of 2)

2.5 COINCIDENT-CROSSED-NOTCH ARRAY (CCN)

The CCN geometry requires a stripline board thickness smaller than the notch gap at its feed point, in order that the vertical and horizontal elements might remain independent. A 0.060-inch thick stripline HP notch array with a 0.090-inch notch feed gap was designed and fabricated to meet this requirement.

The VP elements were then fabricated and configured with the HP elements as depicted in Figure 20. The vertical boards contain three vertically polarized elements, only one of which is actively fed, the other two being used for impedance matching to free space. The vertical and horizontal element designs are identical, except that the stripline feeds are offset to keep the feeds from physically intersecting and interfering electrically. Figure 21 is a picture of the completed array.

Embedded element patterns and gain and impedance measurements were taken every 0.25 GHz from 3.25 to 9.25 GHz. It can be concluded that, except for a rise in the active impedance at around 4 GHz for both the VP and HP elements, array performance is good over the 3.75 to 7.5 GHz frequency band. All the following statements pertain to embedded element measurements over this 3.75 to 7.5 GHz frequency band on the center VP and HP elements.

Figures 22 through 25 show passive and active VSWR as measured on the automatic network analyzer. The VP element has a passive VSWR under 3.5:1, and under 2:1 over most of the band. The VP element active VSWR is under 4.5:1 out to 60 degrees, except for a rise to 7:1 for a 0-degree scan at 4 GHz, and a rise to 6:1 for a 40-degree scan at 7.5 GHz. The rise at 4 GHz is related to the rise in passive VSWR. The HP active match is 4.5:1 out to a 40-degree scan over 4.5 to 7.5 GHz. At 4.25 GHz, VSWR comes up to 6.5, and at 7.5 GHz there is a rise in VSWR to 10:1 for a 60-degree scan.

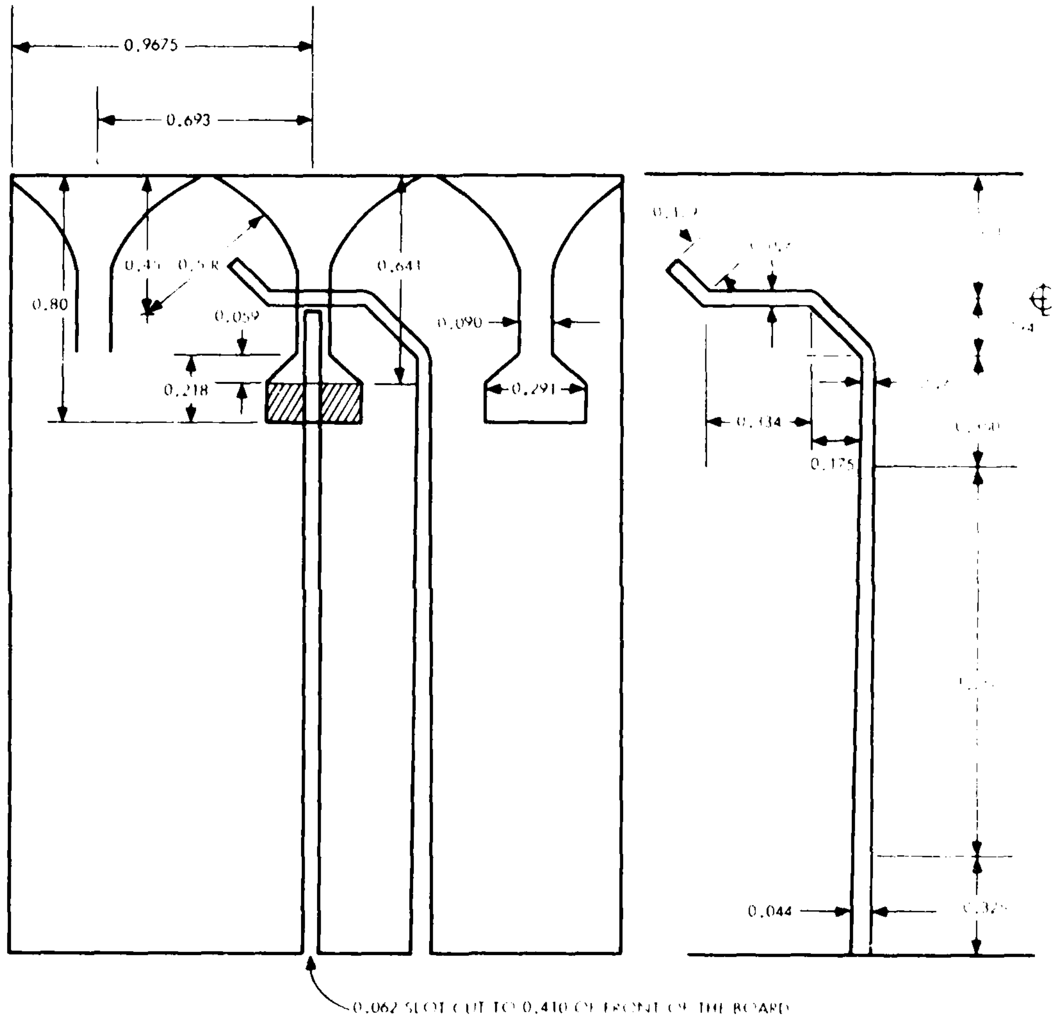

DIELECTRIC THICKNESS = 0.029 INCH
(DUROID 5880)

HORIZONTAL ELEMENTS ARE IDENTICAL IN DESIGN, EXCEPT THAT THE STRIPLINE FEED INTERSECTS THE NOTCH AT 0.4[illegible] INSTEAD OF 0.181

Figure 20. Coincident Vertical Element Geometry (15-Element, Dual-Polarized Notch Array)

14652

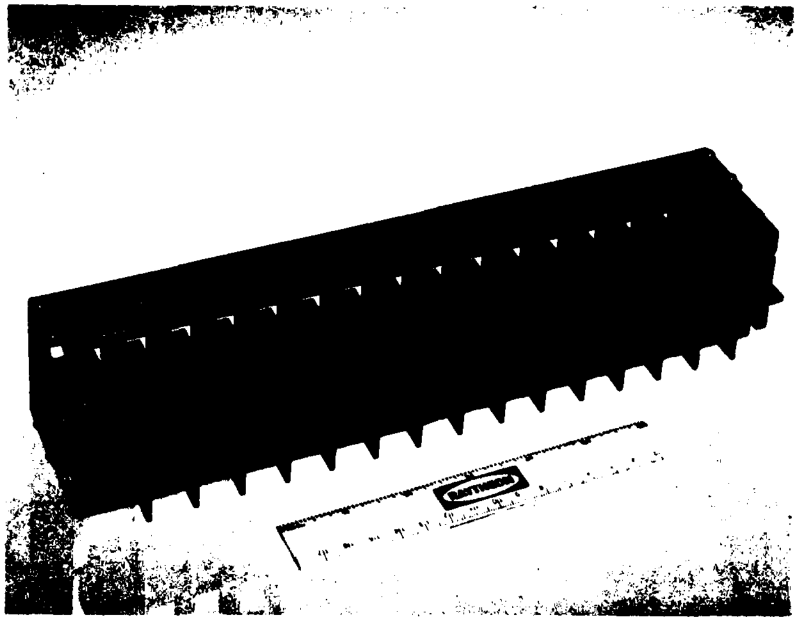

Figure 21. Photograph of Coincident-Center Notch Array

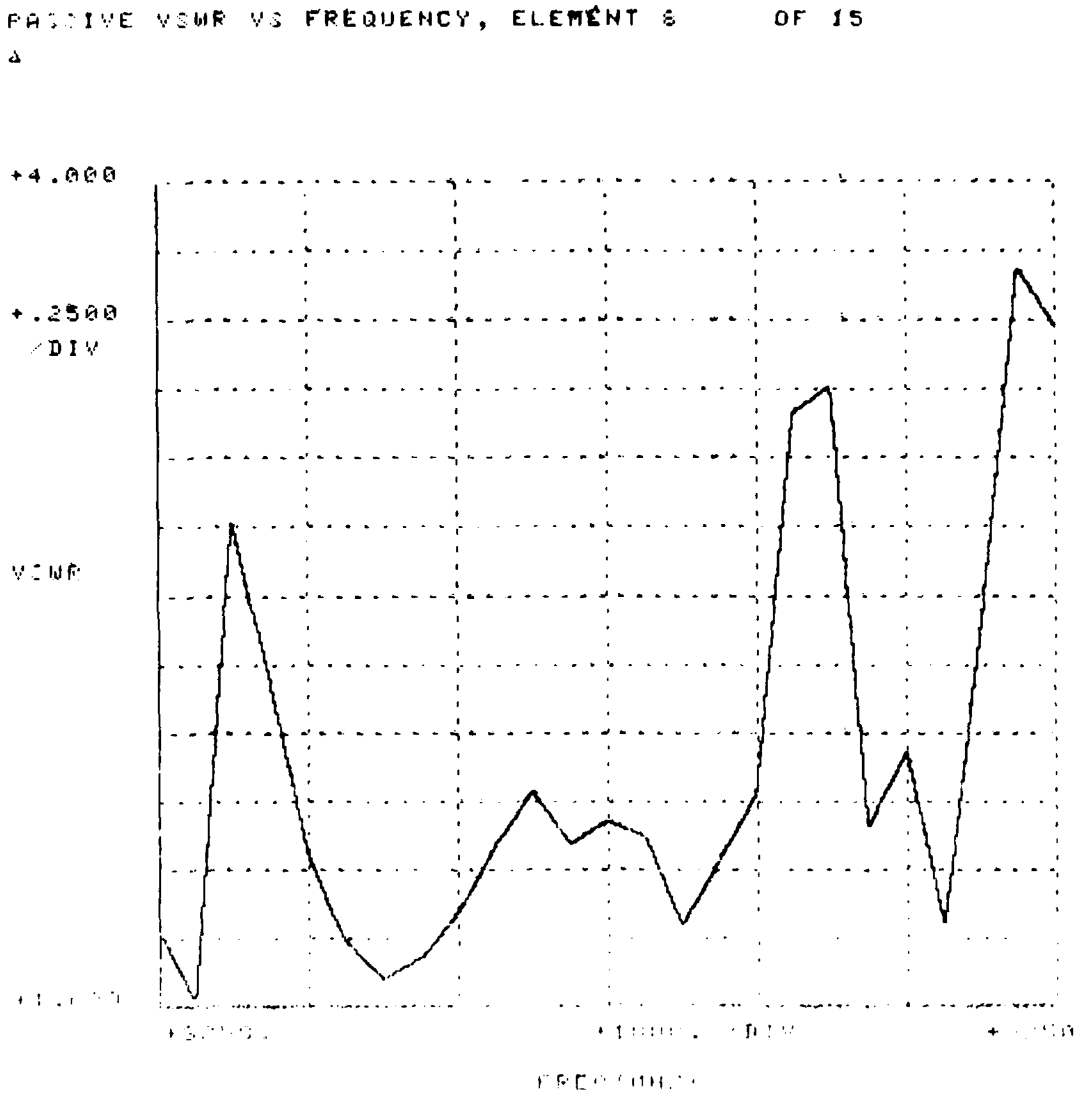

Figure 22. Passive VSWR of Horizontally Polarized Coincident-Crossed-Notch (CCN) Array

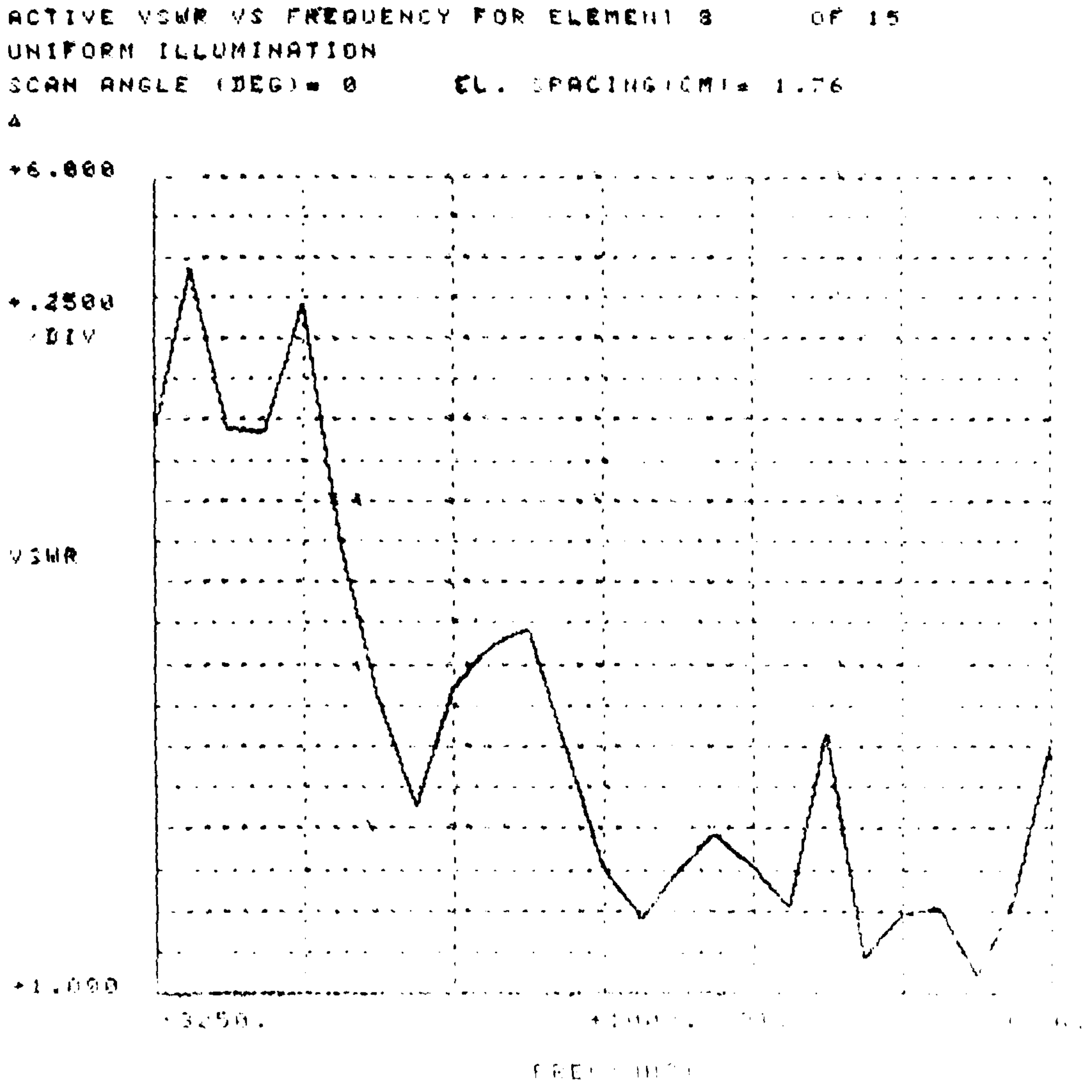

Figure 23. Active VSWR of Horizontally
Polarized CCS Array (Sheet 1 of 3)

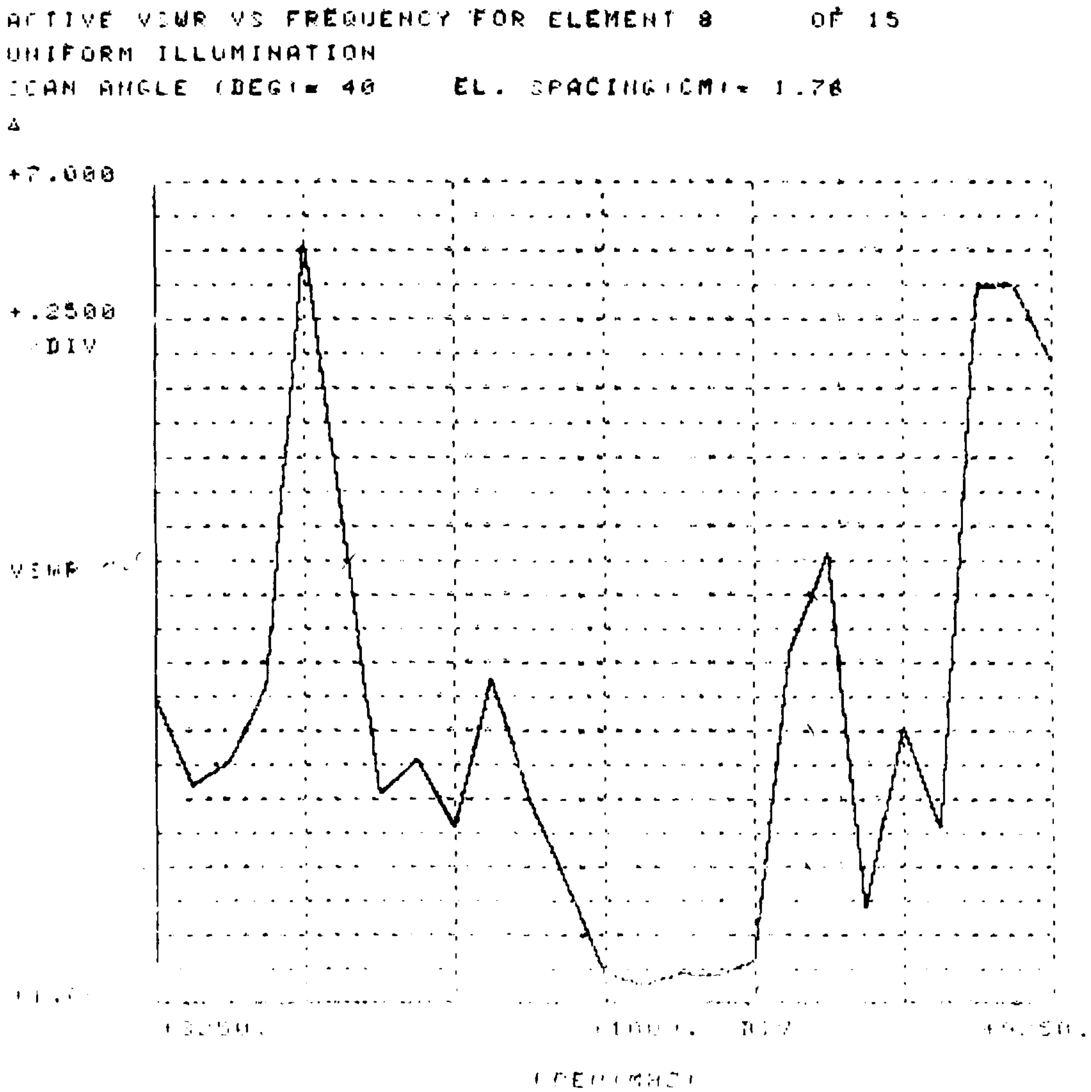

Figure 23. Active VSWR of Horizontally
Polarized CCN Array (Sheet 2 of 3)

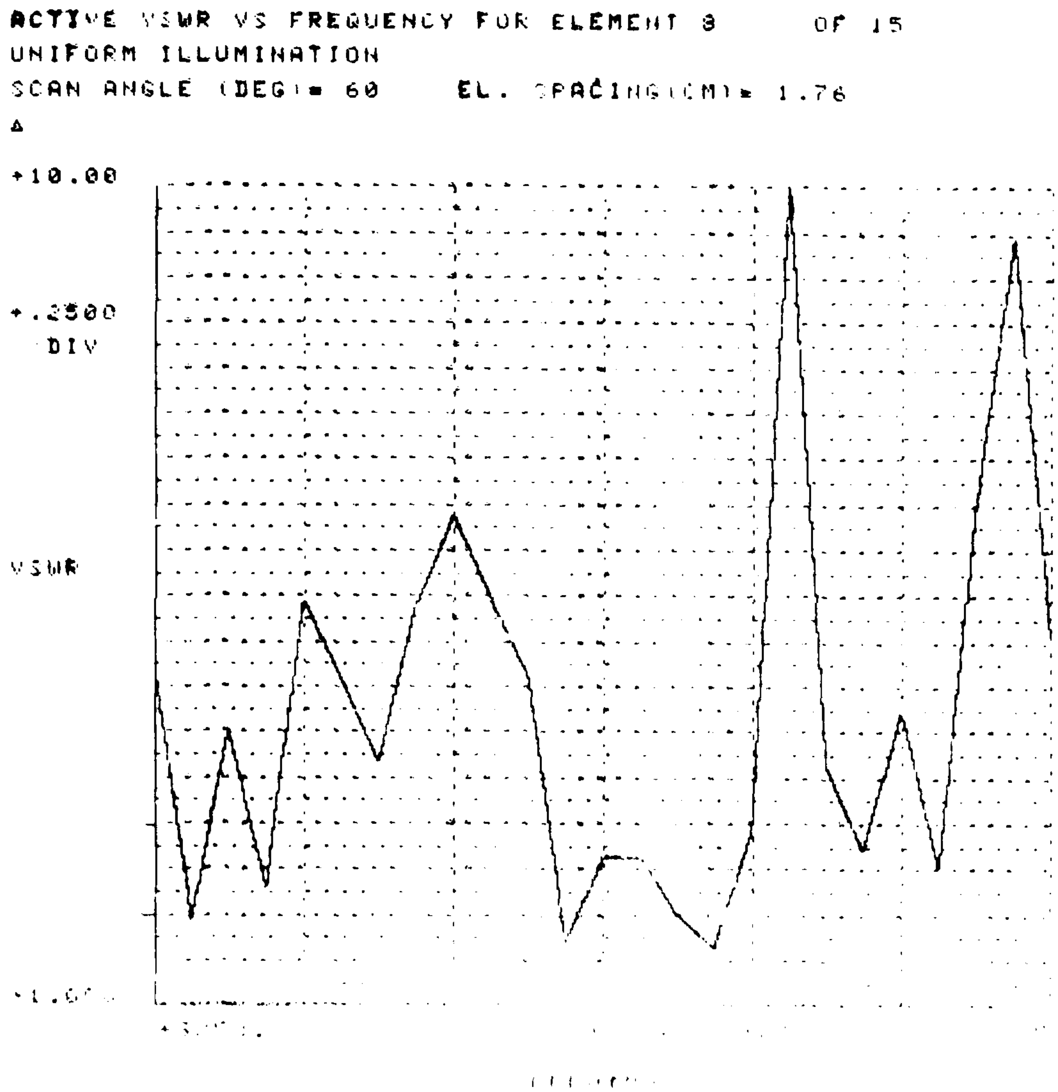

Figure 23. Active VSWR of Horizontally
Polarized CCN Array (Sheet 3 of 3)

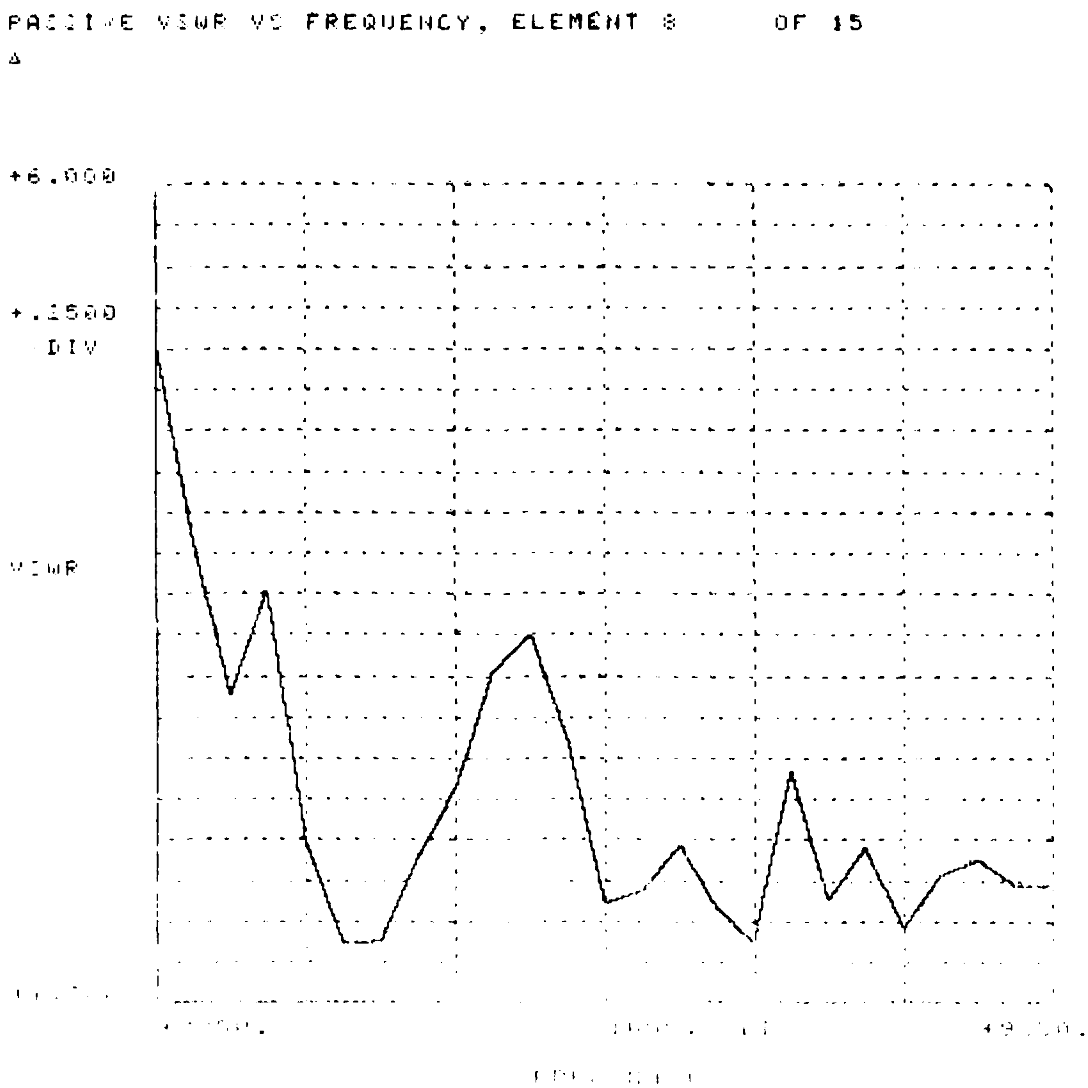

Figure 24. Passive VSWR of Vertically Polarized CCN Array

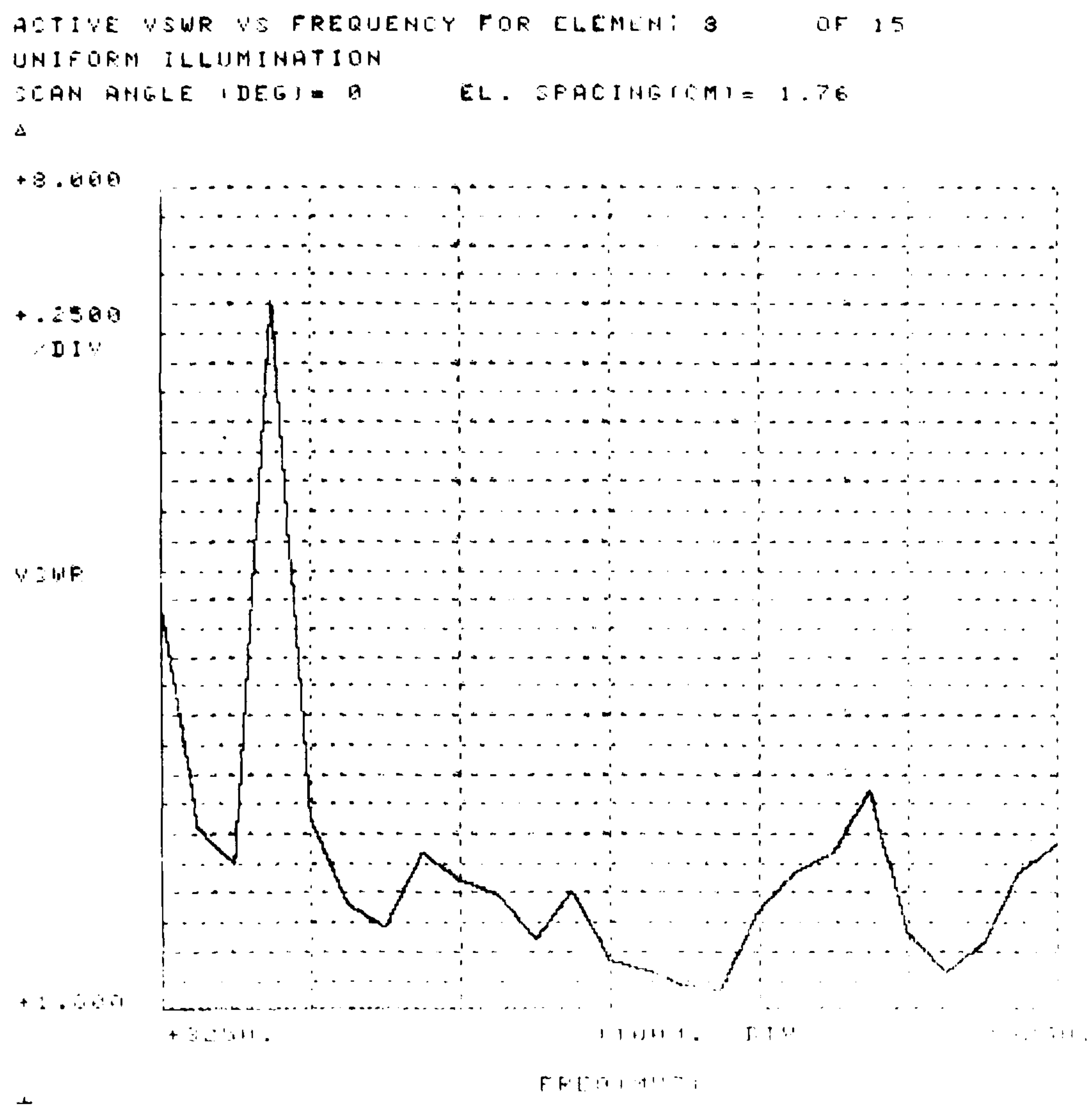

Figure 25. Active VSWR of Vertically Polarized CCN Array (Sheet 1 of 3)

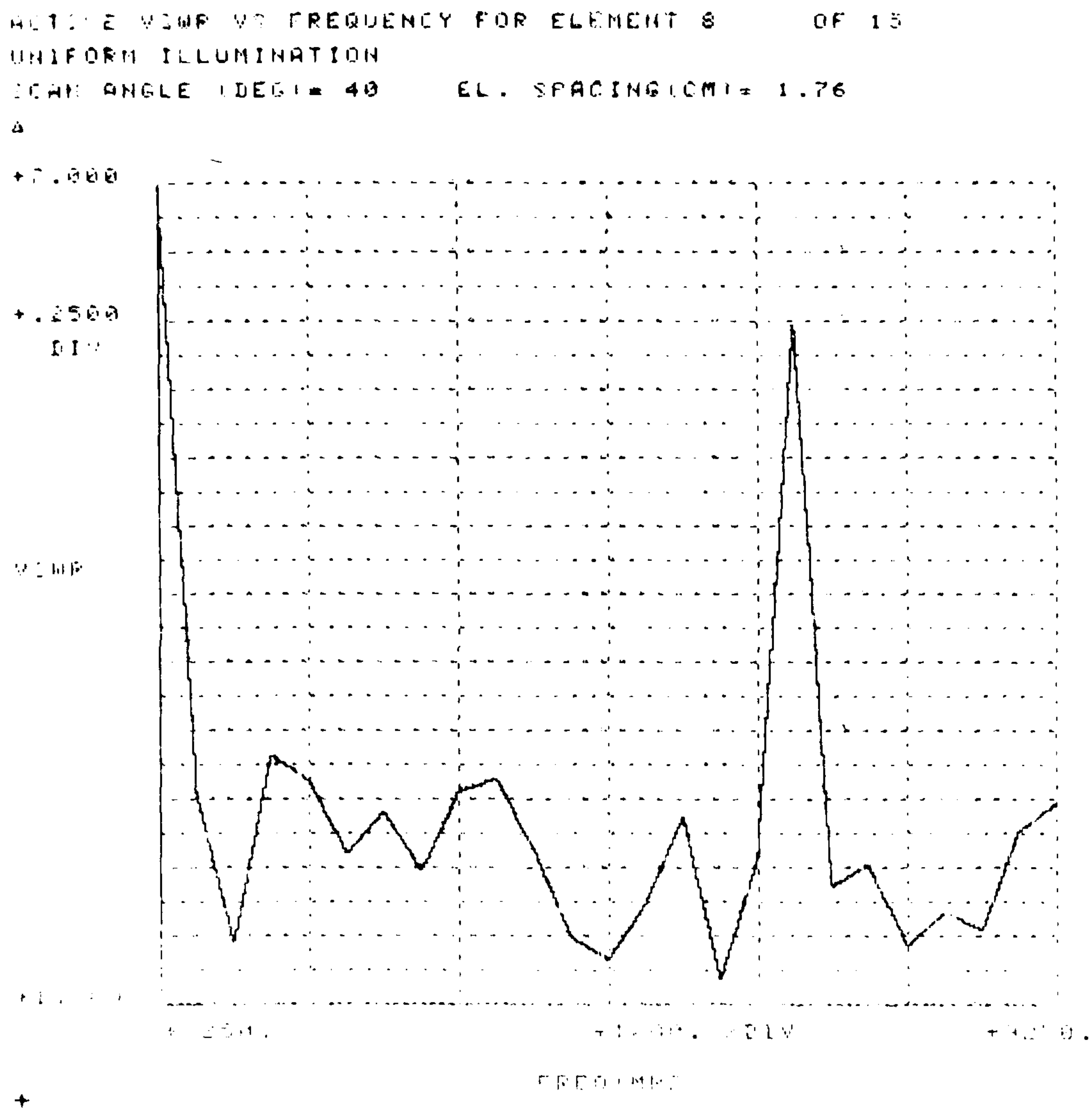

Figure 25. Active VSWR of Vertically Polarized
CCN Array (Sheet 2 of 3)

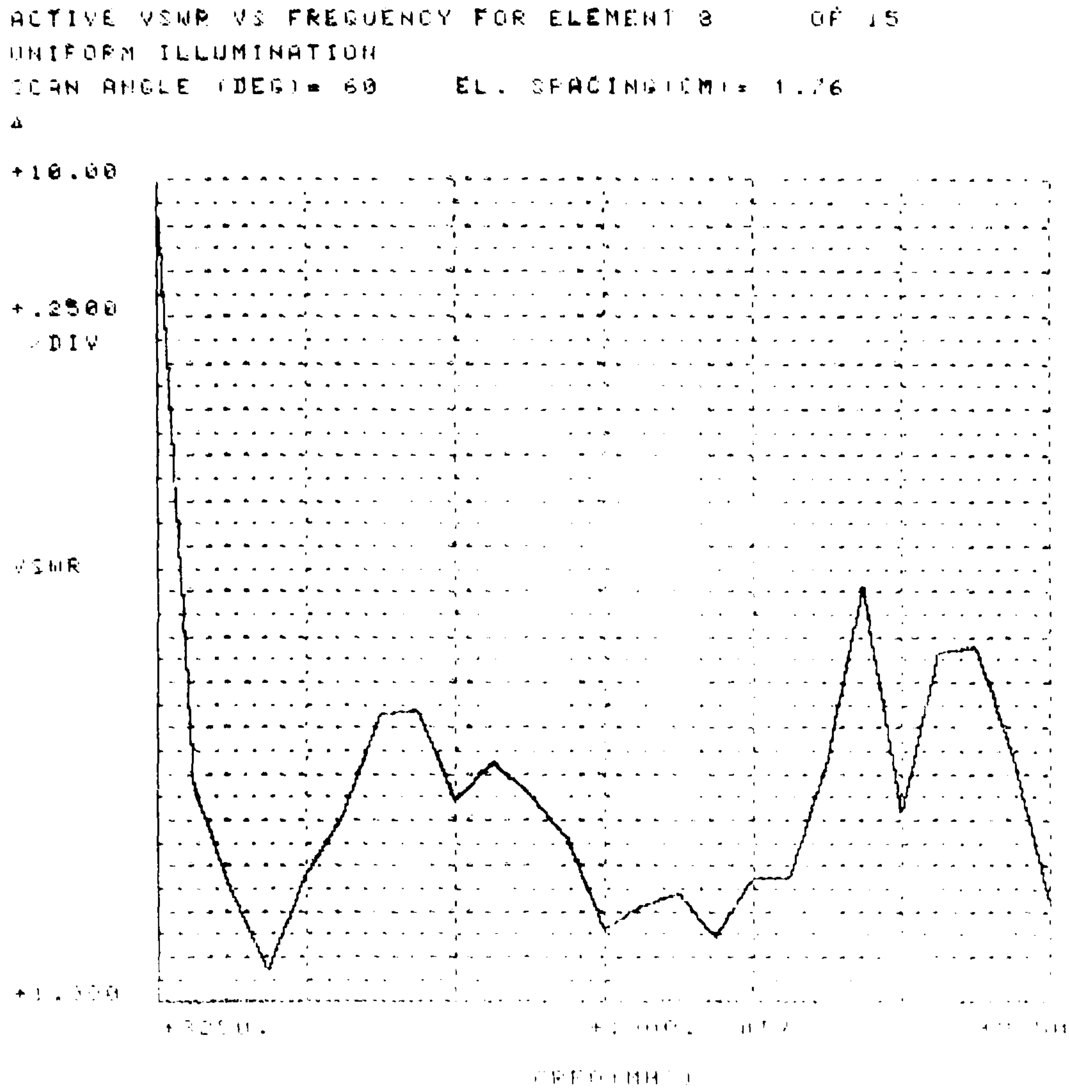

Figure 25. Active VSWR of Vertically Polarized CCN Array (Sheet 3 of 3)

Embedded element patterns of the center elements are shown in Figures 26 and 27. Minimum 3 dB-beamwidths over the band are 74 degrees in azimuth and 91 degrees in elevation for the HP element, and 115 degrees in azimuth and 49 degrees in elevation for the VP element.

Figures 28 and 29 show pattern measurements taken to test the polarization isolation of the VP element to HP incident radiation, and vice versa. The VP element isolation to HP radiation is >14 dB over a ±60 degree scan in azimuth, while HP element isolation over a ±60 degree scan is ≥13 dB.

Phase measurements comparing the VP element phase center to the HP element phase center were taken, and are shown in Figure 30. These give an indication of how differences between locations of the VP and HP element phase centers would affect the quality of polarized radiation which could be generated over the frequency band and azimuth scan.

The graphs should be compared for differences between the VP and HP phase, and not for absolute values, which were adjusted during the tests.

The phase tests were conducted in the following manner. The array face was positioned as accurately as possible over the pedestal center of rotation (CR). At a single frequency, a phase pattern was cut over +90 degrees in azimuth on the center VP element with a VP transmit horn. The transmit horn was then rotated to HP, and a phase pattern cut on the center HP element on the same graph, using the same cable between the phase receiver and the antenna element.

The phase measurements also indicate that, over a ±60 degree scan, the VP and HP element phase centers were at the array face (location of the CR). This is indicated by the flatness of phase over the scan.

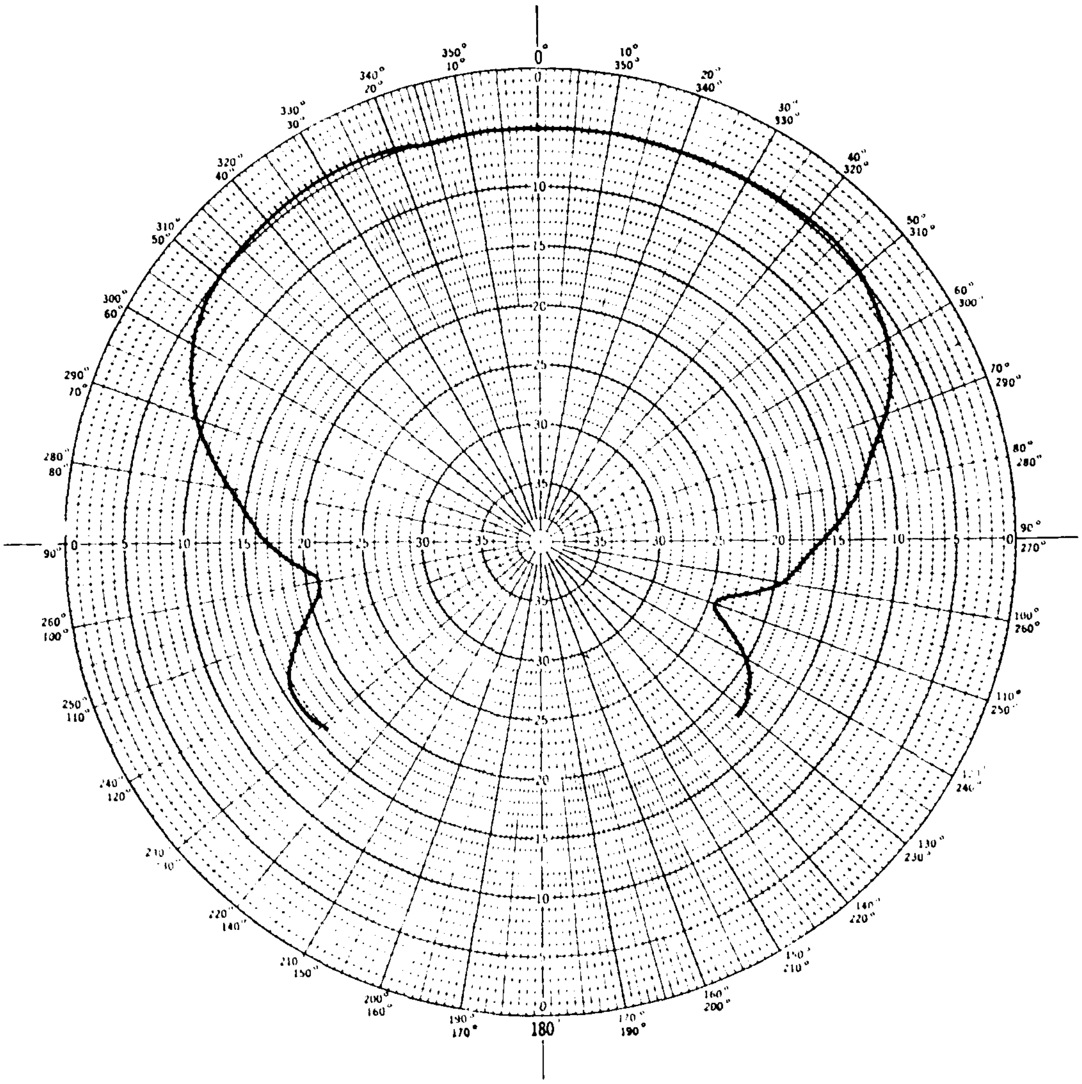

Figure 26. Azimuth Pattern of Vertically Polarized
CCN Array (Sheet 1 of 4)

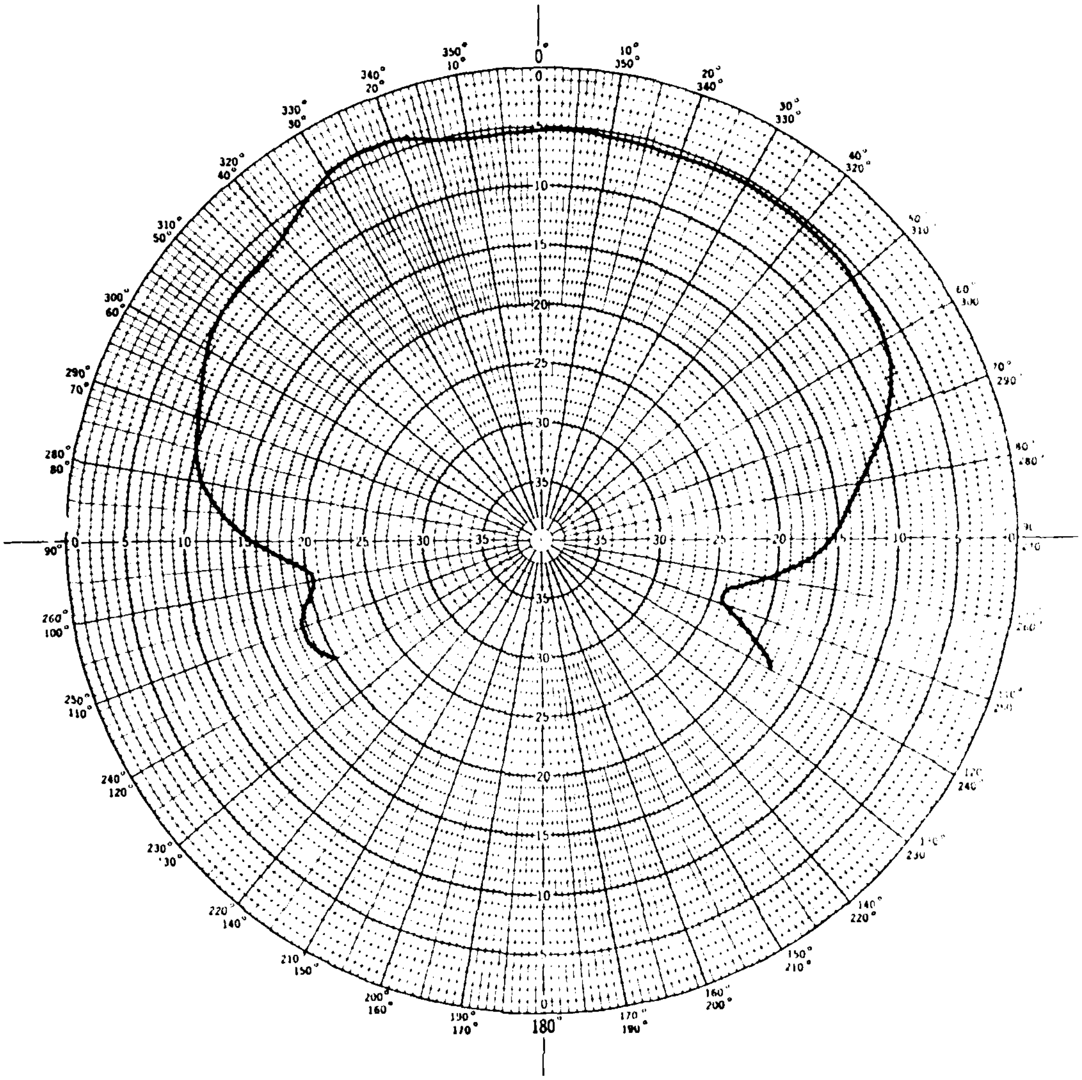

4.75 GHZ

Figure 26. Azimuth Pattern of Vertically Polarized CCN Array (Sheet 2 of 4)

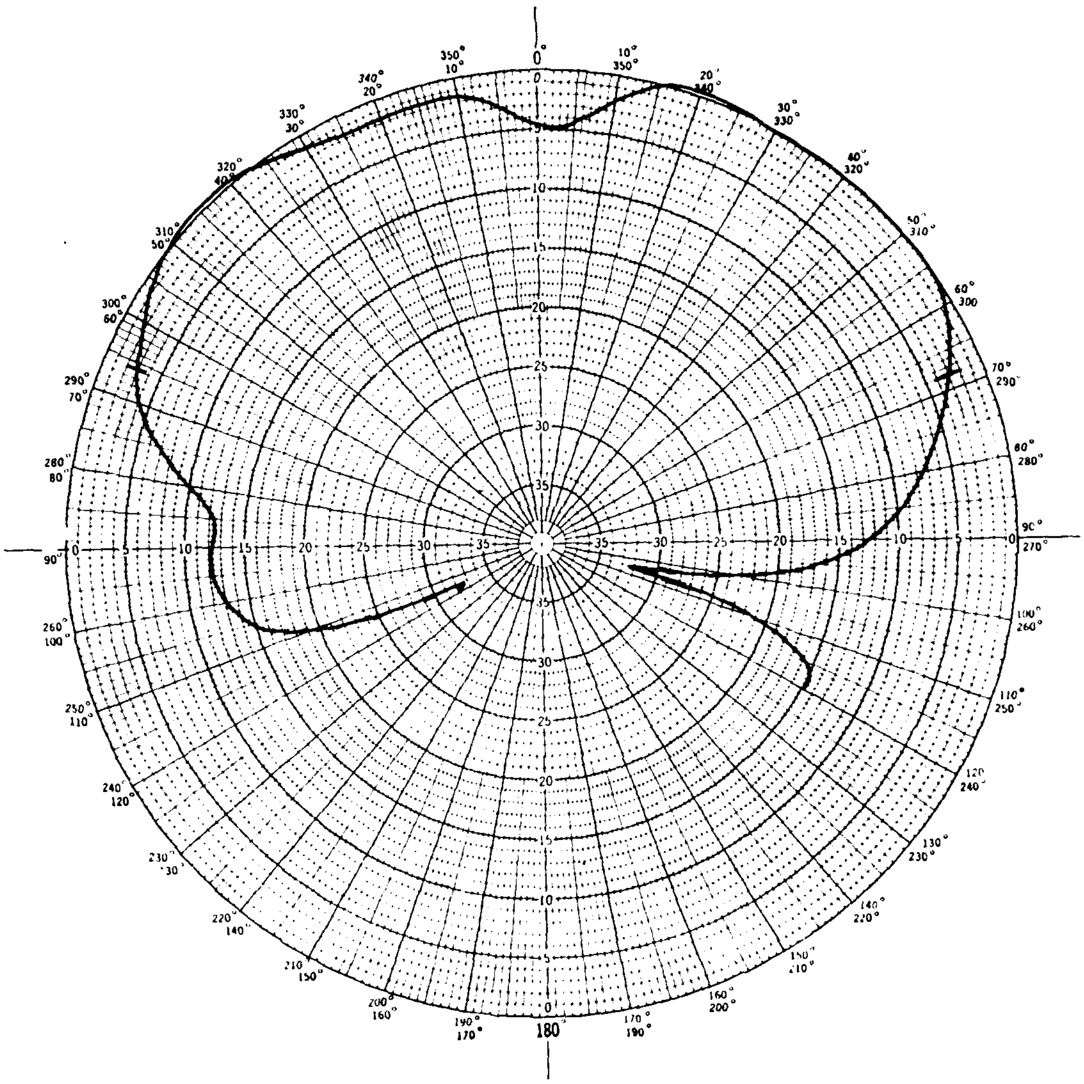

Figure 26. Azimuth Pattern of Vertically Polarized CCN Array (Sheet 3 of 4)

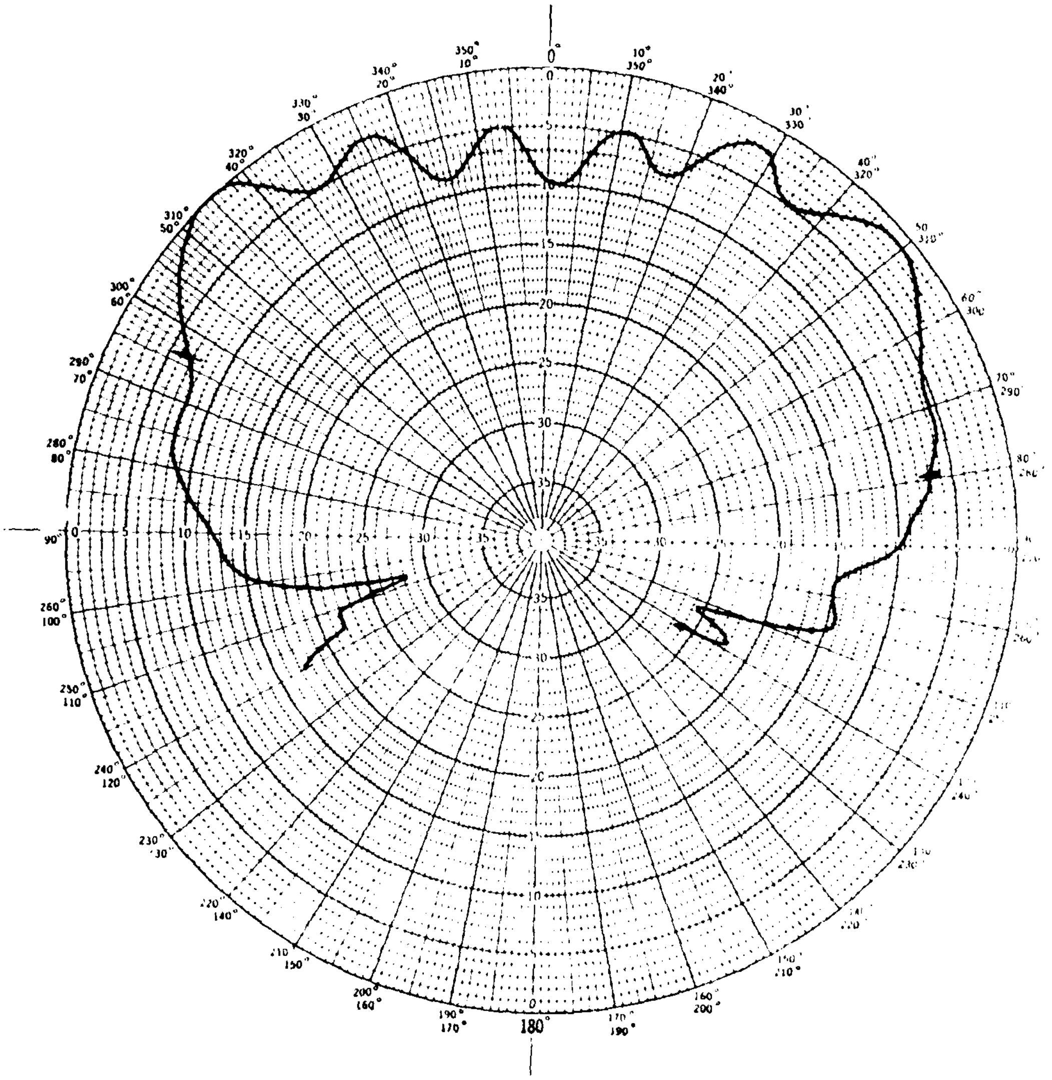

7.5 GHZ

Figure 26. Azimuth Pattern of Vertically Polarized CCN Array (Sheet 4 of 4)

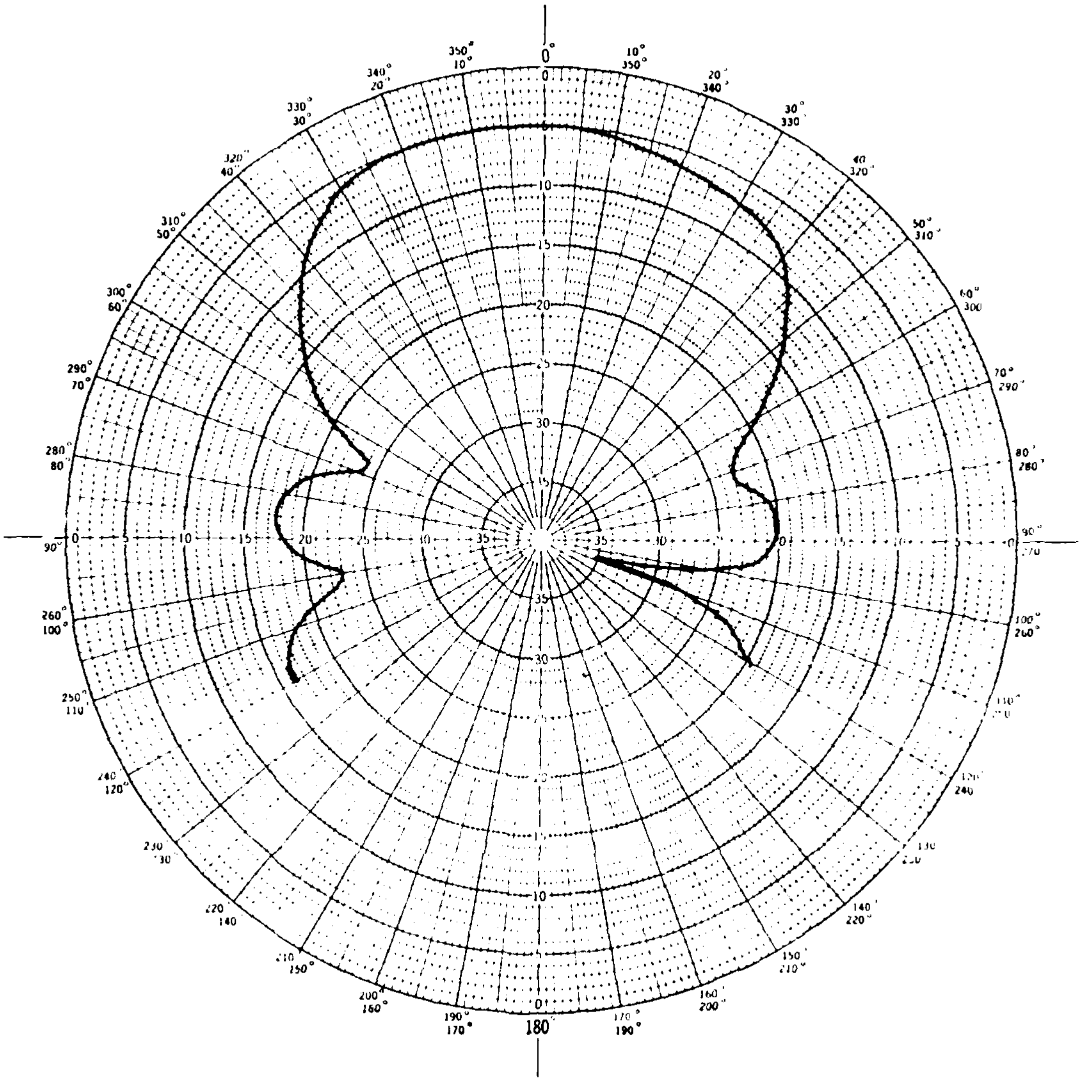

3.75 GHZ

Figure 27. Azimuth Pattern of Horizontally
Polarized CCN Array (Sheet 1 of 4)

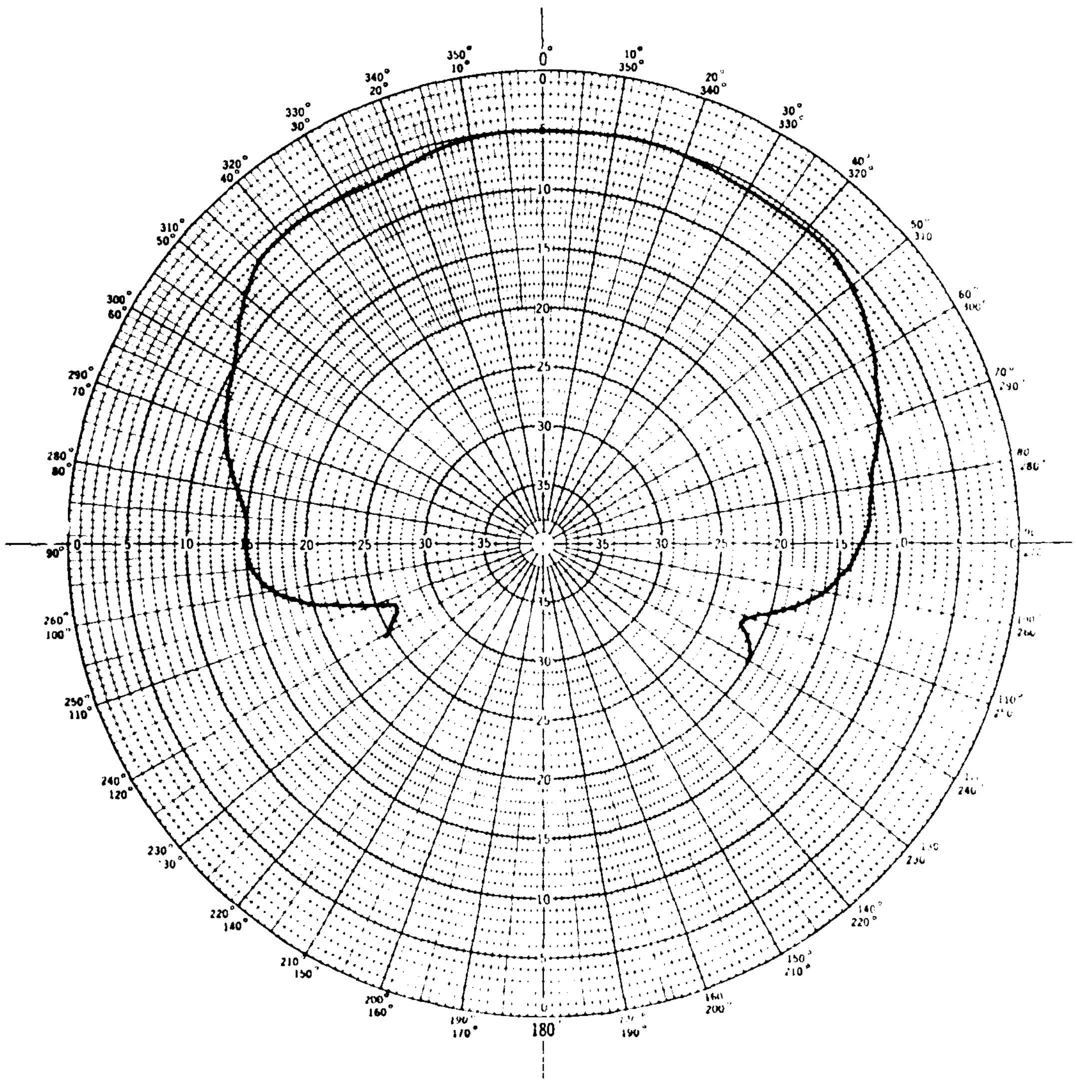

4.75 GHZ

Figure 27. Azimuth Pattern of Horizontally
Polarized CCN Array (Sheet 2 of 4)

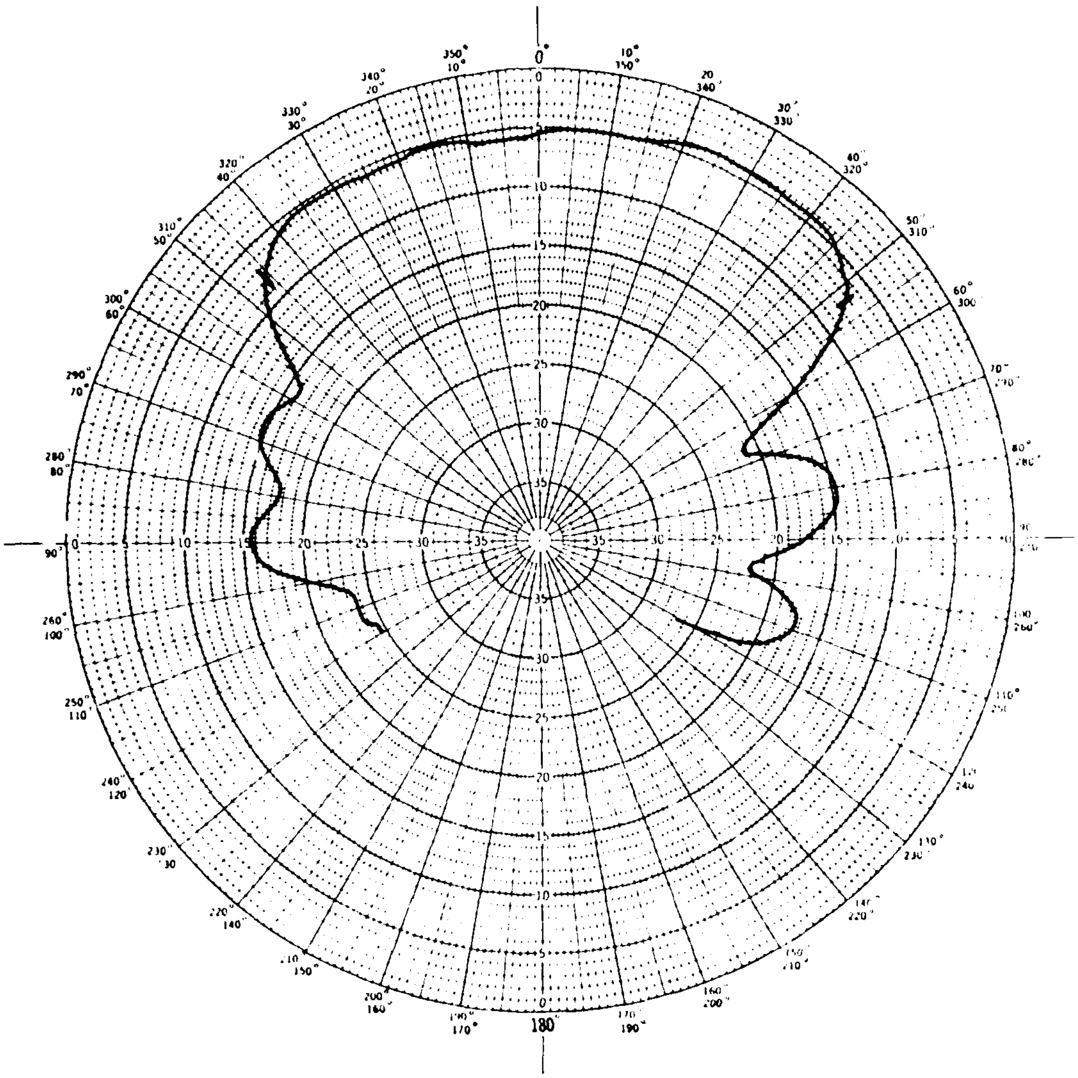

6 GHZ

Figure 27. Azimuth Pattern of Horizontally
Polarized CCN Array (Sheet 3 of 4)

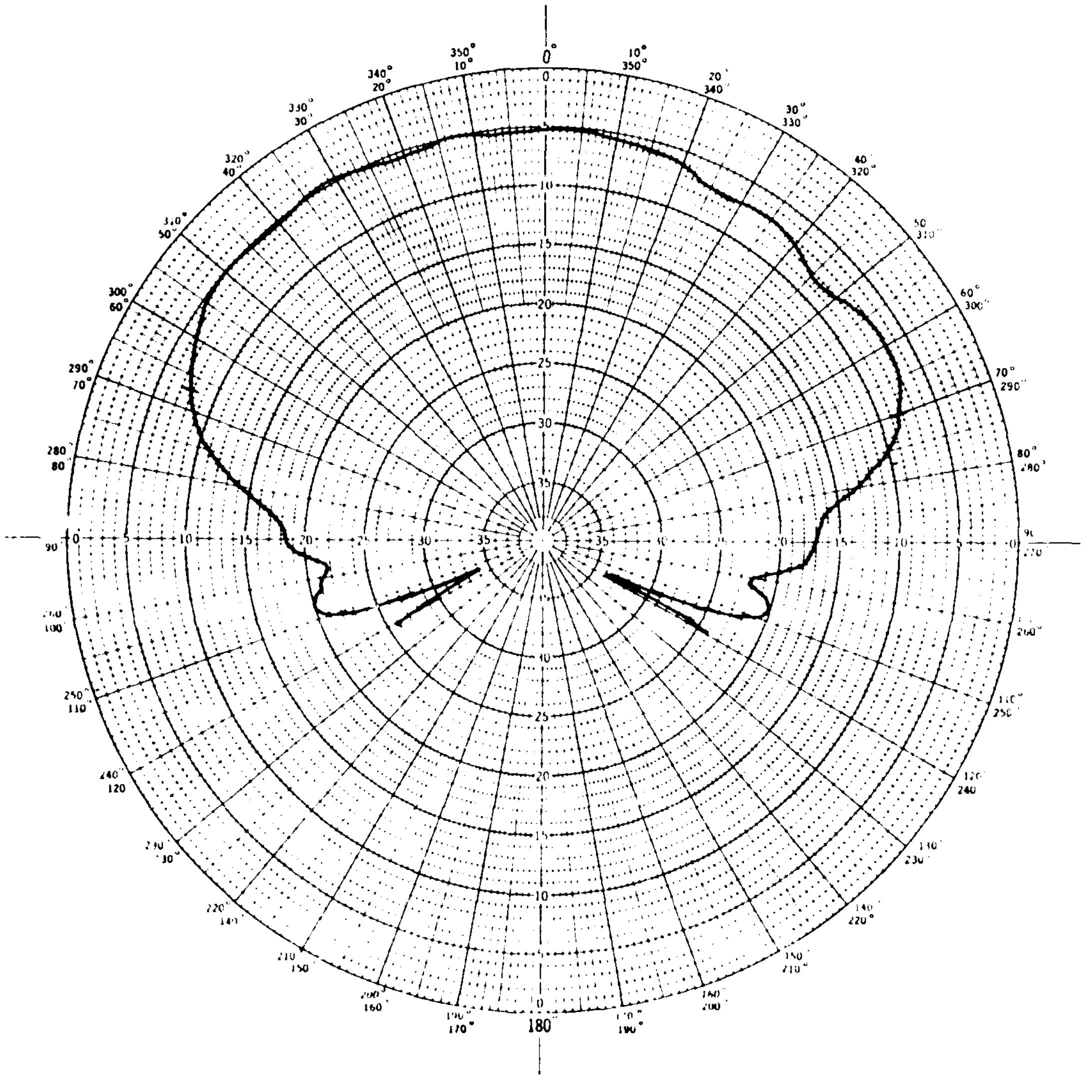

7.5 GHZ

Figure 27. Azimuth Pattern of Horizontally Polarized CCN Array (Sheet 4 of 4)

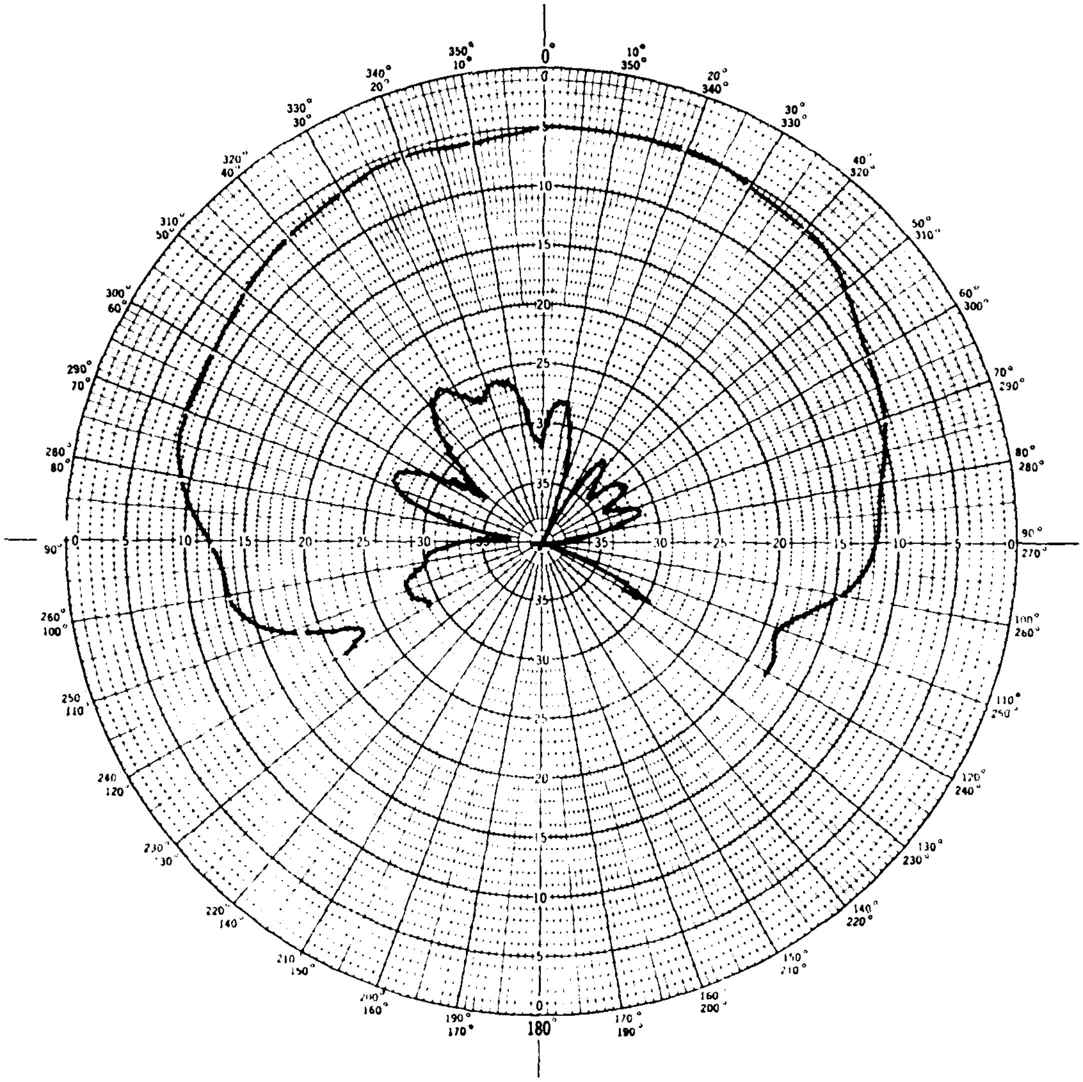

5.25 GHZ

Figure 28. Cross-Polarization (HV) Patterns of CCN Array Element (Sheet 1 of 2)

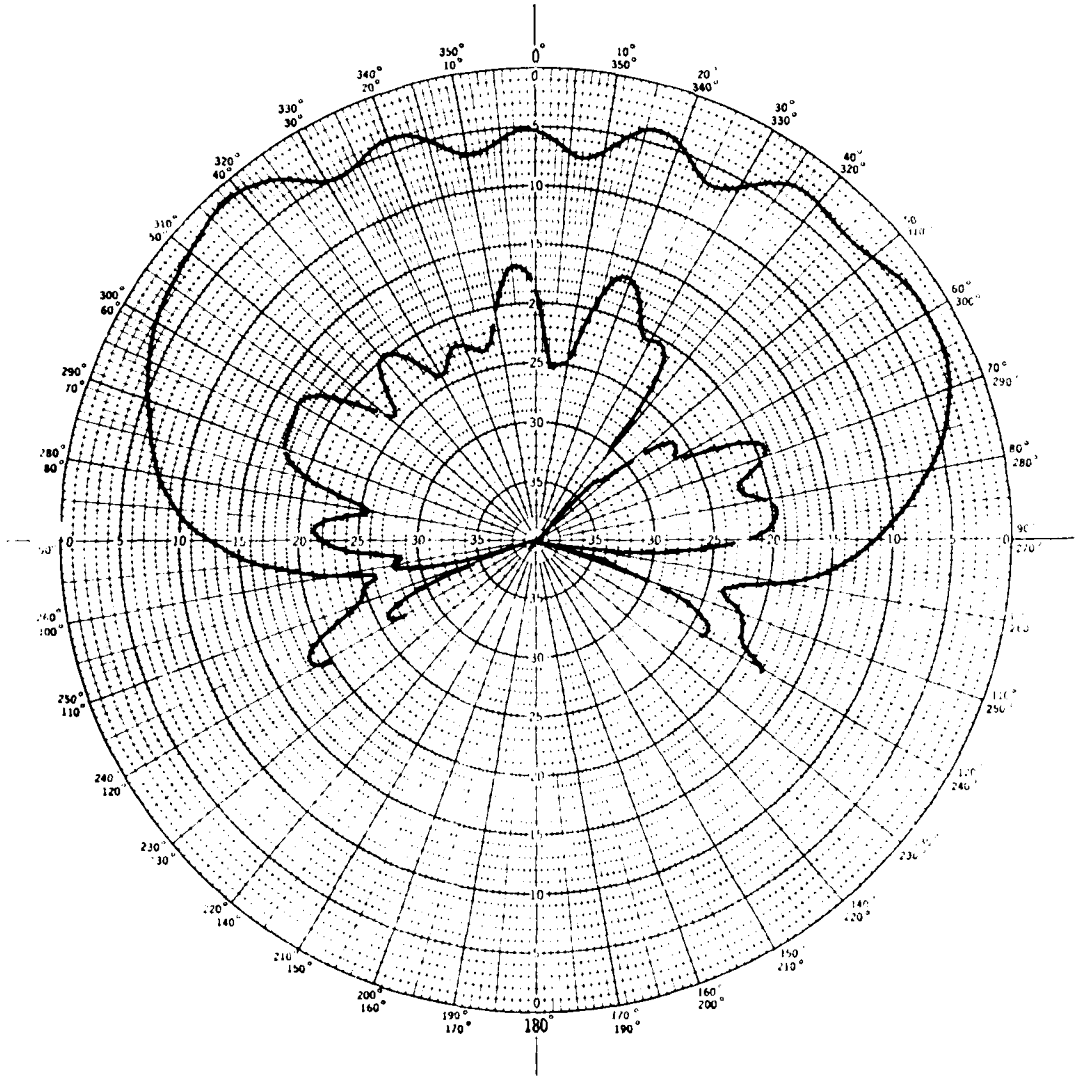

7.25 GHZ

Figure 28. Cross-Polarization (HV) Patterns of CCG Array Element (Sheet 2 of 2)

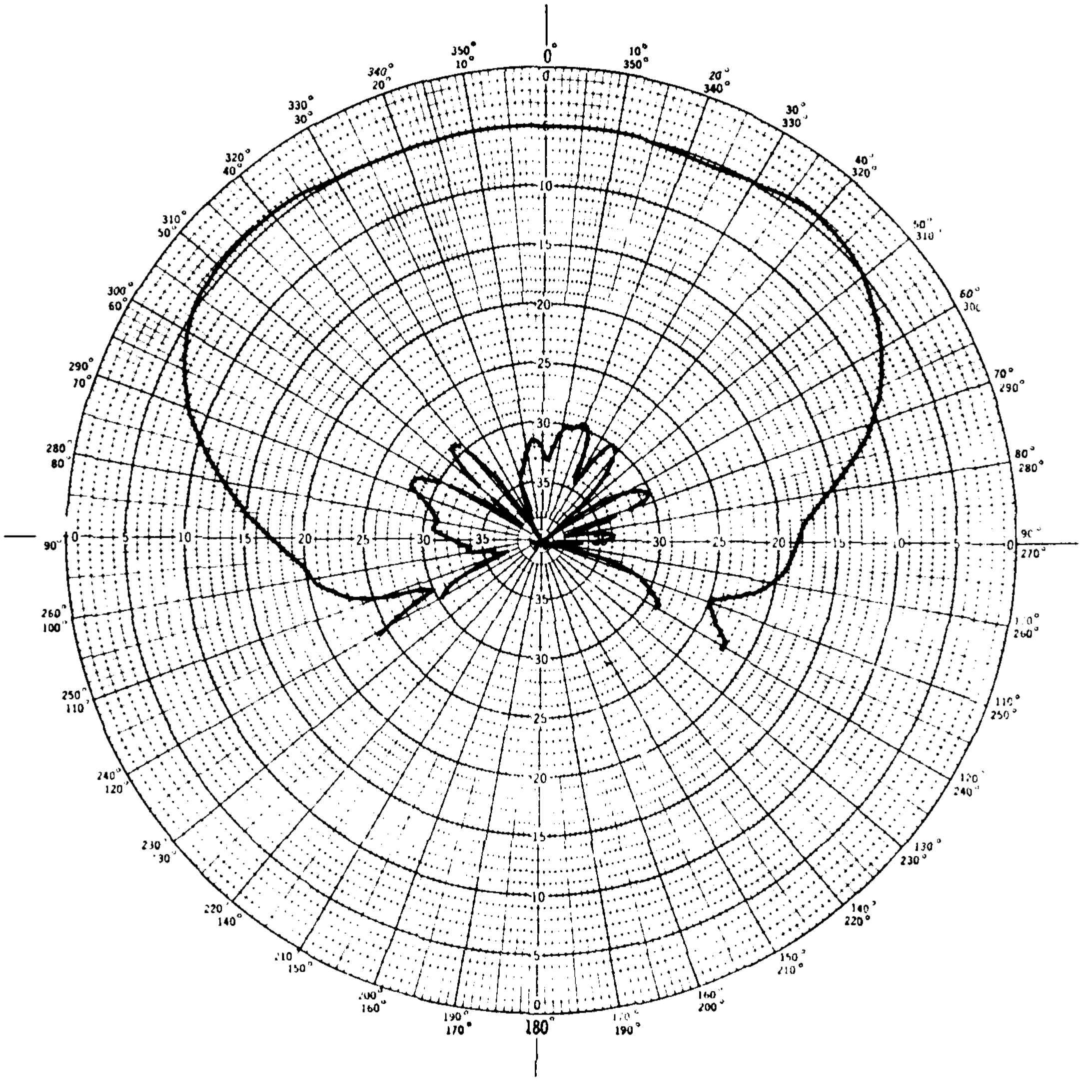

5.25 GHZ

Figure 29. Cross-Polarization (VH) Patterns of CCN Array Element (Sheet 1 of 2)

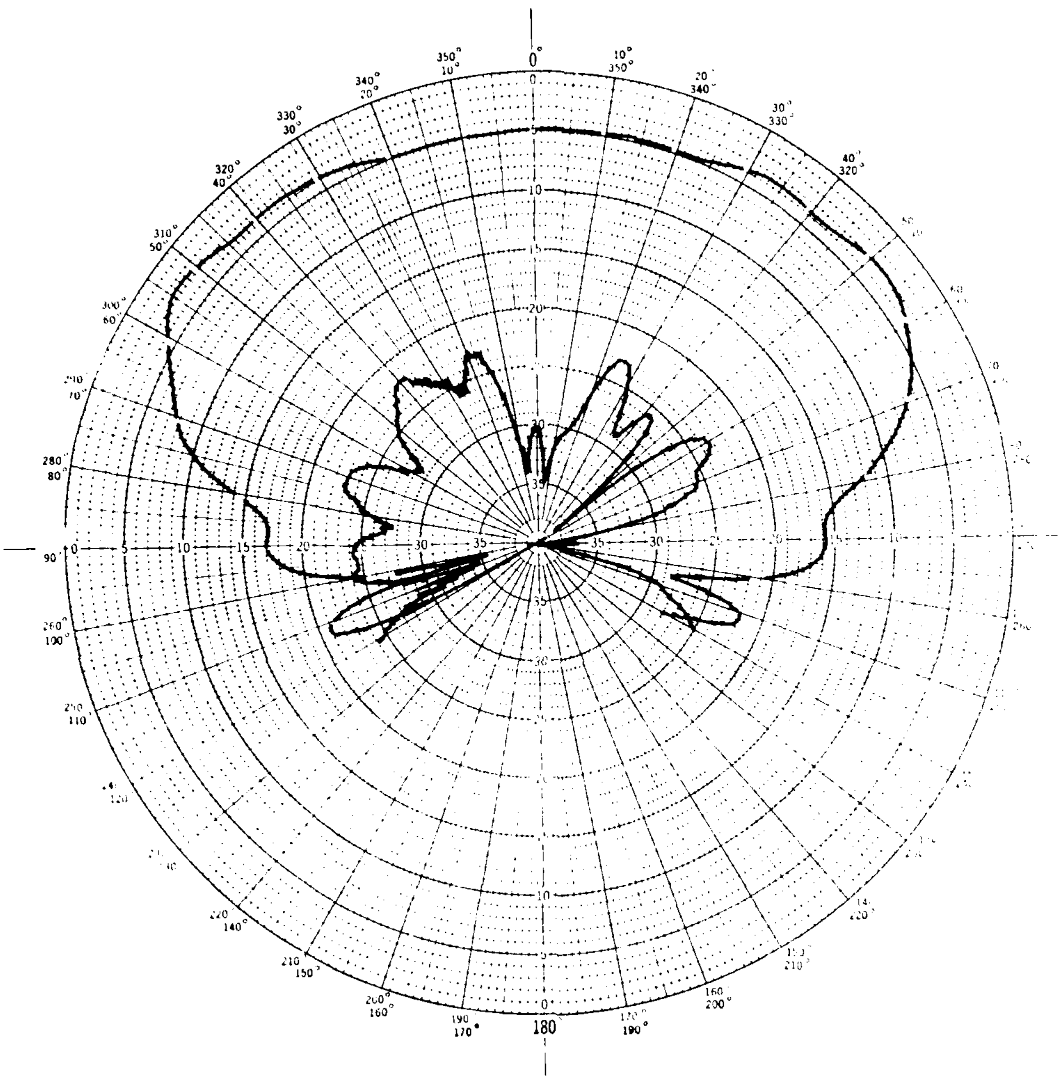

7.25 GHZ

Figure 29. Cross-Polarization (VH) Patterns of CCN Array Element (Sheet 2 of 2)

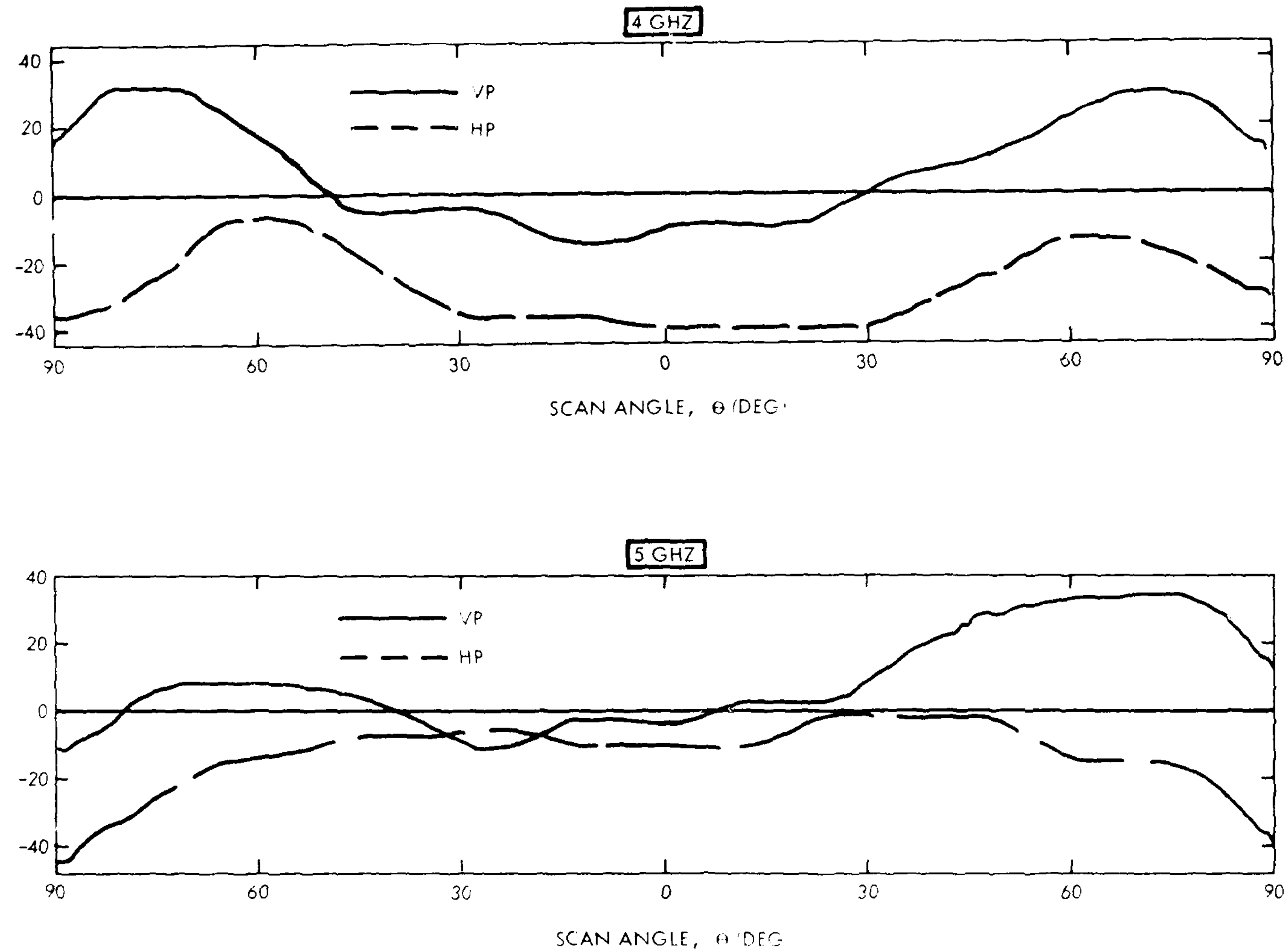

Figure 3[illegible]. Phase Comparison (Part 1 of [illegible])

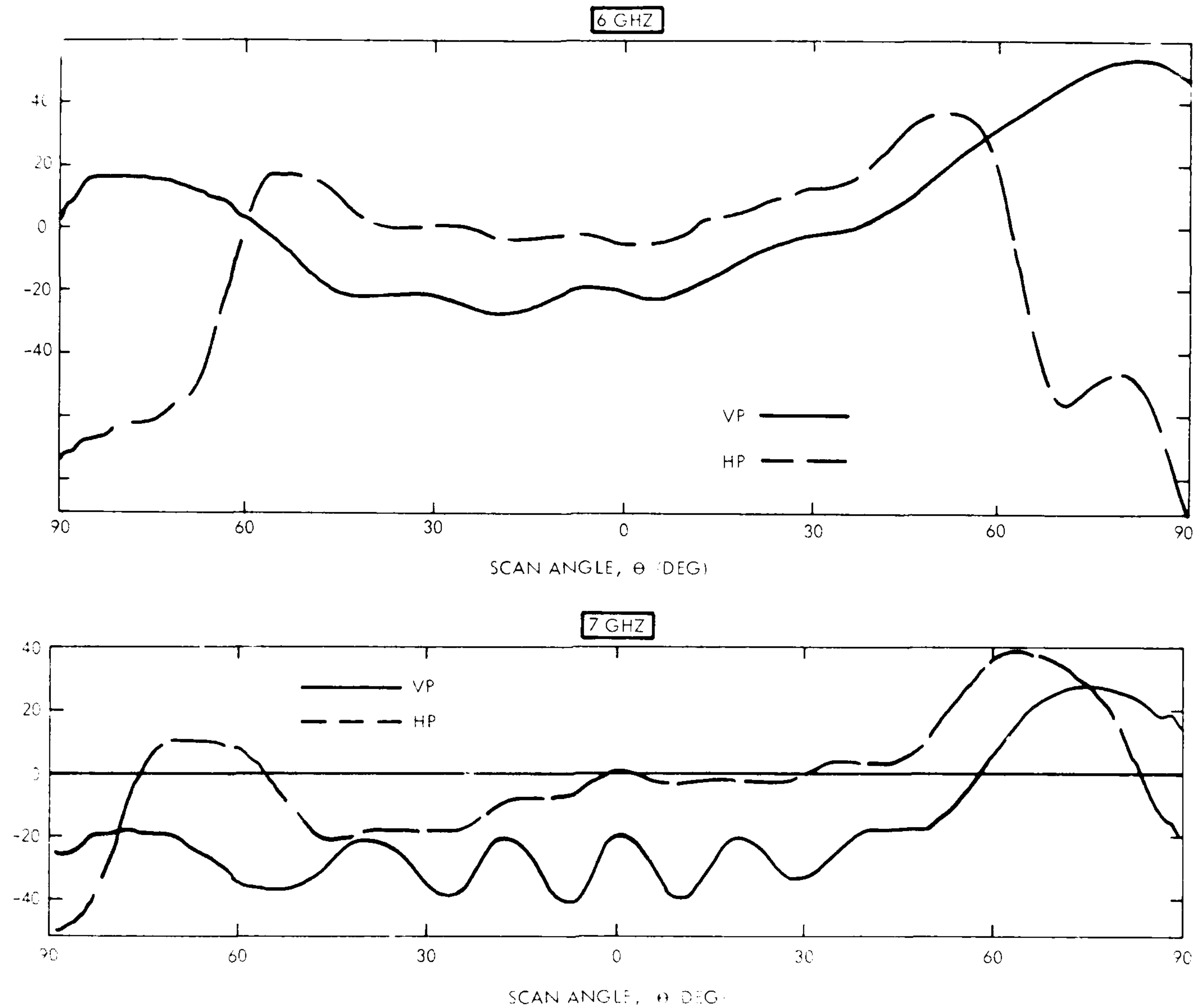

Figure 30. Phase Comparison (Part 2 of 2)

2.6 ESTIMATED GAIN

Actual gain measurements of the present NCN and CCN arrays would be of little use, due to the presence of only three vertical elements. Consequently such data are not presented.

However, estimated directivity of the NCN and CCN elements in a two-dimensional array environment can be derived from a comparison between gain and patterns of the HP linear array, which had very regular patterns, and the HP and VP embedded-element patterns of the NCN and CCN arrays.

A summary of beamwidth appears in Table 1. Notice that, over the 4 to 8-GHz band, the combined beamwidths of the HP linear array and CCN dual-polarization array are in close agreement. Thus one would expect the directivity of the CCN array to closely agree with the directivity of the HP linear element (Figure 12). Element gain may be less in spots, due to VSWR mismatches.

For the NCN array, the VP beamwidth at 5, 6, and 7 GHz is substantially less than the elevation beamwidth of the HP linear array. Consequently, one would expect improved gain at 5, 6, and 7 GHz by about 4, 1.5, and 1 dB, respectively. However, the reduced beamwidth is a significant problem for a wide-scan array.

2.7 PATTERN NULLS IN CROSSED-NOTCH ANTENNAS

The printed-notch element has thus far been found unsuitable for multi-octave, wide-angle scanning in array applications, because of unexplained pattern nulls at angles smaller than those computed by grating lobe criteria. A model for a possible explanation resulting from excitation of a surface wave follows. The frequency of such a pattern null is predicted here, but the strength of the coupling and subsequent depth of the null are not considered.

The crossed-notch array over a ground plane forms a corrugated, reactive structure (Figure 31) which is capable of supporting a guided surface wave. For excitation of the notch elements in the x-z plane (horizontal elements), the polarization is horizontal. This polarization is suitable to couple to a T-M surface wave propagating in the x direction. The governing relation for the surface wave propagation vector in the x direction, k_x, is:

$$k_x{}^2 = k_o{}^2 \, [1 + \tan^2 (k_o t)], \tag{28}$$

where $k_o = \frac{2\pi}{\lambda_o}$ = free-space propagation vector, and t=ground-plane depth.[10]

TABLE 1. BEAMWIDTH COMPARISON

Frequency (GHz)	Beamwidth Degrees 3	4	5	6	7	8	9
Azimuth Beamwidth							
HP Array	160	155	155	119	120	125	123
NCN Array	95	90	100	134	139	143	157
CCN Array	-	97	128	97	130	128	-
Elevation Beamwidth							
HP Array	90	93	95	120	133	140	140
NCN Array	-	-	53	70	90	107	120
CCN Array	-	144	115	133	160	140	-

10 Harrington. "Time Harmonic Electromagnetic Fields." McGraw-Hill, 1961, p 171.

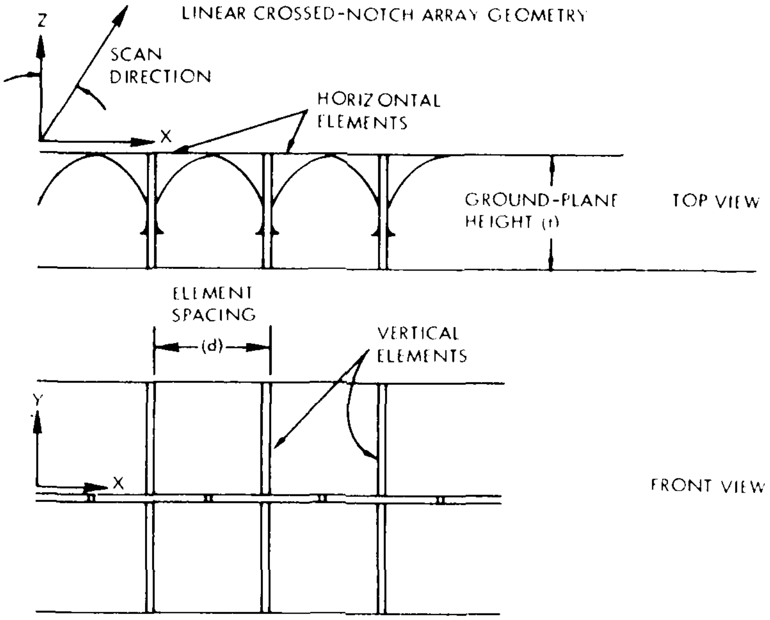

Figure 31. Linear Crossed-Notch Array Geometry

For array scanning at an angle θ, the coupling from all elements to the surface wave will add in phase for

$$k_x = k_0 \sin\theta + \frac{2\pi m}{d}, \tag{29}$$

$$m = \pm 0, 1, 2 \ldots,$$

where d = element spacing. Solving equations (28) and (29) for θ, we have:

$$k_0 \sin\theta + \frac{2\pi m}{d} = \pm \sqrt{1 + \tan^2 (k_0 t)}$$

$$\sin\theta = \pm \frac{1}{k_0 \cos (k_0 t)} - \frac{2\pi m}{k_0 d} \tag{30}$$

For a fixed geometry (t, d constant), we have a surface resonance and pattern null at an angle θ for $k_{o,m}$ such that:

$$\pm \left| \frac{1}{k_o \cos (k_o t)} - \frac{2\pi m}{k_o d} \right| < 1 \qquad (31)$$

Equations (30) and (31) predict nulls which are symetrical with angle, and which move with frequency. Equation (31) has been solved for the design parameters of a 15-element linear, crossed-notch array currently being tested. The frequencies for pattern nulls are listed in Table 2. There are no solutions for the case m = 0. The lowest-order ($m = \pm 1$) solutions are obtained by direct solution of equation (31). Higher moding ($|m|>1$) predictions have been made, taking advantage of the fact that the solutions converge quickly to the same value. We may then take the limit $m = \infty$ in equation (31), and note that the frequency poles for $1/k_o \cos(k_o t)$ are the desired solutions.

TABLE 2. PREDICTED FREQUENCIES OF PATTERN NULLS FOR HORIZONTAL ELEMENTS*

Ground Plane Depth t, Inches	Frequency for Nulls (GHz)	
	Lowest-Order($m = \pm 1$)Modes	Higher-Order Modes
1.4	5.75, 6.75 to 7.5	6.3
1.3	6.0 to 6.25, 7.25 to 8.5	6.8
1.2	6.5 to 6.75, 8.0 to 8.5	7.4
1.1	3.0, 7.0 to 7.5	8.0
1.0	3.5, 7.5 to 8.0	3.0
0.9	3.75, 7.75 to 8.5	3.3
0.8	4.25, 8.0 to 8.5	3.7

* Element spacing d = 0.693 in., variable ground plane depth t, over a frequency band 3.0 to 8.5 GHz.

SECTION III

MICROWAVE CIRCUITS FOR AGILE POLARIZATION

3.1 INTRODUCTION

The 3-D dome allows wide-angle scanning over regions exceeding a hemisphere. Feed arrays for dome applications are simplest if they provide a fixed, linear polarization. However, for such feed arrays, whether flat or curved, the polarization incident on the dome will vary with azimuth direction, resulting in scan-dependent polarization characteristics. For example, a linearly polarized feed array consisting of dipole elements will provide vertical polarization for the plane containing the dipole axis, and horizontal polarization for the orthogonal plane. For intermediate azimuth positions, the polarization will still be linear, but rotating from vertical to horizontal and back again, as azimuth angle is varied. This situation may be circumvented by employing circular polarization in the feed array, but this solution is restrictive and successful only if polarization purity is maintained.

In general, system designs employing dome antennas require some specific polarization over the operating hemisphere. In addition, modern systems are increasingly turning to polarization agility to accomplish their goals. Both situations require that the feed array be capable of providing multiple polarizations, perhaps with high switching rates between the various polarization states. Pervisou analyses have shown that the dome will transmit any incident polarization with essentially no change. The burden of providing polarization agility is therefore placed on the feed array.

One technique for generating polarizations employs a crossed, linear-array element fed with some appropriate polarization selection circuit. Many crossed (dual) linear elements may be employed including crossed dipoles, crossed slots, square or circular waveguide, etc. Reference[11] describes the polarization characteristics for such dual linear elements, using the crossed slot as an example.

While the radiating characteristics of the element are important, the characteristics of the element feed network are equally important in establishing overall antenna performance. Many types of polarization selection circuits are possible, the choice depending on the number of polarizations states desired, the amount of loss which may be tolerated, and the speed required to go from state to state. This discussion addresses three specific feed array polarization requirements:

1. "Rotatable linear polarization," for which the tilt angle may be "continuously" varied over a 180-degree range; this capability allows the polarization external to the dome to remain fixed as a function of scan (azimuth) angle.

2. "Selectable polarization," which allows the feed array polarization to be chosen from among a limited number of fixed states; all of these circuits provide at least one pair of orthogonal polarization states, and the selection of states can be made in a random manner.

3. "Completely arbitrary polarization," which allows the selection of any polarization state; this capability requires the greatest complexity in the polarization selection circuit.

---

11 Holst, D.W. "Cross Slot Polarization Characteristics Over Hem sphere." Raytheon memo 9282/DWH/071, 23 Feb. 1979.

The following paragraphs describe the relevant circuits and some of their operating characteristics.

3.2 ROTATABLE LINEAR POLARIZATION

A feed circuit to provide rotatable linear polarization is presented in Figure 32. This circuit is basically a variable power divider which splits the power to the two crossed linear elements to achieve a polarization rotation. This circuit consists of two 3-dB hybrids and a multi-bit phase shifter. A signal at the input of the network is divided between the crossed linear elements in a ratio determined by the value of the phase shifter. The ouput signals are either in phae or 180 degrees out of phase, regardless of the phase shifter setting. This condition is necessary to maintain a linearly polarized signal in space.

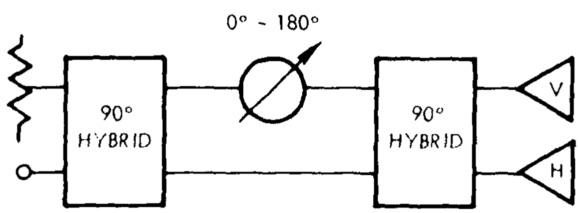

Figure 32. Variable Power-Divider Circuit to Provide Rotatable Linear Polarization

The polarization rotation obtained depends on the granularity of the multi-bit phase shifter. There is a 2:1 relationship between the bit size and rotation. It takes two degrees of phase shift to change the polarization tilt angle by one degree. For dome operation with constant linear polarization independent of azimuth angle, a rotation of up to 180 degrees is required.

Analysis of the circuit of Figure 32 provides the following relations for determining the polarization tilt angle, where ϕ is the phase shifter setting:

$$\left| \frac{E_V}{E_H} \right| = \sqrt{\frac{1 - \cos \phi}{1 + \cos \phi}} \tag{32}$$

$$\text{Tilt Angle} = \tau = \tan^{-1} \left(\frac{E_V}{E_H} \right) \tag{33}$$

$$E_V = (\cos \phi - 1) + i \sin \phi \tag{34}$$

$$E_H = \sin \phi - i(\cos \phi + 1) \tag{35}$$

Results obtained from these expressions are presented in Table 3. The consequences of a limited number of bits n in a multi-bit phase shifter are shown below.

TABLE 3. ROTATABLE LINEAR CHARACTERISTICS

No. of Bits, n	Smallest Bit (Deg)	Polarization Rotation, τ (Deg)	Polarization Crosstalk (dB) $\left\|\frac{E_V}{E_H}\right\|$	Additional Polarization Losses (dB)
1	180	90	∞	∞
2	90	45	0	-3.01
3	45	22.5	-7.65	-0.69
4	22.5	11.25	-14.03	-0.17
5	11.25	5.63	-20.13	-0.04

ϕ (Deg)	$\left\|\frac{E_V}{E_V}\right\|$	$\angle E_Y$ (Deg)	$\angle E_X$ (Deg)	$\angle E_Y - \angle E_X$ (Deg)	τ (Deg)
180	∞	-	-	-	-90
179	114.5887	179.5	-0.5	180.0	-89.5
150	3.7321	165.0	-15.0	180.0	-75
120	1.7321	150.0	-30.0	180.0	-60
90	1.0	135.0	-45.0	180.0	-45
60	0.5774	120.0	-60.0	180.0	-30
40	0.3640	110.0	-70.0	180.0	-20
20	0.1763	100.0	-80.0	180.0	-10
1	0.0087	90.5	-89.5	180.0	-0.5
0	0				0
-1	0.0087	-90.5	-90.5	0	+0.5
-20	0.1763	-100.0	-100.0	0	+10
-40	0.3640	-110.0	-110	0	+20
-60	0.5774	-120.0	-120.0	0	+30
-90	1.0	-135.0	-135.0	0	+45
-120	1.7321	-150.0	-150.0	0	+60
-150	3.7321	-165.0	-165.0	0	+75
-179	114.5887	-179.5	-179.5	0	+89.5
-180	∞	-	-	-	+90

Obviously the polarization rotation increment becomes finer with an increasing number of bits, as shown by the third column. The last two columns refer to a horizontally polarized incident wave. The fourth column provides the $|E_V/E_H|$ ratio as given by equation (32); i.e., the signal response in the vertical element relative to that in the horizontal element for incident horizontal polarization. This is a measure of isolation as a function of the number of bits employed.

The last column provides the polarization loss for an element with the indicated polarization tilt angles corresponding to the horizontally polarized incident wave. This loss must be added to the insertion loss of the polarization circuit. Note that, for three or more bits, the polarization loss is small.

It should be mentioned that one additional phase shifter in the V or H output arm of Figure 32 is required in order to obtain any specified polarization. This phase shifter must be capable of providing 360 degrees of phase shift.

3.3 SELECTABLE POLARIZATION

The circuits shown in Figure 33 through 35 which are capable of providing a number of fixed polarization states. Two, three, four, and six-state circuits are indicated, with circuit complexity obviously increasing with the number of states provided. Each circuit provides at least one pair of orthogonal polarizations, while the four and six-state circuits provide two and three orthogonal pairs, respectively.

Phase shifters used in these circuits are single-bit phase shifters of the value indicated. By use of diode phase shifters, the polarization state may be rapidly changed to implement system requirements. Required phase shifter settings for the available states for each circuit are indicated in the figures.

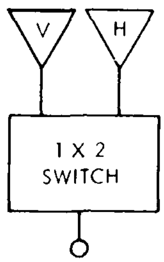

(A) SWITCHABLE ORTHOGONAL LINEAR

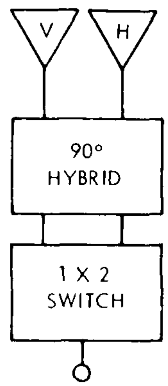

(B) SWITCHABLE ORTHOGONAL CIRCULAR,
TWO-PORT FEED

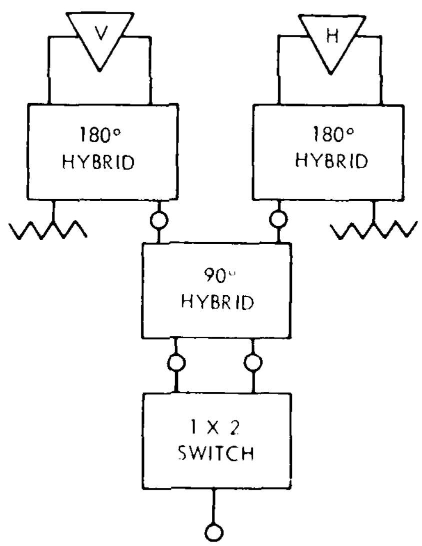

(C) SWITCHABLE ORTHOGONAL CIRCULAR,
FOUR-PORT FEED

Figure 33. Two-State Polarization Circuits

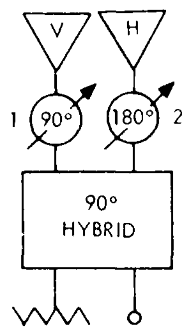

POLARIZATION	STATES
DIAGONAL:	1 = 90°, 2 = 180°
RHCP:	1 = 0°, 2 = 180°
LHCP:	1 = 0°, 2 = 0°

(A) VARIABLE PHASE SHIFTER

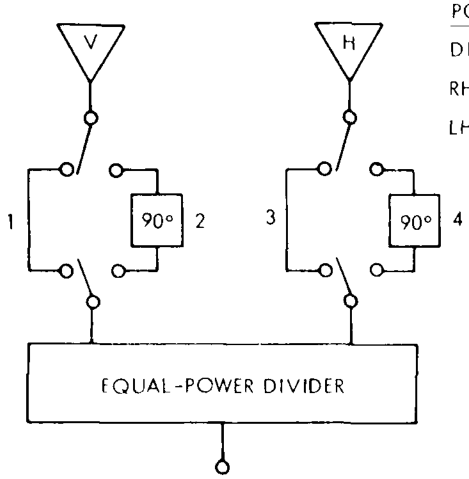

POLARIZATION	STATES
DIAGONAL:	1 AND 3, 2 AND 4
RHCP:	1 AND 4
LHCP:	2 AND 3

(B) FIXED-PHASE SHIFTER

Figure 34. Three-State Polarization

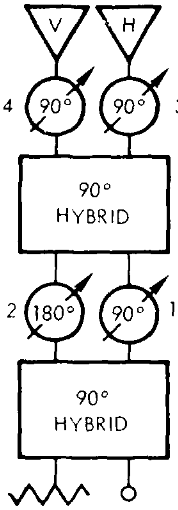

POLARIZATION	STATES
VERTICAL:	1 2 3 4 0°
HORIZONTAL:	2 180°, 1 3 4 0°
RHCP:	1 4 90°, 2 3 0°
LHCP:	1 3 90°, 2 4 0°

(A) FOUR-STATE CIRCUIT

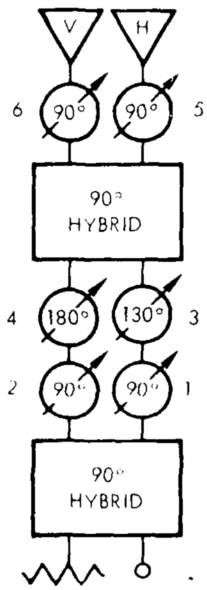

POLARIZATION	STATES
VERTICAL:	1 = 2 = 3 = 4 = 5 = 6 = 0°
HORIZONTAL:	4 = 180°, 1 = 2 = 3 = 5 = 6 = 0°
RHCP:	1 = 5 = 90°, 2 = 3 = 4 = 6 = 0°
LHCP:	1 = 6 = 90°, 2 = 3 = 4 = 5 = 0°
DIAGONAL:	1 = 90°, 2 = 3 = 4 = 5 = 6 = 0°
DIAGONAL:	2 = 90°, 4 = 180°, 1 = 3 = 5 = 6 = 0°

(B) SIX-STATE CIRCUIT

Figure 35. Four- and Six-State Polarization Circuits

AD-A093 214 RAYTHEON CO GOLETA CALIF ELECTROMAGNETIC SYSTEMS DIV F/G 9/5
AGILE POLARIZATION FEED ARRAY FOR 3-D DOME ANTENNA.(U)
NOV 80 D T THOMAS, S D BIXLER, C J LAUER N00014-78-C-0690

UNCLASSIFIED NL

2 of 2

END
DATE FILMED
1-8
DTIC

To obtain an estimate of the insertion loss for each circuit, three typical octave bands were considered. Table 4 gives an estimate of losses for the individual components comprising the various circuits; i.e., hybrids, phase shifters, and switches. Losses are indicated for the 1 to 2, 4 to 8, and 8 to 16-GHz octave bands. These values are representative of the state of the art for these components and frequency ranges. Table 5 gives an estimate of the total loss to be expected for each circuit configuration. The indicated loss figures do not include connecting transmission line loss, since this is a variable which depends on specific system layout. As such, the loss values indicated in Table 5 represent best-case values; they may be expected to increase somewhat, depending on the final layout. For those circuits having phase shifters, the loss is different for the on and off states. In these instances, the appropriate value of loss was selected for each polarization state.

It should be noted that, due to the various combinations of on and off phase-shift states, there generally is an amplitude imbalance between the V and H arms as polarization is changed. This imbalance derives from the differential loss in the two paths resulting from the selected phase-shifter settings, and ranges between 0.2 and 1.0 dB. As a result, signal cancellation in hybrid output arms is not complete, since amplitudes are not equal. This leads to high-amplitude, cross-polarized components, and makes it impossible to achieve high-purity circular polarization.

The speed with which polarization states may be changed depends on the speed of the phase shifters. For diode phase shifters, in-house studies indicate switching speeds under 100 ns and power handling of about 10 watts CW per circuit. Switch rates of the order of 1 MHz and greater appear reasonable.

TABLE 4. TYPICAL COMPONENT LOSSES

Component	Frequency Band		
	1 - 2 GHz	4 - 8 GHz	8 - 16 GHz
90° Hybrid	0.25 dB	0.4 dB	1.2 dB
180° Hybrid	0.5 dB	0.6 dB	1.3 dB
1 x 2 Switch	1.0 dB	1.5 dB	2.2 dB
180° Phase Shifter (off state)	0.75 dB (0.5 dB)	1.0 dB (0.6 dB)	1.4 dB (0.9 dB)
90° Phase Shifter (off state)	0.8 dB (0.5 dB)	1.1 dB (0.7 dB)	1.5 dB (1.0 dB)
45° Phase Shifter (off state)	0.9 dB (0.6 dB)	1.2 dB (0.8 dB)	1.6 dB (1.1 dB)
22-1/2° Phase Shifter (off state)	1.0 dB (0.6 dB)	1.3 dB (0.9 dB)	1.8 dB (1.2 dB)
3-dB Power Divider	0.3 dB	0.7 dB	0.9 dB

TABLE 5. SUMMARY OF POLARIZATION CIRCUIT LOSSES

Polarization Circuit	Figure No.	Polarization State	Losses (dB) 1 - 2 GHz	4 - 8 GHz	8 - 16 GHz
Two-State	33(A)	Vertical	1.0	1.5	2.2
		Horizontal	1.0	1.5	2.2
	33(B)	RHCP	1.25	1.9	3.4
		LHCP	1.25	1.0	3.4
	33(C)	RHCP	1.75	2.5	4.7
		LHCP	1.75	2.5	4.7
Three-State	34(A)	RHCP	1.1	1.4	2.6
		LHCP	0.75	1.1	2.2
		Diagonal	1.1	1.5	2.7
	34(B)	RHCP	0.6	1.4	1.8
		LHCP	0.6	1.4	1.8
		Diagonal	0.3	0.7	0.9
Four-State	35	Vertical	1.5	2.2	4.4
		Horizontal	1.75	2.3	4.8
		RHCP	2.1	3.0	5.4
		LHCP	2.1	3.0	5.4
Five-State	36	Vertical	2.0	2.8	5.3
		Horizontal	2.25	3.2	5.8
		RHCP	2.6	3.6	6.3
		LHCP	2.6	3.6	6.3
		+45° Slant			
		-45° Slant			

3.4 COMPLETELY ARBITRARY POLARIZATION

As mentioned previously, arbitrary polarization may be obtained using the circuit of Figure 32 with the addition of a 360-degree phase shifter in either the V or H output arm. The purity of all polarization states is a function of the amplitude and phase balance achieved in the two output arms. Studies regarding the necessary balances for rotatable linear polarization are described in reference[12]. Similar conclusions are obtained when considering arbitrary polarization states of specified purity.

The circuit of Figure 32 is repeated in Figure 36(A), with the additional 360-degree phase shifter on one output arm. This circuit may be configured into a more balanced structure, as shown in Figure 36(B). Phase shifters have been placed in both arms, and the total required phase shift per device has been reduced by one-half. Amplitude and phase tracking between output arms should be much improved, limited only by the tracking of the individual components. Losses for this circuit depend on the number of bits employed in each phase shifter, and can be as high as 8 to 10 dB.

3.5 CONCLUSIONS

Microwave circuits may be configured to provide diverse polarizations from array antennas. However, circuit complexity, cost, and insertion loss increase rapidly with the number of polarization states to be provided. It is most important to specify polarization requirements carefully to minimize impact on overall system performance.

---

12 Maybell, M.J., and Miller, M.D. "A Linearly Polarized Antenna with an Electronically Agile Polarization Tilt Angle." Raytheon ESD, 20 Mar. 1979.

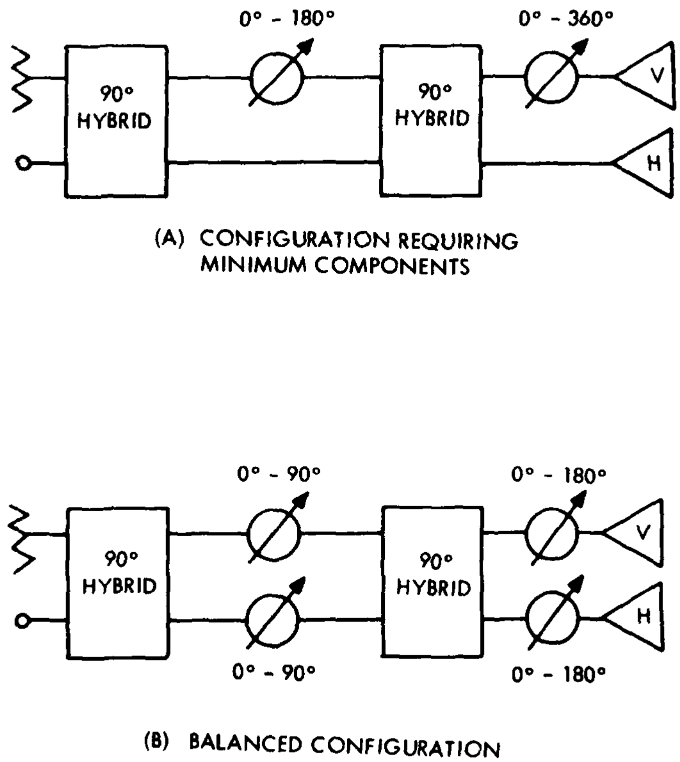

Figure 36. Completely Arbitrary Polarization

SECTION IV
SUMMARY

4.1 PROGRESS MADE

The operational requirements of the 3-D dome antenna were investigated to establish the polarization performance required of the feed array portion. A trade study was conducted to identify potential candidates for octave-bandwidth, dual-polarization elements and the accompanying polarization sensing and agility circuits which meet the required performance.

A typical crossed-slot element was studied to determine its polarization performance over hemispherical coverage. The results show essentially circular polarization for $0 < \theta < 60$ degrees (less than 6-dB axial ratio). The crossed-notch element was then studied to determine its suitability for broadband performance. It was found that predicted pattern nulls would exist at frequencies spaced greater than one octave apart. Thus, the crossed-notch design can serve as an octave-bandwidth approach, with no null distortions. The crossed-notch element was selected as the best element for design, fabrication, and test. Three test pieces were examined.

1. a linear array of crossed-notch elements,

2. noncoincident-crossed-notch (NCN) array, and

3. coincident-crossed-notch (CCN) array.

Tests on these three pieces indicate that:

1. the beamwidth of each is adequate for internal illumination of the dome surface over the octave bandwidth (Table 1);

2. VP to HP isolation is greater than 20 dB for the NCN design;

3. VSWR is smooth enough over an octave bandwidth to provide adequate uniformity of illumination over the dome (the variation of VSWR with scan angle and frequency is a concern which should be addressed to widen the bandwidth); and

4. although the CCN has a broader beamwidth in one polarization, the NCN is favored because beamwidths of orthogonal polarizations more closely aree, making the element more independent of orientation (if the current deeper dome design is used, a slightly narrower element beamwidth can be tolerated, and the NCN design can offer more gain).

Polarization agility circuits were examined to determine the most suitable approach for the chosen element feed. As could be expected, granularity in polarization-setting ability can be traded off against loss, cost, and complexity.

4.2 CONCLUSIONS

Use of a deeper-than-hemispherical dome, such as a prolate spheroid, reduces the scan-angle requirement of the feed array elements. This leads to two improvements:

1. Feed Array VSWR variation over an octave bandwidth is greatly reduced for scan angles less than 40 degrees.

2. Dome illumination is less sensitive to variations in element pattern beyond a 45-degree scan angle.

Although computer-controlled circuits are used in the agile polarization concept described in this report, the complexity of beam steering and shaping control, multiplied by that of the polarization agility control, would represent a great increase in complexity over current, simpler phase-shifted array controls. It is believed that the lens-fed array approach is simpler and more promising than the totally electronic steering approach for the dome feed, especially for wide-band and multiple-beam applications.

4.3 RECOMMENDATIONS

The array elements examined were proven to be adequate for octave bandwidth performance. It is felt that other elements, such as the quad-ridge guide, should be examined for use in order to avoid the pattern nulls inherent in the crossed-notch approach, improve VSWR characteristics, and permit wider-band operation.

Careful thought should be given to tradeoff of depolarization losses associated with circularly polarized elements in linearly polarized radiation compared to the RF losses associated with the circuit necessary for agile polarization. Hardware development of agile polarization circuits and/or concepts is necessary to establish feasibility and performance characteristics.

BIBLIOGRAPHY
POLARIZATION AGILE ARRAYS

POLARIZATION ANALYSIS

1. Chu, T.S., and R.G. Kouyoumjian. "An Analysis of Polarization Variation and Its Application to Circularly - Polarized Radiators." IRE Trans. Ant. & Prop., Vol. AP-10, No. 2, March 1962, p. 188.

2. English, W., et al. "Polarization Diagrams for CP Antenna Analysis." IEEE/AP-S Inter Symp. Digest, October 1976, p. 286.

3. Lewis, R.M. "Geometrical Optics and the Polarization Vectors. "IEEE Trans. Ant. and Prop., Vol. AP-14, No. 1, January 1966, p. 100.

4. Rumsey, et al. "Techniques for Handling Elliptically Polarized Waves with Special Reference to Antenna." IRE Proceedings, Vol. 39, No. 5, May 1951, p. 533.

5. Scott, W.G.. "Antenna Pattern Topology." IEEE/G-AP Inter. Symp. Digest, December 1969, p. 35.

6. Scott, W.G. "Rotating Pseudo-Patterns on the Far Field Sphere of Circularly Polarized Antennas." IEEE/G-AP Inter. Symp. Digest, September 1970,p. 289.

7. Scott, W.G. "Polarization Ellipse Orientation on the Antenna Radiation Sphere." IEEE/AP-S Inter. Symp. Digest, p. 246.

ELEMENTS

8. Alexopoulas, N.G., and J.E. Armstrong. "On the Design of a Circularly Polarized Waveguide Narrow Wall Radiating Element." IEEE/G-AP Inter. Symp. Digest, August 1973, p. 332.

9. Chen, M.H., and G.N. Tsandoulas. "A Wide-Band Square-Waveguide Array Polarizer." IEEE Trans. Ant. and Prop., Vol. AP-21, No. 3, May 1973, p. 389.

10. Chen, M.H., and G.N. Tsandoulas. "Bandwidth Properties of Quad-Ridged Circular and Square Waveguide Radiators." IEEE/G-AP Inter. Symp. Digest, August 1973, p. 391.

11. Fasset, M. and J. Toth. "Broadband Segmented Aperture Feed Program, Final Report, AFAL-TR-76-5." Raytheon Co., Bedford, Mass, AFAL Contract F33615-74-C-1071, April 1974 to November 1975.

12. Fisher, R.E., et al. "Digital-Reflection-Type Microwave Phase Shifters." Microwave Jour., Vol. 12, No. 5, May 1969, p. 63.

13. Goebels, F.J., and K.C. Kelly. "Arbitrary Polarization from Annular Slot Antennas." IRE Trans. Ant. and Prop., Vol. AP-9, No. 4, July 1961, p. 342.

14. Gregorwich, W.S. "A Multipolarization Dual-Band Array." IEEE/AP-S Inter. Symp. Digest, June 1975, p. 189.

15. Herskind, R.E. "A Circular Slot Aperture with Arbitrary Polarization for Missile Applications." 18th Annual ASAF Antenna Res. and Dev. Symp., Robert Allerton Park, October 1968.

16. Hines, J.N., and J. Upson. "A Line Source with Variable Polarization." IRE Trans. Ant. & Prop., Vol. AP-6, No. 1, January 1958, p. 152.

17. Hunt, J., and P. Ventresca. "Large Bandwidth Antenna with Multipolarization Capability." Proc. Ant. Application Symp., Robert Allerton Park, April 1977.

18. Komlos, S.G., et al. "Feed System for Clockwise and Counterclockwise Circular Polarization." IRE Trans. Ant. and Prop., Vol. AP-9, No. 6, November 1961, p. 577.

19. Lamensdorf, D. "A Polarization Independent Element for an Electromagnetic Lens." IEEE/AP-S Inter. Symp. Digest, October 1976, p. 481.

20. Lewis, R.M., M. Fassett., and J. Hunt. "A Broadband Stripline Array Element." IEEE/AP-S, Inter. Symp. Digest, June 1974, p. 335.

21. Lewis, R.M., et at. "Design and Analysis of Broadband Notch Antennas and Arrays." IEEE/AP-S Inter. Symp. Digest, October 1976, p. 44.

22. Lewis, L.R., and J. Pozgay. "Broadband Antenna Study, Final Report., AFCRL-TR-75-0178." Raytheon Co., Bedford, Mass., AFCRL Contract F19628-72-C-0202, January 1972 to March 1975.

23. Lopez, A.R. "Wideband Dual-Polarized Element for a Phased Array." 23rd Annual USAF Antenna Res. and Dev. Symp., Robert Allerton Park, October 1973.

24. Miersch, H.K. "Wideband Polarization Diversity." Microwaves, Vol. 8, No. 10, October 1969, p. 50.

25. Montgomery, J.P. "Ridged Waveguide Phase Array Elements." IEEE Trans. Ant. and Prop., Vol. AP-24, No. 1, January 1976, p. 46.

26. Schennum, G.H. "A Dual-Frequency Coaxial Feed for a Prime Focus Antenna." IEEE/G-AP Inter. Symp. Digest, August 1973, p. 236.

27. Scherer, G., and W. Mohucky. "Wideband Phased Array Element with Rotatable Linear Polarization." 23rd Annual USAF Antenna Res. and Dev. Symp., Robert Allerton Park, October 1973.

BIBLIOGRAPHY (CONT)

28. Stalzer, H.J. "Modes of Crossed Rectangular Waveguide." IEEE Trans. Ant. and Prop., Vol. AP-24, No. 2, March 1976, p. 220.

29. Tung, T.K. and C.C. Liu. "Coaxial Open-Waveguide--A Broadband Multimode Monopulse Antenna." IEEE/AP-S Inter. Symp. Digest, June 1977, p. 108.

30. Wallace, M.E., et al. "Polarization Agile Antennas." 17th Annual USAF Antenna Res. and Dev. Symp., Robert Allerton Park, November 1967.

ARRAY PERFORMANCE

31. Anderson, J.B., et al. "Coupling Between Crossed-Dipole Feeds." IEEE Trans. Ant. & Prop. Vol. AP-22, No. 5, September 1974, p. 641.

32. Bailey, M.C. "Mutual Coupling in a Finite Size Phased Array of Circular Waveguide Elements, IEE/G-AP Inter. Symp. Digest, December 1972, p. 161.

33. Byron, E.V. and J. Frank. "On the Correlation Between Wideband Arrays and Array Simulators." IEEE Trans. Ant. & Prop., Vol. AP-16, No. 4, July 1968, p. 496.

34. Chen, C.C. "Widespread Wide-Angle Impedance Matching and Polarization Characteristics of Circular Waveguide Phased Arrays." IEEE Trans. Ant. & Prop., Vol. AP-23, No. 3, May 1974, p. 414.

35. Chen, C.C. "Quadruple Ridge-Loaded Circular Waveguide Phased Arrays." IEEE Trans. Ant. & Prop., Vol. AP-22, No. 3, May 1974, p. 481.

36. Ermatinger, C.E. and W.G. Scott. "The Crossed Ellipse Array--A System for Reduction of Polarization Axial Ratio." IEEE/G-AP Inter. Symp. Digest, December 1972, p. 21.

37. Haufling, J.D., et al. "Phased Array Polarization--Preduction, Measurement and Design." IEEE/AP-S Inter. Symp. Digest, June 1977, p. 56.

38. Knittel, G.H. and G.N. Tsandoulas. "Square Waveguide Radiating Elements for Dual-Polarization Arrays--Formulation and Solution of the Problem." IEEE/G-AP Inter. Symp. Digest, December 1972, p. 153.

39. Kreutel, R.W. "Coupling in Circularly Polarized Arrays--Polarization Effects." IEEE/AP-S Inter. Symp. Digest, June 1977, p. 189.

40. Lewis, L.R., et al. "Synthesis of a Waveguide Phased Array Element." IEEE Trans. Ant. & Prop., Vol. AP-22, No. 4, July 1977, p. 536.

41. Stalzer, H.J., et al. "Element Pattern of Dually Polarized Element in Infinite Phased Array." IEEE Trans. Ant. & Prop., Vol. AP-26, No. 2 March 1978, p. 347.

BIBLIOGRAPHY (CONCL)

42. Tsandoulas, G.N. and G.H. Knittel. "The Design and Performance of Dually Polarized Square Waveguide Arrays." IEEE/G-AP Inter. Symp. Digest, December 1972, p. 157.

43. Tsandoulas, G.N. and G.H. Knittel. "The Analysis and Design of Dual-Polarized Square Waveguide Phased Arrays." IEEE Trans. Ant. & Prop., Vol. AP-21, No. 6, November 1973, p. 796.

DISTRIBUTION LIST

Defense Documentation Center Cameron Station Alexandria, VA 22314	2*
Office of Naval Research Arlington, VA 22217 Attn: Code 221	5
Director, Naval Research Laboratory Washington, DC 20390	
Attn: Code 2627	1
Attn: Code 4700	1
Commandant of the Marine Corps Scientific Advisor (Code RD-1) Washington, DC 20380	1
Commander Naval Air Systems Command Washington, DC 20360 Attn: AIR 360	1
Commander Naval Ocean Systems Center Attn: Code 7303, J. Whittikar San Diego, CA 92152	1
Commander Naval Sea Systems Command Washington, DC 20360	
Attn: SEA 652	1
Attn: PMS 403	1
Attn: PMS 404	1
Office of Naval Research Branch Office 1030 East Green Street Pasadena, CA 91106 Attn: Code 400	1
Commander Defense Contract Administration Services District 8900 DeSoto Avenue Van Nuys, CA 91304	1

* To be forwarded with DDC Form 50

Enclosure (4)